Università degli Studi di Padova

Department of Pharmaceutical and Pharmacological Sciences

Ph.D. Course in Pharmacological Sciences

Curriculum: Pharmacological and Molecular Sciences

XXXII series

New insights in cisplatin-resistance: role of metabolic reprogramming in cancer cells

Coordinator: Prof. Nicola Ferri

Supervisor: Prof.ssa Monica Montopoli

PhD Student: Veronica Cocetta

Academic year 2018/2019

CONTENT

CONTENT ii

ABSTRACT 1

RIASSUNTO 3

ABBREVIATIONS 5

1 INTRODUCTION 7

1.1 Cancer 7

1.2 Drug resistance and chemotherapy 8

1.3 Cisplatin 9

1.3.1 Drug activation and accumulation 9

1.3.2 Drug resistance 12

Energetic metabolism in healthy cells 17

1.4 Metabolic reprogramming in cancer cells 21

1.4.1 Glycolytic pathway 21

1.4.2 Glutaminolytic pathway 24

1.4.3 Mitochondria involvement in cancer cell metabolism 25

1.4.4 Lipid metabolism 27

2 AIM 35

3 MATERIALS AND METHODS 37

3.1 Cell lines 37

3.1.1 *In vitro* model of acquired cisplatin resistance 37

3.1.2 *In vitro* model of innate cisplatin resistance 37

3.2 Maldi-TOF Mass Spectrometry 38

3.3 Confocal microscopy 38

3.4 Cell viability assays 38

3.4.1 Trypan blue exclusion assay 38
3.4.2 Sulforhodamine B (SRB) test 39
3.4.3 Crystal Violet test 39
3.4.4 Propidium Iodide Assay 39
3.5 Immunoblot assay 40
3.6 Quantitative Real-Time PCR 40
3.7 Flow cytometry 41
3.7.1 Fatty Acids uptake 41
3.7.2 Cell Cycle Analysis 42
3.8 Lipases activity 42
3.9 Liquid chromatography-mass spectroscopy (LC-MS) 42
3.10 BNIP3 silencing 43
3.11 Statistical analysis 43
4 RESULTS 45
4.1 Cisplatin resistance 45
4.1.1 Lipid profile in Sensitive (2008-A431) and Resistant (C13-A431pt) to cisplatin cancer cell lines 46
4.1.2 Glutamine metabolic profile in CDDP sensitive and resistant ovarian cancer cells (2008-C13) and in sensitive and resistant Triple Negative Breast Cancer cells (MDA-MB-468, HCC1143, HCC1937) 64
4.2 Pharmacological targeting of metabolic reprogramming in CDDP-resistant cells 73
4.2.1 Targeting lipid metabolism 73
4.2.2 Targeting mitochondria Remodeling 86
5 DISCUSSION 91
6 REFERENCES 97

ABSTRACT

Cisplatin is one of the most potent anticancer agents used in the treatment of various solid tumors. Unfortunately, the onset of resistance still limits its use in therapy and severely compromises the treatment effectiveness. Although several studies have been performed, the molecular mechanisms involved in cisplatin resistance are not completely understood. Recently, a metabolic rewiring has been shown to play a prominent role in the response of cancer cells to first-line chemotherapeutic agents, indicating the metabolic pathways as powerful mediators of resistance to cancer treatments.

Previous studies of our laboratory had already demonstrated a metabolic switch of cisplatin-resistant cells toward glycolysis and to an altered mitochondrial functionality and morphology. So, in order to better characterize the metabolic fingerprint of cisplatin-resistant cells, in this work the lipid metabolic pathway and the glutamine metabolism have been investigated in models of gynecological cancer cells and Triple-negative breast cancer cells, sensitive and resistant to cisplatin. Aerobic glycolysis, mitochondrial reprogramming, and deregulation of lipid metabolism are not independent pathways but rather they cooperate to sustain cells proliferation and to allow cells survival in a challenging environment induced also by chemotherapeutic drugs. The characterization of the metabolic fingerprint of cells and the interconnection between the different pathways is essential to identify specific targets in cisplatin-resistant cancer cells useful to design pharmacological strategies to bypass resistance. Results indicate a deregulation of the lipid homeostasis in resistant cells which induces a significant lipid accumulation; moreover, preliminary results indicate that resistant cells rely more on glutamine for their survival. From this study and previous observations of our laboratory, different possible metabolic targets specific of cisplatin-resistant cells have been identified, and different pharmacological approaches able to target the identified alterations in lipid metabolism and mitochondria remodeling have been tested.

This work fits in the research panorama aimed at providing new insights into the differential metabolic dependencies of cisplatin-resistant tumors. Results may provide novel therapeutic targets exploitable to overcome cisplatin resistance and to enhance the efficacy of the current chemotherapy.

RIASSUNTO

Il cisplatino è uno dei più potenti agenti antitumorali utilizzati nel trattamento di vari tumori solidi. L'insorgenza di fenomeni di resistenza al farmaco è uno dei fattori che ne limita l'utilizzo in terapia e compromette gravemente l'efficacia del trattamento. Nonostante numerosi studi siano stati condotti negli ultimi anni, i meccanismi molecolari coinvolti nella resistenza al cisplatino non sono ancora stati completamente elucidati. Recentemente è stato dimostrato che un ruolo chiave nella risposta cellulare ai farmaci antitumorali è svolto da una riprogrammazione del metabolismo cellulare, indicando le vie metaboliche come potenti mediatori della resistenza ai trattamenti chemioterapici. Studi precedentemente condotti nel nostro laboratorio su cellule di carcinoma ovarico avevano già dimostrato uno shift metabolico verso la glicolisi e alterazioni a livello di funzionalità/morfologia mitocondriale nei cloni resistenti al cisplatino (C13). L'obiettivo di questo lavoro quindi è stato quello di studiare i pathways del metabolismo lipidico e della glutammina allo scopo di ottenere una caratterizzazione più completa del profilo metabolico delle cellule resistenti. Per questo studio sono stati utilizzati diversi modelli cellulari di tumore ginecologico e diverse linee cellulari di tumore mammario triplo negativo, sensibili e resistenti al cisplatino. È importante sottolineare come glicolisi aerobica, riprogrammazione mitocondriale e del metabolismo lipidico non sono vie indipendenti, ma cooperano per sostenere l'omeostasi cellulare e consentire la sopravvivenza delle cellule in ambienti ostili, indotti anche da farmaci chemioterapici.

Caratterizzare il profilo metabolico delle cellule e le interconnessioni tra i diversi pathways è essenziale per l'identificazione di target molecolari tumore-resistente specifici sfruttabili per approcci farmacologici innovativi. I risultati ottenuti indicano come le cellule resistenti al cisplatino presentino una alterazione dell'omeostasi lipidica che induce un significativo accumulo intracellulare di lipidi; inoltre gli studi preliminari riguardanti il ruolo della glutammina indicano come la sopravvivenza delle cellule resistenti sia particolarmente dipendente dal metabolismo di questo aminoacido.

Da questo studio, e da precedenti osservazioni del nostro laboratorio, sono stati identificati diversi possibili target metabolici specifici delle cellule cisplatino-resistenti, sia a livello di vie metaboliche lipidiche sia a livello mitocondriale.

Questo lavoro si inserisce nel panorama di ricerca volto ad approfondire le specifiche dipendenze metaboliche di tumori cisplatino-resistenti. I risultati ottenuti potranno fornire nuovi target terapeutici sfruttabili al fine di superare la resistenza al cisplatino e migliorare l'efficacia dell'attuale trattamento chemioterapico.

ABBREVIATIONS

ACLY:	ATP-citrate synthase
ATP:	Adenosine triphosphate
Bnip3:	BCL2 Interacting Protein 3
CD36:	Cluster of differentiation 36
CDDP:	Cis-diamminedichloroplatinum II
CPT1/2:	Carnitine palmitoyltransferase I/II
ETO:	Etomoxir
FABP:	Fatty acid-binding protein
FAD/$FADH_2$:	Flavin adenine dinucleotide
FA:	Fatty acid
FAO:	Fatty acid oxidation
FASN:	Fatty acid synthase
FATP:	Fatty acid transport protein
FBS:	Fetal Bovine Serum
G6PDH:	Glucose-6-phosphate dehydrogenase
Gln:	Glutamine
GPAT:	Glycerol-3-phospate acyltransferase
GSH:	Glutathione
LC3:	MAP1LC3B (Microtubule-associated protein 1A/1B-light chain 3)
LDs:	Lipid droplets
MHY908:	2-[4-(5-chlorobenzo[d]thiazol-2-yl) phenoxy]2-methylpropanoic acid
NAD/NADH:	Nicotinamide adenine dinucleotide

P62: Ubiquitin-binding protein p62 (Sequestosome-1, SQSTM1)

PPARa: Peroxisome proliferation-activated receptor alpha

ROS: Reactive oxygen species

RT-PCR: Real Time-PCR

TOM20: Mitochondrial outer membrane translocase complex

VPS34: Vacuolar protein sorting-34 (Class III PI 3-Kinase enzyme family)

1 INTRODUCTION

1.1 Cancer

Cancer is a multifactorial disorder involving complex modifications in the genome affected by the interactions between host and environment. According to estimates from the World Health Organization (WHO) in 2015, cancer is the first or second leading cause of death before age 70 years in 91 of 172 countries, and it ranks third or fourth in an additional 22 countries[1].

The incidence of cancer is growing worldwide, mostly in countries economically developed. The reasons are complex but mainly linked to the aging of population and the adoption of cancer-associated lifestyles, reflectors of socioeconomic development[2].

Cancer cells differ from healthy cells by distinct biological features acquired during the multi-step development of the disease, which allow them to elude the proliferation control mechanism evading apoptosis and to become invasive. Cancer is a multifactorial disorder involving complex alterations, due to mutations in oncogenes and tumor suppressor genes[3]. Oncogenes derive from protooncogenes that, once undergone the mutation, alter their protein synthesis, through the production of wrong proteins, alter activity of proteins or can also have qualitative effects on their transcriptional specificity leading to the stimulation of autocrine/paracrine loops and activation of multiple signaling pathways.[4,5]. The tumor suppressors, instead, usually control the overexpression of oncogenes, but in different types of cancer they are destroyed or altered leading to a decrease in their functionality. The deregulation of tumor suppressor may alter checkpoints and growth pathways, leading to cancer progression[6]. These mutations or loss-of-function alterations lead to an increase in the metabolic demand of cancer cells which require an adaptive response of metabolism in order to sustain cell proliferation[7]. On the other side, some metabolites produced by cancer cells possess oncogenic roles, modifying cellular dynamics and tumor microenvironment. A variety of non-transformed cells such as immune cells, fibroblasts, endothelial cells, undergo phenotypic changes by interaction with cancer cells, sustaining tumor growth[8].

Since the recognition of the tumor, the selection of the treatment and its progress depends on the type of tumor, localization, and stage of progression. The traditional and most used

treatment methods comprehend surgery, radiotherapy, and chemotherapy while the most recent modalities include immunotherapy, hormone-based therapy, stem cell therapies, etc[9]. The high proliferation rate of tumor cells makes them susceptible to a wide range of drugs which targets mainly processes involved in cellular replication; however, as these processes also drive normal cells, the effect is not unique, and a wide range of side effect comes with these drugs. Moreover, in some cases tumors may resist to drug treatment leading to therapeutic failure.

1.2 Drug resistance and chemotherapy

Resistance to chemotherapy and molecularly targeted therapies is the major problem of current cancer research. In fact, some tumors may be refractory to treatment with certain drugs due to some genetic characteristic or, in many cases tumors may develop resistance following exposure to the drug. A huge effort in research has been made to identify factors that can predict the onset of resistance in order to adapt the therapeutic strategy. Temporary respite is obtained by the combination of different drugs; the rational to choosing which drug to combine is that they present different modes and sites of action in other to give a complementary/synergistic effect as well as the present minimally overlapping toxicity. Different combinations are currently used in therapy (like platinum and taxane, docetaxel and gemcitabine in ovarian cancer, etc)[10]. This approach can eventually result in the phenomenon of multi-drug resistance[11].

The mechanism of resistance is complex and multifactorial and is object of several studies. A variety of factors have been demonstrated to be involved in chemoresistance, including the reduced intracellular concentrations of drugs, alterations in drug targets, activation of pro-survival pathways, ineffective induction of cell death and interactions between cancer cells and the tumor microenvironment[12]. Moreover, it is increasingly evident that tumors contain a high level of molecular heterogeneity[13]; indeed, drug resistance can occur through a therapy-induced selection of the most favorable cell phenotype able to survive in presence of the drug.

Recent studies show that the metabolic state of cells influences the response to chemotherapy and that cancer cells reprogram their metabolism in response to chemotherapeutic drugs. These observations indicate that the metabolic rewiring is an

important mechanism of acquired resistance and can be exploited for improving the efficacy of the treatment[14].

1.3 Cisplatin

Cis-diamminedichloroplatinum II, best known as Cisplatin (CDDP) is a metallic coordination compound, which is one of the most potent and most employed alkylating chemotherapeutic agents (Figure 1). The compound was first prepared by Michele Peyrone in 1845 but its properties where casually bring to light in 1965 by Barnett Rosenberg and co-workers[15]. During his experiments on the effect of an electric field on *Escherichia Coli* growth, Rosenberg discovered that a platinum compound released from the electrodes that he was using, blocks cells division. In 1969 Rosenberg has demonstrated that cisplatin has the ability to inhibit leukemia L1210 and sarcoma 180 in mice [16]. Subsequent tests on the drug showed the action of cisplatin against a variety of tumor systems; the *trans*-isomer is not effective due to the trans-arrangements of the chloro ligands that leads to faster inactivation of the drug, and to the stereo-conformation which render *trans*-platin unable to form the 1,2 intrastrand adducts with DNA[17]. Results on cisplatin were so promising that preclinical and toxicological tests were started, leading in 1978 to the approval in clinical use for testicular and ovarian cancer by the Food and Drug Administration[18].

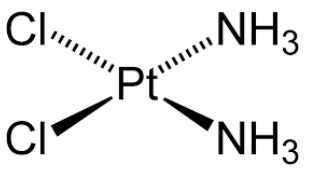

Figure 1: Cis-diamminedichloroplatinum II

Nowadays cisplatin plays a major role in the treatment of several cancers, including testicular, ovarian, bladder, head and neck, cervical, colorectal and lung cancer[19].

The drug is used intravenously and primarily eliminated by kidney while only the 10% takes the bile duct. The main side effects are nephrotoxicity, ototoxicity, neurotoxicity, and myelosuppression[20].

1.3.1 **Drug activation and accumulation**

Cisplatin has a planar structure formed by a central atom of platinum in the oxidation state of +2 to which are linked two chlorine atoms and two NH_3 molecules, thus obtaining

a framework-planar geometry. The molecule exists in two isomers *cis* and *trans* but it is only the *cis*-isomer which presents a strong anti-tumor activity [21].

The *in-vivo* molecular mechanism of cisplatin, which behaves as a classical prodrug, is conditioned by the environment; in fact, the activation inside the cell is due to the different chloride concentration between the bloodstream and the cell cytoplasm. The concentration drops from ~100 mM in the blood plasma to ~4 mM in cell cytoplasm, facilitating the reaction of mono or di-aquation of the drug, making it a potent electrophile ($[Pt(H_2O)Cl\ (NH_3)_2]^+$ and $[Pt(H_2O)_2(NH3)_2]^{2+}$ cations) prone to react with nucleophilic species within the cells (DNA, RNA and proteins) (Figure 2) [22].

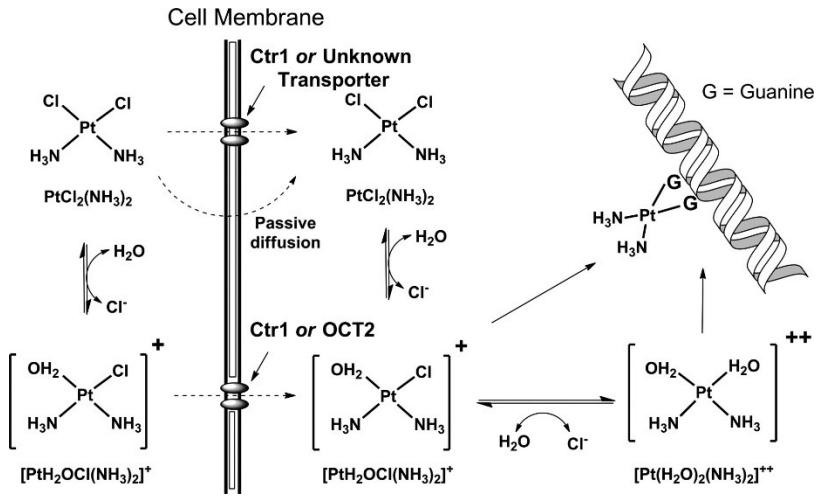

Figure 2: Schematic representation of cisplatin uptake and activation [23].

The platinum atom of CDDP forms covalent bonds with the purine bases (with the N7-position) producing 1,2 or 1,3-intrastrand crosslinks and a lower percentage of interstrand crosslinks. The crosslinks, cause alterations in the double helix structure of DNA blocking the replication and or/preventing the transcription process. Moreover, the formation of crosslinks disrupts the structure of DNA which is recognized by cellular proteins to repair the DNA damage[24]. In particular, preventing or hindering the polymerase binding to DNA, a failure in DNA duplication occurs, and this block primarily affects tumor cells, which are in fast replication. In addition to preventing these fundamental processes, cisplatin seems to damage cancer cells by inducing apoptosis[25]; also the production of ROS induced by cisplatin can lead to irreversible damage to the cells[26].

Although DNA is commonly accepted as major target of cisplatin, only the 1% of the drug appears to interact with nuclear DNA, while the largest amount interacts with sulfur donors (such as cysteines, methionines, thiols, etc.), proteins or mitochondrial structures, as well as with the mitochondrial DNA (mtDNA),[27,28]. Indeed, the process of protein-cisplatin recognition is reputed crucial in determining cisplatin uptake, transport, biodistribution and toxicity profile. Once CDDP is intravenously administered to the patient, it diffuses into tissues and is highly bound to plasma proteins as result of its strong reactivity with sulfurs of thiol groups[29]. Also, a significant portion of Pt is bound to glutamyl-cysteine-glycine (glutathione, GSH) and/or other cysteine-rich biomolecules like a few small proteins of the metallothionein family [30].

The biochemical mechanism by which cisplatin crosses the cell membrane is still not completed understood. The passive diffusion across the plasma membrane has initially been proposed as process responsible for cisplatin transport into the cells[31]. Nowadays it is accepted that uptake of cisplatin into cells occurs via multiple mechanisms which involve passive diffusion as well as active transport systems. Different transporters have been associated with CDDP transport across the plasma membrane: in the last years, some proof of evidence have demonstrated that cisplatin may enter cells by the copper trafficking system which includes the copper transporters members of the Copper Transport (Ctr) protein family, like Ctr1 and Ctr2 [32]. Also, the copper pumps ATP7A and ATP7B has been shown to be responsible for sequestration and efflux of cisplatin. Moreover, the copper chaperone Atox1 has been shown to possibly play a role in delivering cisplatin to ATPases[33].

1.3.2 **Drug resistance**

Despite the success of cisplatin treatment against several cancers, the effectiveness of the therapy is limited because of acquired or intrinsic resistance which leads to therapeutic failure. In particular prostate, colorectal, and lung cancer are intrinsically resistant to cisplatin while acquired resistance is more often observed in ovarian cancer patients[34]. Intense research has been conducted in the past 30 years and the acquired resistance appears to be a multifactorial phenomenon which involves a plethora of unrelated mechanisms. Studies highlighted how the acquisition of resistance can be due to pre-target alterations (that involve steps preceding the binding of cisplatin to DNA), on-target alteration (directly relate to DNA–cisplatin adducts), post-target alterations (related to lethal signaling pathway(s) elicited by cisplatin-mediated DNA damage) and off-target resistance (which affect other molecular pathways that do not present obvious link with cisplatin)[28] (Figure 3).

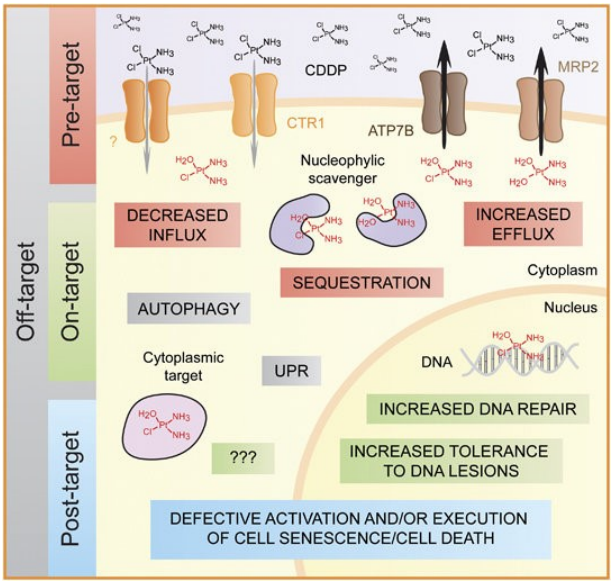

Figure 3 Molecular mechanisms of CDDP resistance [28]

- **Reduced drug accumulation:** The predominant cause of cisplatin resistance is the reduced effective concentration of intracellular drug[35]. As consequence of reduced uptake or retention, the formation of platinum-DNA adducts is obviously decreased resulting in reduction of cytotoxicity and, thus, resistance to the drug. Decreased influx could result from defective transporters or channels, or functional/structural changes in organelles or membrane potential. Active efflux could result from increased export, secretion, or exocytosis of the platinum compounds[27,34]. As said, the platinum compound is taken up by cells by passive diffusion or trough facilitate transport. Decrease expression of these transporters seems to be involved in cisplatin resistance. Cisplatin uptake is performed by the copper transporters CTR1 and CTR2 as well as from the solute carrier (SLC) transporter family, specifically the SLC22 family members in which OTC2

seems to be more involved in cisplatin uptake[23]. Cisplatin resistant cells show decreased levels of CTR1 mRNA and decreased cisplatin uptake; mouse embryonic fibroblasts (MEF) null for CTR1 provide 3.2 fold increased resistance compared to transfected cells; moreover, in the clinic, CTR1 has been shown to be decreased in ovarian and lung cancer resistant to cisplatin[36]. Regarding the OTC2's role in cisplatin resistance, there are not a lot of clinical studies primarily due to the fact it is expressed in the kidney. The other shuttle coppers between the Golgi and the plasma membrane, ATP7A, and ATP7B which belong to the transporter family of P-type ATPases, are instead involved in the efflux of the drug. The copper, in fact, competes with the drug for cellular uptake but is also able to reduce the outflow of cisplatin, increasing its accumulation. The overexpression of ATP7B is associated with a worse prognosis in patient with esophageal cancer [37] and squamous cancer cells of the head and neck[38] indicating an implication in the resistance. The main protein involved in the effective elimination of the drug from the cells is an ATP-binding cassette transporter, located on the cell membrane and able to recognize different anticancer drugs, including platinum-based compounds[39]. Overexpression of this transporter has been observed in resistant ovarian tumors, sarcomas and breast tumors[40]. In additions, other ABC transporters including Multidrug-resistant proteins (MRPs) are possibly involved in cisplatin resistance by increasing drug efflux[28].

Once in the cytoplasm, platinum-based agents undergo acquation-reactions with the formation of electrophilic sites, prone to react with intracellular nucleophilic species such as glutathione (GSH), methionine, metallothioneins (MTs), and thiol-containing proteins. Increased concentration of these compounds is known to lead to resistance through the binding and inactivation of the drug[27]. Elevated levels of GSH, of γ-glutamylcysteine synthetase (the enzyme which catalyzed GSH synthesis), or of the glutathione S-transferase which mediate the conjugation of GSH with CDDP, have been observed in cisplatin resistance both *in vivo* and *ex vivo*[41]. Glutathione S-conjugates are then extruded via MRP1 or MRP2 thus explaining the associated cell resistance to cisplatin[28]. Besides glutathione, also thioredoxin (Trx) system and metallotionines (MTs) are involved in cell protection from oxidative stress.

Metallotioneins are low molecular weight-thiol containing proteins, which are thought to be involved in controlling levels of copper and zinc, as well as protecting cells from oxidative stress and toxicity associated with heavy metals[42]. The presence of these compounds is associated to resistance in ovarian carcinomas, cervical and lung, therefore, the association of MT levels with cisplatin resistance may be tissue-specific and may play a minor role depending on the cellular environment[43],[44]. Thioredoxin system play a major role in regulation of redox-cell homeostasis and also, it is involved in several cellular functions, as DNA replication and repair, regulation of transcriptional factors, etc[45]. Trx is reduced by thioredoxin reductase (TrxR), which involves the oxidation of NADPH. In clinical samples, Trx levels correlate with cisplatin resistance in bladder, prostate, liver, gastric, lung and colon cancer cells [46],[47].

- **Increased repair of platinum-DNA adducts:** The well-known mechanism of action of cisplatin is the alteration in the structure of the DNA molecule, then, the amount and the extent of the DNA-damage determine cell survival or death[48]. Cisplatin-induced DNA adducts block transcription and DNA synthesis, which in turn triggers an intricate intracellular signal transduction cascade in attempt to eliminate the lesions. Studies have revealed that tumor cells can have intrinsic differences in DNA repair mechanism when compared to their healthy counterparts, although alterations may also be acquired. The role of DNA repair systems in platinum resistance has been studied for many years, in preclinical and clinical settings (Figure 4).

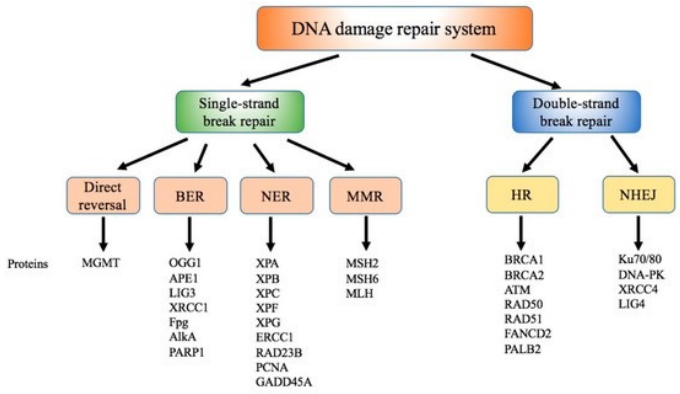

Figure 4: DNA damage repair systems. DNA damage repair systems include BER (base-excision repair), NER (nucleotide repair), MMR (mismatch repair), HR (homologous-recombination repair) and NHEJ (non-homologous end joining repair) pathways[49].

The nucleotide excision repair (NER) system is believed to resolve the majority of DNA lesions caused by CDDP[50], although components of mismatch repair (MMR) machinery have also been implicated in this process[51]. NER is an ATP-dependent multiprotein complex that recognizes 1,2 intrastrand cross-links and subsequently excises the DNA; the gap that remains is then filled by DNA polymerase. An increased NER proficiency has been associated with CDDP resistance in vitro in murine models as well as in cohorts of cancer patients[28]. In particular, the excision repair cross-complementation group 1 (ERCC1) protein plays a key role in nucleotide excision repair. ERCC1 dimerizes with xeroderma pigmentosum complementation group F, and this complex is required for the excision of the damaged DNA. Several studies in cancer cell lines linked the deficiency of in ERCC1 levels and xeroderma pigmentosum complementation group F to cisplatin resistance[52]. Multiple studies with human ovarian cancer cell lines, including cell lines with intrinsic cisplatin resistance, showed an increased sensitivity to cisplatin after antisense RNA inhibition of ERCC1[53]. In addition, cell lines that develop resistance in vitro after exposure to cisplatin chemotherapy were found to have increased expression of ERCC1[54]. Recently many single nucleotide polymorphisms have been identified in ERCC1 and ERCC2 genes, and some have been shown to affect the DNA repair capacity and concomitantly the tumor's sensitivity to cisplatin[55].

The MMR system is responsible for correcting single-strand DNA (ssDNA) errors, such as insertion/deletions or mismatches. MMR consists of recognition, excision, re-synthesis, and ligation of the newly synthetized strand; it is believed to detect DNA adducts caused by CDDP, fail in their repair, thus transmitting a pro-apoptotic signal[56]. Many studies have linked MMR deficiency to cisplatin resistance and genes encoding for MMR components; mutS homolog 2 (MSH2) and mutL homolog 1 (MLH1) are frequented altered in cisplatin acquired resistance[57],[58]. Loss of MLH1 in colon cancer cells resulted in a 2-fold increase in cisplatinum resistance and genetic complementation of MHL1 in deficient cells has been showed to restore cisplatin sensitivity[57],[59].

MSH2 deficiency resulted in increase in cisplatin resistance in endometrial cancer cell line HEC59 as well as in muscle-invasive bladder cancer[57],[60]. Defects

in MMR system may be inherited (as in hereditary nonpolyposis colorectal carcinoma) or may occur through epigenetic silencing of genes (mostly through Mut L homologue 1 (Hmlh1) promoter hypermethylation) as has been shown in colorectal, gastric and ovarian carcinoma[61]. It is to note that high expression levels of MMR components may exert a positive influence both on the probability to acquire CDDP resistance and on the propensity to chemotherapy-naïve tumors to relapse (because MMR limits the accumulation of genetic alterations)[28].

- **Genetic alterations and apoptosis inhibition:** The induction of the apoptotic pathway is essential for cisplatin efficacy. CDDP stimulated apoptosis by triggering both extrinsic death pathway and intrinsic mitochondrial pathway. Several studies showed that CDDP-resistant cells present a decrease in the apoptotic machinery caused possibly by alterations in genes, proteins, and pathways of pro or anti-apoptotic signal[62]. Numerous proteins such as Bcl-2 family proteins and p53, and multiple pathways including nuclear factor-kB (NF-kB) and mitogen-activated protein kinase (MAPK), are involved in extrinsic and intrinsic apoptosis[35].

  In the induction of pro-apoptotic proteins by DNA-damage-induced signaling, the tumor suppressor p53 play a major role. In fact, up-regulation of proapoptotic proteins such as PUMA or Bax is mediated by acetylation and phosphorylation of p53[63]. It has been observed that alterations in p53 are associated with cisplatin resistance and other studies underlined how the frequency of protein mutations is higher in resistant ovarian cancer cell lines than the sensitive counterpart[64]. Also, the phosphatidylinositol-3-kinase/Akt (PIK3/Akt/mTOR) pathway is a key regulator in cell survival and plays an important role in chemotherapy resistance by inducing anti-apoptotic proteins[65]. It has been shown that inhibition of (PI3K)/Akt pathway sensitizes different cell lines to cisplatin, as human lung cancer cells and Triple Negative breast cancer cells[66 67].

  Other proteins involved in resistance are those of the Bcl-2 family which contains both pro and anti-apoptotic proteins. The alteration in the balance between these different proteins has been shown to be linked with resistance phenomena leading to the activation of the multi-domain (BH1, 2, 3) effector proteins BAK and

BAX, which assemble into multimeric pores in the mitochondrial membrane and facilitate mitochondrial outer membrane permeabilization (MOMP) and cytochrome c release into the cytosol[68 69].

The mitogen-activated protein kinase (MAPK) pathway also plays a critical role in the intracellular signaling network which regulates gene expression in response to several stimuli. Defects in several pro-apoptotic signal transducer, including mitogen-activated protein kinase 14 (MAPK14, best known as $p38^{MAPK}$) and c-Jun N-terminal kinase 1 (JNK1) has been observed in cisplatin resistance[70,71] and inhibition of JNK, p38 kinase, or ERK attenuates cisplatin-induced apoptosis and cell death [72]. Finally, several studies both *in vitro* and *in vivo*, demonstrated that constitutive activation of NF-Kb inhibits chemotherapy-induced apoptosis in several cancer types, including cervical cancers[73,74].

Recent interest has been given to the role of mitohormesis in cell adaptations to different stresses. Evidence shows that various form of mitochondrial stress, can cause an adaptive response that can benefit the cells. It has been shown that moderate levels of ROS protect against several disease inducing upregulation of mitochondrial capacity and endogenous antioxidant defense[75,76]. This still poorly unexplored mechanism can be involved in the remodeling of the metabolism that confers resistance following drug treatment.

Energetic metabolism in healthy cells

In healthy cells a large amount of energy provided by ATP is required to replicate all cellular contents: glucose participates with two ATP molecule synthesis through glycolysis and up to 36 ATPs through its complete catabolism by the TCA cycle and OXPHOS (oxidative phosphorylation). The large requirements for nucleotides, amino acids, and lipids are sustained by intermediate metabolites of these pathways. In addition to glucose, also glutamine is catabolized for most mammalian cells growing in culture. Therefore, glucose and glutamine both supply carbon, nitrogen, free energy, and reducing equivalents necessary to support cell growth and division. This means that glucose, in addition to being used for ATP synthesis, should also be diverted to macromolecular precursors such as acetyl-CoA for fatty acids, glycolytic intermediates for non-essential amino acids, and ribose for nucleotides to generate biomass (Figure 5).

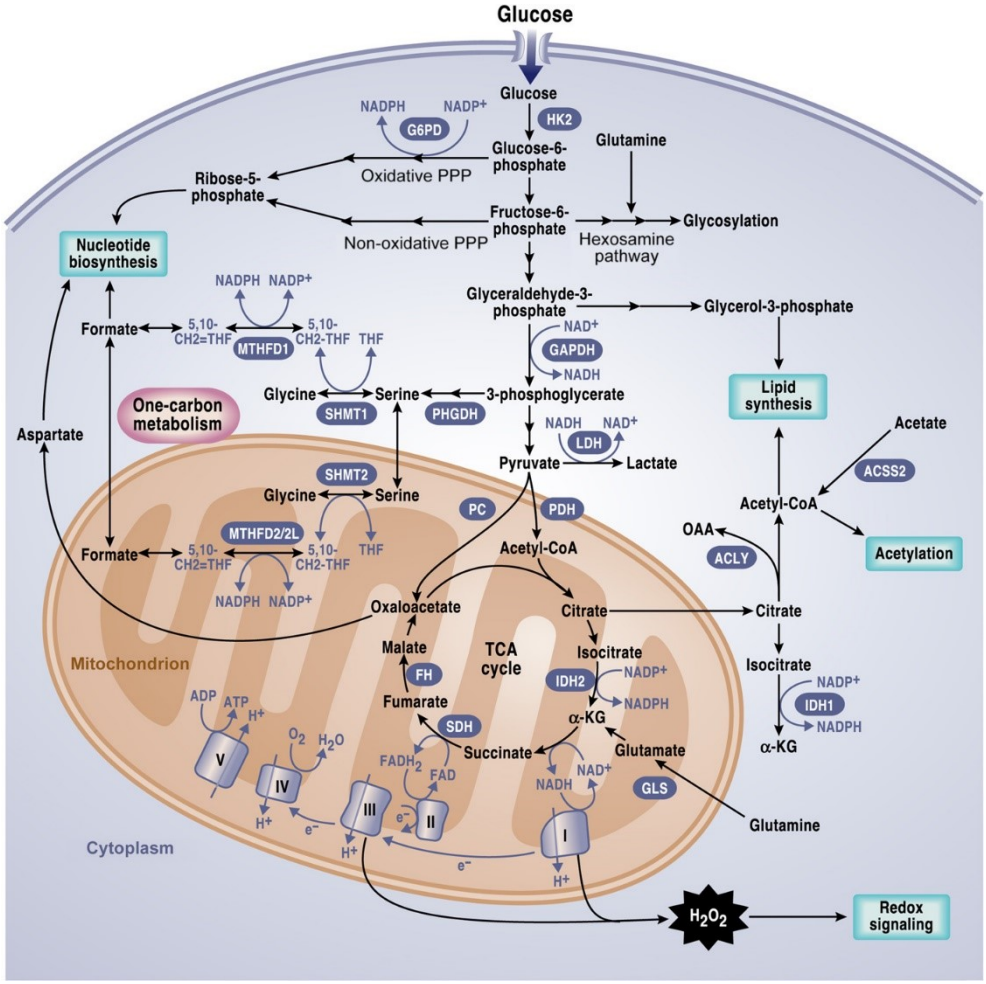

Figure 5:Anabolic pathways that promote cancer growth. Glucose- metabolism, generates glycolytic intermediates to support cell growth; Mitochondrial TCA cycle intermediates are used for several biosynthetic reactions leading to nucleotides and lipid synthesis. Moreover, mitochondria are also implicated in redox homeostasis [77]

- **Glycolytic pathway**: Glycolysis is the first step in the breakdown of glucose to generate energy. Glucose enters the cell through glucose transporters (GLUTs) and is then phosphorylated to glucose-6-phosphate (G6P) by hexokinase 1 (HK1). Phosphoglucose isomerase catalyzed the conversion of G6P to fructose-6-phosphate (F6P) which yields fructose-1,6-biphosphate (F1,6-BP) by phosphofructokinase 1 (PFK1); Aldolase A catalyzed the hydrolysis of 1 F1,6-BP in dihydroxyacetone phosphate and glyceraldehyde 3-phosphate. The 2 products of aldolase equilibrate redly in a reaction catalyzed by triose phosphate isomerase. Succeeding reactions of glycolysis utilize glyceraldheyde-3-phosphate as substrate. Glyceraldehyde 3-phosphate dehydrogenase catalyzed its oxidation to 1,3-biphosphoglycerate which is converted in 3-phosphoglycerate

by phosphoglycerate kinase; the following step involves reaction of phosphoglycerate mutase 1 (PGAM1) which catalyzes the production of 2-phosphoglycerate (2PG); enolase 1 (ENO1) catalyze 2PG conversion in phosphoenolpyruvate (PEP) that is finally transformed in pyruvate by Pyruvate kinase (PK) . Ultimately, glycolysis produces two ATP molecules and six NADH molecules per glucose. In normal tissues, most of the pyruvate is directed into mitochondria to be converted into acetyl-CoA by the action of pyruvate dehydrogenase (PDH) or transaminated to form alanine[78,79].

Pentose phosphate pathway (PPP): This is a metabolic pathway that generates NADPH and pentose sugars from G6P. PPP is divided into two biochemical branches: an oxidative and non-oxidative branch. The oxidative converts G6P to ribulose-5-phosphate (Ru5P), CO_2 and NADPH by glucose-6-phosphate dehydrogenase (G6PD) while producing two molecules of NADPH. NADPH is both a major cellular antioxidant, maintaining glutathione in a reduced state to prevent oxidative damage, and a required cofactor in the reductive biosynthesis of fatty acids, nucleotides, and amino acids. NADH is also used in mitochondrial OXPHOS[80]. The non-oxidative branch yields the glycolytic intermediates fructose 6-phosphate (F6P), glyceraldehyde 3-phosphate (G3P) and sedoheptulose sugars, resulting in the production of sugar phosphate precursors for amino acid synthesis and ribose-5-phosphate (R5P), which is essential for nucleic acid synthesis[81].

- **Tricarboxylic acid (TCA) cycle:** Pyruvate produced by glycolysis is converted to acetyl-CoA, which enters the TCA cycle, and citrate, α-ketoglutarate, succinyl-CoA, fumarate, malate, and oxaloacetate are produced as intermediate products; acetyl-CoA cannot cross the inner mitochondrial membrane, but intramitochondrial acetyl-CoA and oxaloacetate combine to form citrate, which is transported out of the mitochondria and broken back down into its constituents by ATP citrate lyase (ACLY). Acetyl-CoA is converted to malonyl-CoA by acetyl-CoA carboxylase, and acetyl-CoA and malonyl-CoA are then both used by the multi-subunit enzyme fatty acid synthase (FAS) for the synthesis and elongation of fatty acid chains. Oxaloacetate is used for the synthesis of non-essential amino acids. Cytosolic and nuclear acetyl-CoA is also a precursor for

the post-translational modification of proteins (for example, histones) by acetylation. Like citrate, malate produced in the TCA cycle leaves the mitochondria, and it is converted to pyruvate plus NADPH. Citrate might also be converted to isocitrate and then to α-ketoglutarate, generating another molecule of NADPH by the action of isocitrate dehydrogenase 1 (IDH1).

- **Glutaminolysis:** After glutamine is taken into the cell, it is first converted into glutamate by glutaminase (GLS/GLS2). Glutamate is then converted in α-ketoglutarate via two different pathways: the first via the activity of glutamate dehydrogenase (GLUD) which generates ammonium and NADH or NADPH. The second is via the activity of a group of transaminases, including glutamate–oxaloacetate transaminase (GOT), glutamate–pyruvate transaminase (GPT), and phosphoserine transaminase (PSAT) which promote the generation of other non-essential amino acids including alanine, aspartate, and phosphoserine. α-Ketoglutarate thus generated can serve as an anaplerotic substrate in the TCA cycle. Glutamine anaplerosis in the TCA cycle provides critical precursors for NEAAs, nucleotides, and lipids.
- **Lipid metabolism:** the homeostasis of this pathway is required to maintain cellular structure, provide energy and is involved in cell signaling.

  De novo lipid synthesis is the process that, converting nutrient-derived carbons into fatty acids, can supply with phospholipids for biological functions[82,83]. Fatty acids have different turnovers in the body. They can be broken down through a series of mitochondrial β-oxidation processes into acetyl-CoA, which then enters the tricarboxylic acid cycle to aid ATP generation. Alternatively, fatty acids can be incorporated into TAG, phospholipids or cholesterol esters.

  Fatty acids, in fact, can be used to generate many different types of lipids: they are converted in diacylglycerides (DAGs) and triacylglycerides (TAGs) via the glycerol phosphate pathway. TAGs are mainly used for energy storage in the form of lipid droplets. Intermediate of this pathway can also be converted in building blocks for biological membranes like phosphatidylcholine (PC), phosphatidylethanolamine (PE), phosphatidylglycerol (PG) and phosphatidylserine (PS). Another class of lipids essential for membrane function are sterols, mainly cholesterol and cholesteryl-esters (CEs). Cholesterol

modulates the fluidity of the lipid bilayer and it provides the structural backbone for the synthesis of steroid hormones such as progesterone and estrogen. Sphingolipids, phosphoinositides, and eicosanoids are as well generated from FAs, and play important roles in signaling functions and tissues[84].

1.4 Metabolic reprogramming in cancer cells

Cancer metabolic reprogramming has been recognized as one of the ten cancer hallmarks by Drs. Hanahan and Weinberg[85] (Figure 6) and in the last decade several works have well documented this metabolism rewiring. In order to support rapid proliferation, survival in severe microenvironment, invasion, and metastasis, cancer cells need to reprogram their catabolic and anabolic processes; the reprogram allows cells to adjust the energy metabolism, in order to dispose of the necessary large amount of energy and biomass. Moreover, the reprogramming of cell metabolism has also been linked to the survival of cancer cells upon treatment with chemotherapeutic drugs. Several altered oncogenes and tumor suppressor genes, directly control different metabolic pathways which gather to alter cellular metabolism and provide the necessary support for rapid cell division[86]: ATP to maintain the energetic status, biosynthesis of macromolecules and maintenance of the redox homeostasis[87]. To sustain these needs, cancer cells undergo alterations in the metabolism of all the four major classes of macromolecules: carbohydrates, proteins, lipids, and nucleic acids[88].

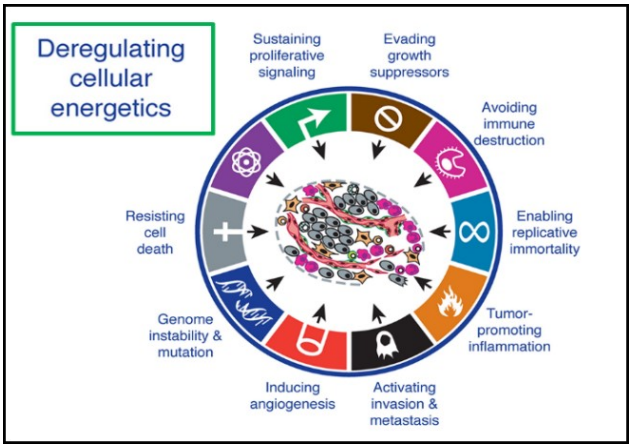

Figure 6: Hallmarks of cancer (Adapted from [74])

1.4.1 Glycolytic pathway

While normal cells rely primarily on mitochondrial oxidative phosphorylation (OXPHOS) for energy supply and metabolic activities, cancer cells avidly take up glucose for aerobic glycolysis[89–91]. This effect is correlated to hypoxia, but it is present also in normoxia conditions[90]. This phenomenon is known as “Warburg Effect” because of Dr.

Otto Warburg's discover in the 1920s. Warburg observed that cancer cells exhibit significant alterations in energy metabolism and mitochondrial respiration compared to normal cells [92]. Having observed a preferential use of glycolysis for ATP generation even in presence of oxygen, he postulated a shift from OXPHOS to glycolysis as a result of an impaired mitochondrial function which induces a respiratory injury finally leading to cancer development. Many decades later, a multitude of studies has provided additional insights into the abnormality of cancer metabolism. However, in contrast to Warburg's original hypothesis, damaged mitochondria are not the reason for the shift to aerobic glycolysis exhibited by most tumor cells. In fact, most tumor mitochondria are not defective in their ability to carry out oxidative phosphorylation. Instead, also mitochondrial metabolism is reprogrammed to meet the challenges of macromolecular synthesis. This possibility was never considered by Warburg and his contemporaries[90].

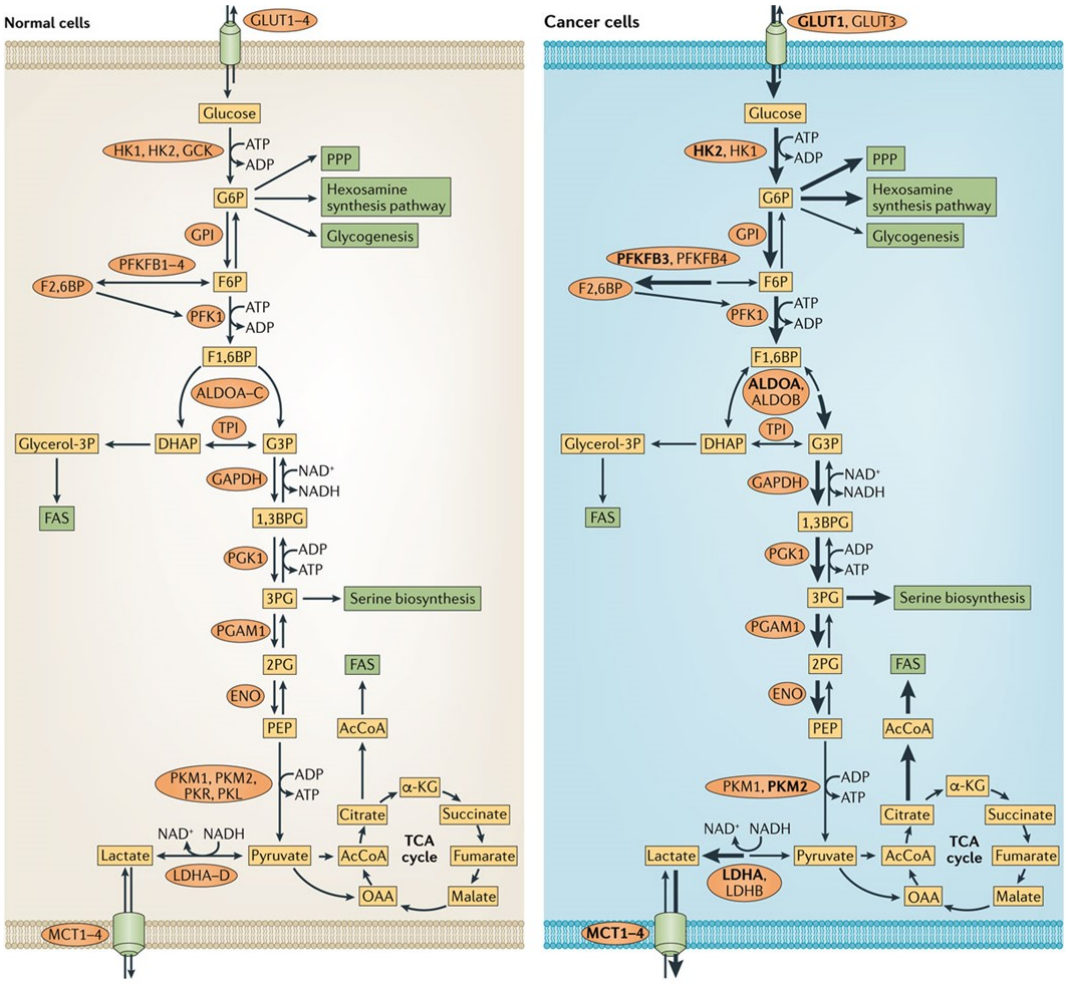

Figure 7: Alterations in glucose metabolism in cancer cells. Compared with normal cells (left), cancer cells (right), present an increased flux of glucose metabolism and glycolysis, overexpressing different enzymes, in order to sustain rapid proliferation [93].

In normal cells, glucose is catabolized to pyruvate, which can be converted to acetyl-CoA to fuel the tricarboxylic acid cycle (TCA). TCA cycle generates $FADH_2$ and NADH to fuel with electrons the mitochondrial respiratory chain. Thanks to mitochondrial respiration, each molecule of glucose can produce 36 molecules of ATP, thus generating a large amount of energy. In healthy cells, glycolysis is preferred only when oxygen is limited. This phenomenon in cancer cells is related not only to hypoxic conditions, but also in presence of oxygen (a process also called "aerobic glycolysis"). Glycolysis generates only 2 ATPs per molecule of glucose, so cells have to compensate for the lack of energy. One of the strategies is an upregulation of glucose transporters (GLUT1-2-3-4) to increase the uptake of the substrate (Figure 7). The Warburg effect has been demonstrated in several types of tumors and the increase in glucose uptake, confirmed through 18F-deoxyglucose positron emission tomography (FDG-PET), positively correlated with poor prognosis and higher metabolic potential in clinical, supporting the theory that alterations in cellular metabolism may contribute to the malignant phenotype[94,95].

The reasons why cancer cells prefer aerobic glycolysis to oxidative phosphorylation are several. Firstly this shift allows cancer cells to live in fluctuating oxygen conditions, that would be lethal for OXPHOS dependent cells[96]. Secondly, the end product of glycolysis is lactate and generation of lactic and bicarbonic acids sets up an acid environment which may activate metalloproteinase and matrix remodeling enzymes, favoring cancer invasion and metastasis[97–99]. Moreover, the lactate extrudes from tumor cells participates in the rearrangement of the tumor micro-ecosystem which integrate anaerobic components (cancer cells) and aerobic components (non-transformed stromal cells)[97]. Third, to ensure cell's antioxidant defenses glucose metabolism could be redirected through the Pentose Phosphate Pathway, leading to the formation of nicotinamide adenine dinucleotide phosphate (NADPH). NADPH can also contribute to fatty acid synthesis [95]. Finally, and most importantly, the entire metabolism is reorganized to increase anabolic reactions providing a biosynthetic advantage for tumor cells to sustain growth and proliferation. In fact, cancer cells exploit the intermediate of glycolysis for anabolic reactions providing building blocks and precursors for the synthesis of DNA and fatty acids (glycogen and ribose 5-phosphate are synthesized from glucose 6-phosphate, triacylglycerides and

phospholipids from dihydroxyacetone, and alanine and malate form pyruvate)[95]. Pyruvate can also enter a truncated the TCA cycle resulting in acetyl-CoA export from mitochondria. Thus, it becomes available for the synthesis of cholesterol, fatty acids, and isoprenoids[94].

1.4.2 **Glutaminolytic pathway**

Besides the glucose dependence, another metabolic characteristic of many cancer cells is a dependence from an exogenous supply of glutamine, despite this being a semi-essential amino acid that hepatocytes can synthesize *de novo*. Deprivation of glutamine in these cells results in growth arrest and cell death owing to their glutamine addiction. Glutamine is the most abundant amino acid in the blood and muscle and is used as precursor of biomass and for energy production to sustain rapid proliferation[100]. Glutamine plays a pleiotropic role providing not only carbon but also nitrogen for nucleic acid synthesis and it's also involved in cellular redox homeostasis (Figure 8); so, it is important to consider both the catabolism and the anabolism of this amino acid in the context of diseases and cancer. Findings from recent years underlined how glutamine requirements are very heterogeneous among different cancer cell lines, varying from glutamine auxotrophs to those that can survive in absence of exogenous glutamine supply[101]. Pieces of evidence suggest that genetics, tissue origin, and microenvironment dictate the glutamine usage in cancer[102].

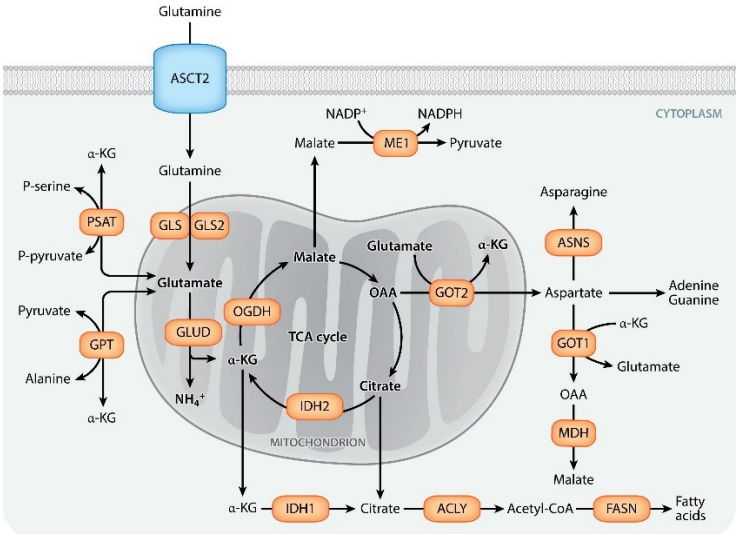

Figure 8: Glutamine metabolic pathways [103].

Several cancer cells can obtain glutamine from the environment; the uptake is mediated by different transporters, which can also be implied in the efflux of glutamine in exchange for other amino acids. These transporters are upregulated in many cancers and under various oncogenic drivers[104,105]. The master transcriptional regulator of metabolism c-Myc has been shown to increase sodium-dependent neutral amino acid transporter type 2 (ASCT2) expression by directly binding the promoter, leading to increase in glutamine uptake and catabolic usage in several cancer types including prostate cancer[106]. Furthermore, overexpression of *c-Myc* transcriptionally repress miR-23a and miR-23b promoting mitochondrial glutamine synthetase (GLS) expression[106]. Moreover, c-MYC also directly targets genes involved in deoxyribonucleotides triphosphate metabolism to enhance glutaminolysis driving nitrogens to nucleotides synthesis[107].

From of studies available so far, it appears that glutamine dependency of cancer cells may be a metabolic vulnerability of cancer and that inhibitors of enzymes involved in glutamine metabolism or therapeutics that inhibit the transcriptional properties of *c-MYC* may be exploited for cancer therapy. Asparaginase, is a chemotherapeutic enzyme indicated for patients with acute lymphoblastic leukemia, which presents dual asparaginase and glutaminase activities and is approved by the FDA[108]. However, while many other drugs have been synthesized to target different stages of glutamine metabolism (from the uptake to its conversion), most are still in preclinical stages[109].

1.4.3 **Mitochondria involvement in cancer cell metabolism**

Mitochondria play a central role in bioenergetics and metabolism since they harbor enzymes responsible for TCA cycle, oxidative phosphorylation (OXPHOS), β-oxidation (FAO), biosynthesis of lipids, nucleotides and amino acids and maintenance of reducing equivalents and homeostatic levels of Ca^{2+} (Figure 9). Thus, mitochondria are capable of rapidly sensing stress signals, coordinating biochemical pathways necessary to permit cells survival in environmental changing conditions[110].

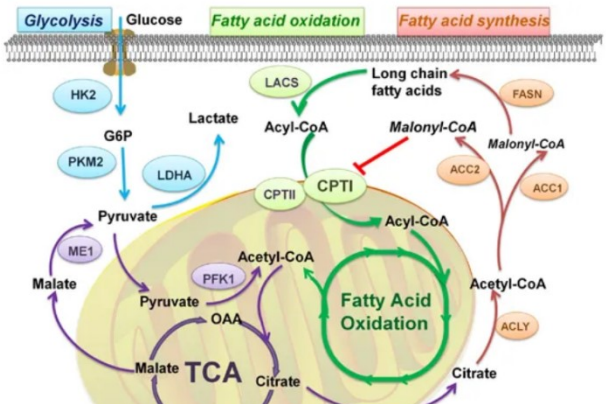

Figure 9: Mitochondria involvement in energetic metabolic pathways[97]:

Despite the initial Warburg's proposal that that mitochondrial dysfunction causes the necessity of cancer cells to rely on glycolysis for ATP production, nowadays it is known that tumor cells mitochondria not only retain their functionality but are also able to adjust the metabolic asset of cells.

In many tumor cells types, OXPHOS activity is downregulated therefore the ATP production is mainly dependent on glycolysis. Enhanced use of glucose also increases the metabolic flux through the Pentose Phosphate Pathway (PPP) which provides building blocks for nucleotides synthesis and NADPH for redox cell homeostasis[80]. These changes limit pyruvate, NAD^+, and FAD availability thus mitochondria must activate anaplerotic mechanisms to feed the TCA cycle; this is mainly done by increasing glutamine utilization[107]. Also, Fatty Acid Oxidation (FAO) might provide some of the metabolic plasticity needed by tumors by enabling the production of ATP and NADPH when required, by providing metabolic intermediates for cell growth, eliminating potentially toxic lipids and inhibiting pro-apoptotic pathways[111]. In addition to their central role in various biochemical pathways, mitochondria are key regulators of apoptosis, and they participate in developmental processes and ageing[112].

Mitochondria are extremely dynamic organelles which balance is maintained through fusion and fission processes. In the last years, pieces of evidence underlined how the mitochondrial dynamic contributes to the metabolic rewiring of cells, influencing neoplastic transformation, cancer metastasis or resistance to chemotherapeutic drugs[113]. Even if the role of imbalanced mitochondrial dynamic in several types of cancer is established and well documented in multiple works, the results remain still controversial.

1.4.4 **Lipid metabolism**

Commonly disregarded in the past, alteration in lipid- and cholesterol- associated pathways are now well recognized and largely described in tumors[84,114].Studies now reveal that abnormalities in lipid metabolism promote cancer development, invasion and metastasis via multiple signaling pathways (Figure 10) which suggests that targeting lipid metabolism might be a novel strategy for cancer prevention and treatment[115]. Highly proliferative cancer cells show a strong lipid and cholesterol activity which is satisfy by either overactivation of endogenous synthesis or by increasing the uptake of exogenous lipids. The excess of lipids in cells are stored in lipid droplets (LDs) and high level of LDs is considered a marker of cancer aggressiveness[116,117] and resistance to chemotherapy[118].

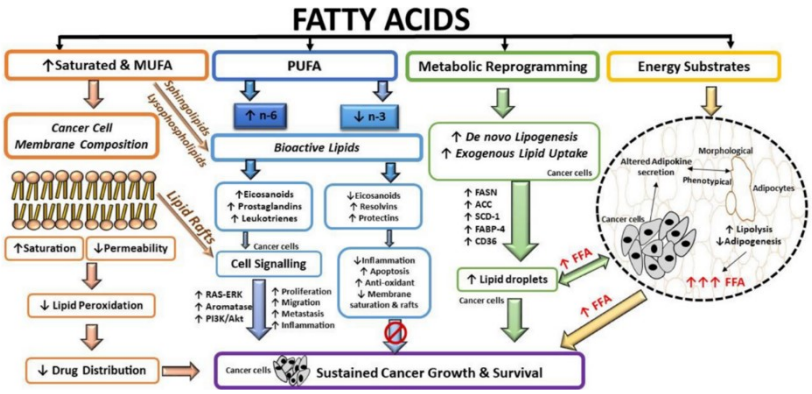

Figure 10: Role of fatty acids in cancer growth and survival. The role of lipids in progression and anticancer treatment is complex: they solve a role in membrane composition, energy source, source of bioactive lipids [119]

1.4.4.1 Lipid uptake

Fatty acids and lipids play a variety of functions in mammalian homeostasis but, largely due to their hydrophobic properties, they can also exert harmful effects and may cause cellular injuries. Thus, their transport into tissues need to be carefully controlled and in the last years, the knowledge about the regulation of fatty acid uptake has largely increased[120]. The uptake has long been considered to occur by passive diffusion, however, from a physiological perspective, the fine regulation of the uptake is necessary to satisfy the metabolic needs avoiding possible detrimental effects of excessive fatty acid accumulation. Various membrane proteins have been associated with fatty acid uptake

including fatty acid translocase (FAT)/CD36, plasma membrane fatty acid-binding proteins (FABPpm), long-chain fatty acyl-coenzyme A synthetase (ACSL), and fatty acid transport proteins (FATPs)[121].

The most characterized protein involved in fatty acid uptake is cluster differentiation 36/fatty acid translocase (CD36/FAT). CD36 overexpression has been observed in various tumors (ovarian cancer, gastric cancer, glioblastoma, and oral squamous cell carcinoma)[122] and has been proposed to induce tumor progression and chemotherapy resistance in several human cancers[123]. Another class of proteins, the FATP family, also known as solute carrier family 27 which contains 6 members, has been shown to be involved in fatty acid transport. The precise mechanism by which FATPs function in lipids uptake is still unclear. It has been proposed that FATPs can directly transport fatty acids, can work as enzymes that activate lipids through inherent acyl-CoA synthetase (ACS) activity, or can act as bifunctional proteins with independent transport and enzymatic activity. Studies regarding the subcellular localization of FATPs, underline their membrane and cytosolic localization, supporting their role in both uptake as well as activation[121,124].

The fatty acid binding proteins (FABPs) are members of intracellular lipid-binding proteins family involved in the reversible binding of hydrophobic ligands and traffic them to different intracellular compartments including mitochondria, endoplasmic reticulum, lipid droplets, peroxisome, etc. FABPs are ubiquitously expressed throughout tissues that are highly active in FA metabolism and comprise several isoforms.[125] FABPs are expressed in most malignancies such as prostate, breast, liver, bladder and lung cancer which are associated with the incidence, proliferation, metastasis, invasion of tumors[126].

1.4.4.2 Lipogenesis

Lipogenesis or *de novo* fatty acid synthesis is a metabolic pathway that synthesizes fatty acids from carbohydrates (Figure 11). The first step of this series of reactions is the conversion of citrate to acetyl-CoA by ATP-citrate lyase (ACLY). Acetyl-CoA is then carboxylated to malonyl-CoA by acetyl-CoA carboxylase (ACACA); the conversion of malonyl-CoA to palmitate is mediate by fatty acid synthase (FASN) which is the rate-limiting step of the process. Moreover, Glycerol-3-phosphate acyltransferase (GPAT) initiates the pathway of TAG synthesis by esterifying a long-chain fatty acyl-CoA to a

glycerol-3-phosphate backbone to form lysophosphatidic acid. Four isoforms have been identified with different subcellular localization: GPAT1-2 at mitochondrial level while GPTA3-4 at endoplasmic reticulum level[127].

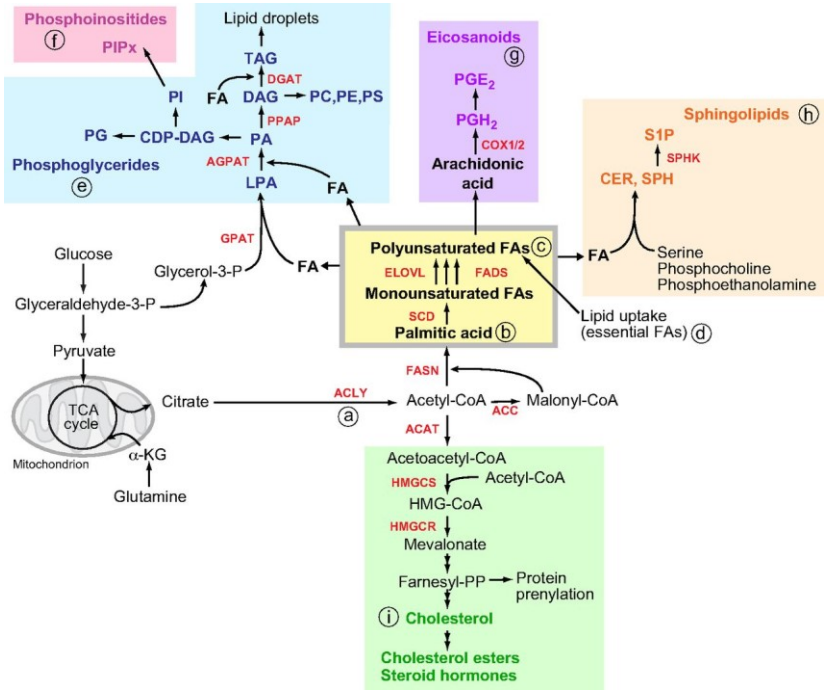

Figure 11: Schematic overview of the pathways involved in lipid biosynthesis[84]

The up-regulated FA synthesis has been observed in several tumor cells which present a significant increase in expression and activity of various enzymes involved in lipogenesis pathway[128].

Initially, the lipogenic phenotype of cancer cells have been linked to an increased expression and activity of the fatty acid synthetase (FAS), which is responsible for the terminal catalytic step in fatty acid synthesis[129,130]. Tumors with an overexpression of FASN exhibit a more aggressive phenotype and this overexpression is correlated with poor prognosis in breast cancer patients[131]. Besides FASN other enzymatic mechanisms are involved. A markedly increased ACLY expression and activity has been reported in cancer cells, and its inhibition suppresses the proliferation of certain types of cancer cells[132]. Similarly, acetyl-CoA carboxylase (ACC), the rate limiting enzyme for the long FAS synthesis, has been shown to be overexpressed not only in advanced breast

carcinomas but also in preneoplastic lesions associated with increased risk for the development of infiltrating breast cancer[133].

1.4.4.3 Lipid storage - lipid droplets

Lipid droplets are dynamic organelles that play a pivotal role in the management of lipid uptake, distribution, and consumption. Lipid droplets (LDs) are intracellular deposit of neutral lipids, mostly triacylglycerol (TAG) and sterol esters, surrounded by a layer of phospholipids and numerous peripheral and embedded proteins. The LDs are formed *de novo* following the synthesis of TAGs and sterol esters between the two leaflets of the ER membrane[134]. Lipid droplets are synthesized in response to lipid overload, to dampen the potentially toxic effect of excessive lipids, but their biogenesis is also induced in various type of stress (nutrient or oxygen deprivation, treatment with pro-oxidants, chemotherapeutic agents, inducer of ER stress)[117]. This suggests that LDs synthesis is regulated by imbalance in energy metabolism and redox homeostasis of cells and that they can contribute to cancer cell survival and growth. Originally considered as inert fat depots for energy storage, LDs are now considered to play a pivotal role in cellular homeostasis during challenging conditions.

Firstly, LDs provide not only FAs for energy production but are also involved in the maintenance of the redox homeostasis. In fact, in conditions of increased FA uptake or production, they concur to protect cells from reactive oxygen species (ROS) by supporting NADPH synthesis[135].

Lipid droplets are the main anti-lipotoxic organelles that control FA, DAG, and CE lipotoxicity by sequestering these potential toxic lipids into inert lipid forms. This protective effect is exerted not only to protect cells from exogenous lipid overload but also from endogenous lipids accumulated within the cells during high autophagic flux[117].

Another function performed by LDs is the regulation of fatty acid trafficking within the cells. Their dynamic interaction with mitochondria allows an efficient channeling of FA to these organelles maximizing the FA oxidation during nutrient stravation[136].

Besides, LDs turnover is closely related to autophagy. Autophagy can lead to LDs formation by providing lipids recycled form organelles, but it can also promote LDs breakdown through lipophagy process. Moreover, LDs have been shown to provide lipids for the autophagosome-membrane formation or stimulation of signaling processes for autophagy[137]. In the end, FAs and other lipids derived from LDs breakdown act as signaling molecules by themselves or by interaction with transcriptional factors[138] (Figure 12).

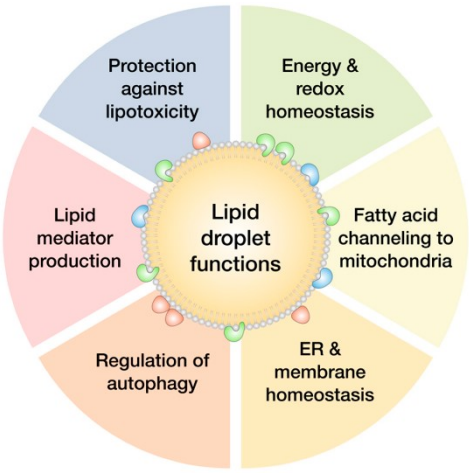

Figure 12: Lipid droplet functions in conditions of stress[103].

LDs accumulation has been observed in several human cancers including ovarian, breast, prostate, lung, liver, colon, brain, etc. and a high lipid accumulation has been considered a marker of cancer aggressiveness. Emerging evidence suggested that changes in lipid droplets metabolism are an important hallmark of cancer metabolic reprogramming.

1.4.4.4 Lipolysis and Lipophagy

Both lipid uptake and *de novo* lipogenesis can be enhanced in cancer cells, thus complementary lipid degradation mechanisms are required to furnish intermediates for energy generation, biosynthesis of membranes, and synthesis of other biomolecules.

Breakdown of the lipid droplets can occur by two distinct pathways: Lipolysis and Lipophagy.

Lipolysis is the catabolic process of the FA cycle that provides FAs in conditions of metabolic need and removes them when they are in excess. The hydrolysis of TGs to FAs and glycerol requires three subsequent steps catalyzed by three different lipases: adipose triglyceride lipase (ATGL) catalyzes the rate-limiting first step, converting TAG into diacylglycerol (DAG) and a free FA. The Hormone-sensitive lipase (HSL) converts DAGs in monoacylglycerol (MAG) and free FA, and finally, the monoglyceride lipase (MGL) converts MAG into glycerol and a third free FA. The three FAs released can be re-esterified in new TAG or can be shuttled to mitochondria for generation of energy via fatty acid oxidation or they can be used for anabolic processes[139]. In response to lipolytic

stimuli, ATGL is recruited to LDs to facilitate the initial step of TAG catabolism and this pathway was thought to be the primary mechanism through which TAG in LDs were degraded[140]. Recent evidence suggests deregulation of ATGL in different cancer types even if the specific role and effect are still controversial. Most *in vitro* studies have proposed pro-neoplastic activity of ATGL[141]; in fact, depletion of ATGL has been shown to reduce proliferation in non-small-cell lung carcinoma cell lines and colorectal cancers while upregulation contributes to aggressiveness of breast cancer[142] and pancreatic ductal adenocarcinoma[143]. Conversely, numerous *in vivo* studies in ATGL knockout mice have proposed a tumor-suppressive role of ATGL[144,145].

In addition to the action of cytoplasmatic lipases, the fairly recent discovered autophagic degradation of lipids or lipophagy can be used to mobilize LDs during fasting periods[146,147]. Lipophagy is, in fact, the pathway involved in the specific turnover of LDs which is mediated by the autophagic machinery delivering LDs or parts of lipid droplets to the lysosome for degradation by lysosomal acid lipases (LALs) deposit in the autolysosomes[148]. The breakdown of LDs by lipophagy degrades all storage and structural LDs associated lipid or proteins, thereby releasing FAs, cholesterol, amino acids, etc.

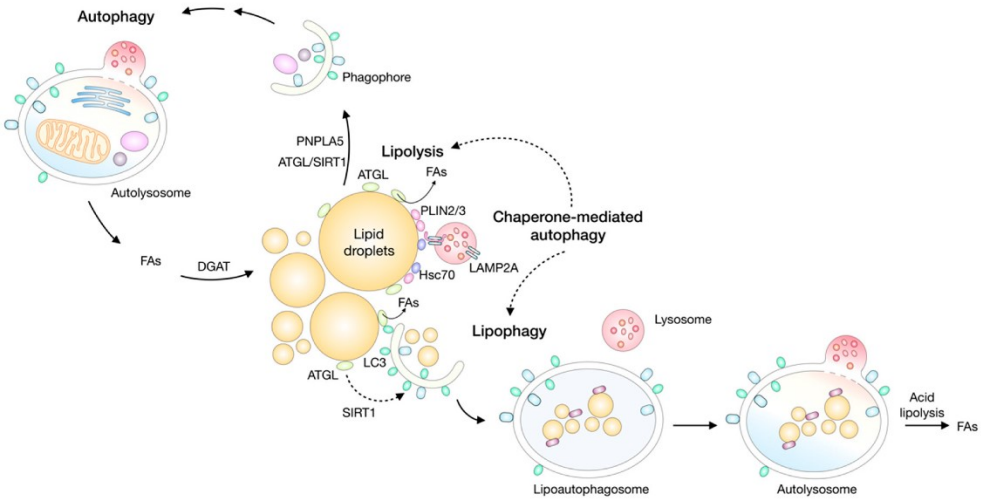

Figure 13: Crosstalk between Lipid droplets and autophagy [117].

The role of lipophagy in cancer is controversial and under investigation: several reports indicate lipophagy as a tumor-promoting event[149] while most of the studies suggest a suppressive role of lipophagy in tumorigenesis[150]. So, it is possible that the role of lipophagy will be determined by the metabolic and oncogenic dysregulation of cancer cells and their stress status (Figure 13).

1.4.4.5 B-oxidation

Another process by which fatty acids molecules are broken down in the β- oxidation, in mitochondria (Figure 14). This process leads to the generation of Acetyl-CoA which enters the TCA cycle, and NADH and $FADH_2$ used as cofactors in electron transport chain. The mitochondrial inner membrane is impermeable to long-chain acyl-CoAs, thus the carnitine palmitoyltransferase (CPT) system is required. This enzymatic complex is made up of two distinct proteins: carnitine palmitoyltransferase 1 (CPT1) at the outer mitochondrial membrane and Carnitine palmitoyltransferase II (CPT2) at the inner mitochondrial membrane.

Several studied have demonstrated that alteration in CPT expression are related to cancer progression and metastasis. Knockdown of CPT1A leads to down-regulation of mTOR signaling and increases of apoptosis promoting prostate cancer cells growth[151]. it is also reported that CPT1 is related to enhance tumorigenesis in breast cancer[152] and leukemic cells[153]. Moreover, CPT1 has also been linked to many other cellular signaling pathways often altered in cancer (such as FAS, aerobic glycolysis, mTOR and STAT3 signaling etc.), indicating a possible role in cancer pathogenesis and resistance to treatments[154].

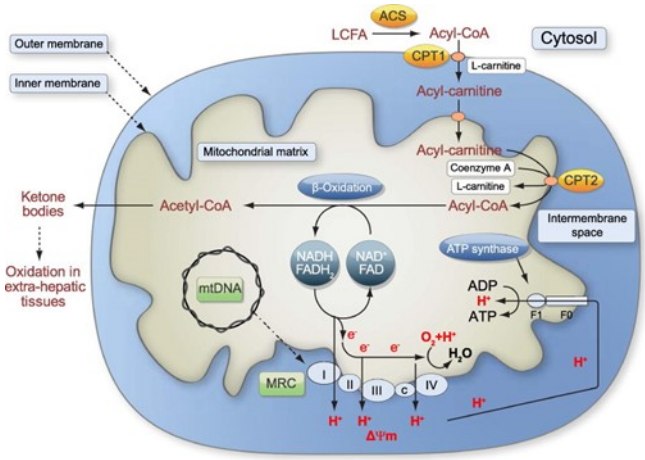

Figure 14: Schematic representation of mitochondrial fatty acid β-oxidation and oxidative phosphorylation in mitochondria[155].

2 AIM

Cancer metabolism has emerged as an important area of research in recent years. Recently, metabolic rewiring has been shown to play a prominent role in the response of cancer cells to first-line chemotherapeutic agents, suggesting that the metabolic pathways are indisputable mediators of resistance to cancer treatments.

The focus of this work is to gain insights into the compensatory mechanism and/or relevant processes that turn energetic metabolism specifically in cisplatin-resistant cancer.

Previous studies of our laboratory had already demonstrated a metabolic switch of cisplatin-resistant cells toward glycolysis and to an altered mitochondrial functionality and morphology[156,157]. So, in order to better characterize the metabolic fingerprint of cisplatin-resistant cells, in this work, the lipid metabolism has been investigated and the study on the implication of glutamine was started. Two different models of cisplatin resistance have been investigated: a model of acquired cisplatin-resistance using ovarian carcinoma cells (2008-C13) and cervix squamous cancer cells (A431-A431pt), and a model of intrinsic resistance to cisplatin using several lines of Triple Negative Breast cancer cells (TNBC: MDA-MB-468, HCC1143, and HCC1937). The investigations regarding TNBC cells have been performed in Professor Toker's laboratory (Department of Pathology at the Beth Israel Deaconess Medical Center, Harvard Medical School, Boston, USA).

From this study and previous observations of our Lab, different possible metabolic targets have been identified, allowing the development of the second part of this work. In fact, the second aim has been the use of pharmacological approaches able to target the identified alterations in lipid metabolism and mitochondria remodeling.

The results obtained in this work might lead to the identification of novel prognostic and predictive biomarkers for chemosensitization, and possibly open up new possibilities of therapeutic strategies for tumors resistant to cisplatin.

3 MATERIALS AND METHODS

CDDP for in vitro experiments was purchased from Teva, PIK-III (#S7683) and SAR405 (#S7682) were purchased from Selleckchem.

3.1 Cell lines

3.1.1 *In vitro* model of acquired cisplatin resistance

Human ovarian carcinoma (2008 wild type and C13 cisplatin-resistant cells) and human vulvar epidermoid carcinoma (A431 wild type and A431Pt cisplatin-resistant cells) cell lines were used for this study. The CDDP-resistant variant (C13, A431Pt) were selected by exposure to increasing CDDP concentrations for a period of 9 months.

All cell lines were grown in Roswell Park Memorial Institute medium (RPMI 1640 LOBE12167F) supplemented with 10% fetal bovine serum (FBS), 4 mM glutamine, 100 U/ml penicillin and 100 µg/ml streptomycin and the cells were grown in humidified condition at 5% CO_2 and 37°C. For all the glutamine deprivation experiments dialyzed FBS was used.

All reagents for cell culture were from Cambrex-Lonza (*Basel, Switzerland*) and FBS from Gibco, Invitrogen (*Carlsbad, CA, USA*).

3.1.2 *In vitro* model of innate cisplatin resistance

(Experiments were mainly performed in Toker's Laboratory, BIDMC, Harvard Medical School, Boston)

Human Triple Negative Breast cancer, basal like cells MDA-MB-468, HCC1143, and HCC1937 were obtained from the American Type Culture Collection (ATCC) and authenticated using short tandem repeat (STR) profiling. All cell lines were maintained in RPMI 1640 (*CellGro*) supplemented with 10% FBS (*Gemini*), 2 mM glutamine, in humidified condition at 5% CO_2 and 37° C. Cells were passaged for no more than 6 months and routinely assayed for mycoplasma contamination.

For all the glutamine deprivation experiments dialyzed FBS was used.

3.2 Maldi-TOF Mass Spectrometry

The lipid fingerprint of human cancer cell lines was delineated by MALDI-TOF spectrometry. The complete lipid pool was analyzed in total extracts.

$1x10^6$ cells were plated in 100 mm cell culture dishes and allowed to attach overnight. After 48 hours, cells were washed and gently scraped with PBS. $5x10^6$ were collected and centrifuged at 1400 rpm. The pellet was therefore resuspended in 1 mL of PBS and the protein content was determined by Lowry procedure (*Bio-rad DC Protein Assay, MA, USA*). The lipidomic Maldi-TOF Mass Spectrometry analysis was performed by Professor Agostini (Fondazione Città della Speranza, Padova).

3.3 Confocal microscopy

Lipid droplet content

Cells were plated on glass coverslips in 12-well plates and, following overnight incubation, were exposed to different treatments according to experimental protocols. After 24 hours, cells were stained with 50 nM Mitotracker Orange (*Invitrogen*), fixed with 4% formaldehyde, washed with PBS and labelled with Bodipy 493/503 (*Molecular Probes Invitrogen, Paisley, UK*). After washing, 4′,6-Diamidino-2-phenylindole (DAPI) was used to stain the nucleus, and then the coverslips were mounted on glass slides by using Mowiol 40–88 (*Sigma, St Louis, MO*). Images were acquired by confocal microscope Zeiss LSM 800 e analyzed with ZEN 2.0 imaging software. Lipid droplet area and number were quantified using ImageJ software.

3.4 Cell viability assays

3.4.1 Trypan blue exclusion assay

Cells were plated on 12-well plates and, following overnight incubation, were exposed to different treatments according to the experimental protocol. After treatment, cells were washed, detached with 0.25% trypsin-0.2% EDTA and suspended in trypan blue (*Sigma-Aldrich, St Louis, MO, USA*) at 1:1 ratio in medium solution[158]. Cells were counted using a chamber Burker hemocytometer.

3.4.2 **Sulforhodamine B (SRB) test**

Cells were plated on 96-well plates and, following overnight incubation, were exposed to different treatments according to experimental protocol. After treatments cells were fixed with trichloroacetic acid (*Sigma-Aldrich, St Louis, MO, USA*) and stained with SRB (*Sigma-Aldrich, St Louis, MO, USA*), which stoichiometrically binds proteins. The bound SRB was therefore dissolved by adding 10 mM TRIS and the absorbance was measured at 570 nm using a Victor3X multilabel plate counter (*Wallac Instruments, Turku, Finland*).

3.4.3 **Crystal Violet test**

Cells were plated on 96-well plates and, following overnight incubation, were exposed to different treatments according to experimental protocol. After treatments cells were fixed with 4% p-formaldehyde (*Sigma-Aldrich, St Louis, MO, USA*) and stained with Crystal violet dye (*Sigma-Aldrich, St Louis, MO, USA*), which binds to proteins and DNA, for 20 minutes. The bound Crystal Violet was therefore dissolved by adding acetic acid 1%, and the absorbance was measured at 570nm using a Victor3X multilabel plate counter (*Wallac Instruments, Turku, Finland*).

3.4.4 **Propidium Iodide Assay**

Cell viability was assayed with a propidium iodide-based plate reader assay, as previously described[159]. Cells were seeded in 96-well plates and exposed to different treatments, according to experimental protocol. Then cells were treated with a final concentration of 30 μM propidium iodide for 20 min at 37°C. The initial fluorescence intensity was measured in a SpectraMax M5 (Molecular Devices) at 530nm excitation/620nm emission. Digitonin was then added to each well at a final concentration of 600 μM. After incubating for 20 min at 37°C, the final fluorescence intensity was measured. The fraction of dead cells was calculated by dividing the background-corrected initial fluorescence intensity by the final fluorescence intensity. Viability was calculated by this formula: 1-fraction of dead cells.

3.5 Immunoblot assay

Cells were plated in 100 mm cell culture dishes and allowed to attach overnight. After 48 hours, cells were washed and lysed with ice-cold lysis buffer [TRIS 25 mM pH 7,4; NaCl 150 mM; IGEPAL 1%; sodium deoxycholate 1%; SDS 0,1%; EDTA 1 mM] supplemented with the protease inhibitor cocktails (*Roche Molecular Biochemicals, Mannheim, Germany*). Cell lysates were then centrifuged at 14000 rpm for 15 minutes at 4°C and the supernatant protein content was determined by Lowry procedure (*Bio-rad DC Protein Assay, MA, USA*). Equal amounts of protein were loaded on a 10% polyacrylamide gel and electrophoretically separated in running buffer. After electrophoresis, the proteins were blotted onto a Hybond-P PVDF membrane (*Amersham Biosciences, Buckinghamshire, UK*) and non-specific binding sites were blocked with a 10% skim milk solution. The membrane was therefore exposed to the elected primary antibody: anti-CD36 (1:1000, Rabbit, 18836-1-AP, *Protein Tech*.), anti e-FABP (1:200, Mouse, sc-365236, *Santa Cruz Biotech*), anti-FATP2 (1:500, Mouse, sc-393906, *Santa Cruz Biotech*), anti-LDL receptor (1:100, Mouse, *Santa Cruz Biotech*.), anti-Caveolin1 (1:1000, Rabbit, *Abcam*) anti-BNIP3 (1:1000, Rabbit, ab109362, *AbCam*) and, following overnight incubation, was washed and exposed to the HRP-conjugated anti-mouse (1:10000, *Dako)* or anti-rabbit secondary antibody (1:3500; *PerkinElmer, MA, USA*). The signal was visualized with enhanced chemoluminescent kit (*Amersham Biosciences*) according to the manufacturer's instructions and analyzed by Molecular Imager VersaDoc MP 4000 (*Bio-Rad, Hercules, CA, USA*). The integrated intensity was normalized to antibodies: Tom20 (1:2000; Rabbit, sc-11415, *Santa Cruz Biotech*), beta-actin (1:5000; Mouse, ab6276, *AbCam*).

3.6 Quantitative Real-Time PCR

Total mRNA was extracted as per manufacturer's instructions using a Direct-zol™ RNA MiniPrep kit (*Zymo Research, Irvine, CA, USA*) and measured with a NanoDrop 2000 (*Thermo Fischer Scientific Inc., Waltham, MA, USA*). The relative expression of each gene was determined by quantitative real-time PCR (*Eco™ Illumina, Real-Time PCR system, San Diego, CA, USA*) using One Step SYBR PrimeScript RT-PCR Kit (*Takara Bio, Inc., Otsu, Shiga, Japan*) and the primers designed as in Table 1.

GENE	FORWARD SEQUENCE	REVERSE SEQUENCE
ACLY	5'-CCAGATGGCAAGATCCTCAT-3'	5'-GACTTCTCCCATCACCCGTA-3'
CD36	5'-AGATGCAGCCTCATTTCCAC -3'	5'-GCCTTGGATGGAAGAACAAA -3'
GPAT1	5'-GCCGCTTCTGTTTCTACCAG -3'	5'- CCTTCCGTCCATCTGGTGTT-3'
GPAT3	5'-GCCAGAGGCAGAACCTACAG-3'	5'-GTTTGGGCATTTTTGGAGAA -3'
GPAT4	5'-TCTGGGGTTTCACCAGTTTC -3'	5'- TGCAAAGTGGATCTGTCTGC-3'
FASN	5'-GGTCTTGAGAGATGGCTTGC-3'	5'-AATTGGCAAAGCCGTAGTTG-3'
FABP5	5'-AGGAGTGGGAATAGCTTTGCG -3'	5'-GCTGAACCAATGCACCATCT -3'
BNIP3	5'-GAATTTCTGAAAGTTTTCCTTCCA-3'	5'- TTGTCAGACGCCTTCCAATA -3'
FABP3	5'- GCATCACTATGGTGGACGCT-3'	5'- GTGGTAGGCTTGGTCATGCT-3'
TOM20	5'-GGGGCAGTTAGAGGGAGAAC-3'	5'-CCAGCTCATACTGCACTCCA -3'
G6PDH:	5'-AAGAGACCGTGGATGCTGAA-3'	5'-CCTGCTCACTGTAAGACTGG-3'
βACTIN	5'-CCAACCGCGAGAAGATGA-3'	5'-CCAGAGGCGTACAGGGATAG-3'
18R	5'-CGGCGACGCCCCATTCGAAC-3'	5'-GAATCGAACCCTGATTCCCCGTC-3'

Table 1: Sequences of genes primers

Melt-curve analysis was used to confirm the specificity of amplification and absence of primer dimers. All genes were normalized to β-Actin, TOM20 or 18R.

Expression levels of the indicated genes were calculated by the ΔΔCt method using respectively the dedicated StepOne software or Eco™ Software v4.0.7.0.

3.7 Flow cytometry

3.7.1 Fatty Acids uptake

Cells were seeded in 6-well plates and allowed to attach overnight and treated as experimental protocol. For cell starvation culture media were substituted with HBSS for the defined time. After washing, a Bodipy FL C_{16} solution (500nM in HBSS) was added for 5 and 15 minutes. Cells were then washed with PBS and collected with Trypsin-EDTA. After centrifugation for the elimination of the supernatant, cell pellets were fixed for 15 minutes at room temperature with 4% p-formaldehyde solution. p-formaldehyde was removed by centrifugation and pellets were resuspended in 300 µl PBS. Fluorescence intensity was analyzed using an Epics XL flow cytometer (*Coulter Systems, Fullerton, CA, USA*) equipped with a 488 Argon laser. The emission of Bodipy was measured at 528 nm.

3.7.2 **Cell Cycle Analysis**

Cells were plated in 6 wells-plates, allowed to attach overnight and treated according to the protocol. Cells were washed with PBS and collected with Trypsin-EDTA. After centrifugation for the elimination of the supernatant, cell pellets were fixed for 20 minutes at 4°C with 70% EtOH. EtOH was removed by centrifugation and cells were incubated for 20 minutes at room temperature with 300 µl PBS+RNAsi+Propidium Iodide. Fluorescence intensity was analyzed using an Epics XL flow cytometer (*Coulter Systems, Fullerton, CA, USA*) equipped with a 488 Argon laser. The emission of propidium was measured at 580 nm.

3.8 Lipases activity

Cells were seeded in 100mm dishes and allowed to attach overnight. Cells were then treated as experimental protocol. Starvation has been induced by treatment with HBSS buffer for 4 hours.

Cells were washed with PBS and gently scraped with PBS. $1x10^6$ cells were collected and centrifuged at 1400 rpm. The cell pellets were sonicated in 0,5 ml of cold PBS (*Bandelin electronic, Berlin, EU*) and centrifugated at 10000 rpm for 15 minutes at 4°C.

The enzymatic activity of lipases was evaluated on the supernatant by Cayman's Lipase Activity Assay Kit (*Cayman Chemical Company, MI, USA*) according to the manufacturer instruction. The fluorescence intensity (λex: 390 nm, λem:520 nm) was measure with VICTOR™X3 2030 (*Multilabel Reader, Perkin Elmer*) at 37°C. Lipase activity was evaluated by the following formula: [RFU/ml / Slope form standard curve (RFU/µM)] * sample dilution. Enzymatic activity has been normalized on the protein content obtained by Lowry procedure.

3.9 Liquid chromatography-mass spectroscopy (LC-MS)

Cells were plated in 6-well plates and after 48 hours quickly washed with ice-cold PBS on an ice bath. Cells were lysed with a dry ice/methanol solution (−80°C) of 50% methanol/30% acetonitrile in water and quickly scraped. The extracts were mixed at 4°C for 15 minutes and pelleted in a cooled centrifuge (4°C). The supernatant was evaporated

using a refrigerated SpeedVac. Samples were resuspended using 20-µl HPLC grade water for MS and submitted for LC-MS analysis. The amount of extraction solution was calculated according to the number of cells present in the sample dish, extrapolated using a "counter dish" cultured in the same conditions of the sample dishes and proteins were quantified using the Bio-Rad DC protein assay.

Intermediates were separated using a liquid chromatography system. Data acquisition was controlled with Xcalibur 2.0 (*ThermoElectron Co, San Jose, CA, USA*). The mass accuracy was maintained below 1 ppm due to the use of a lock mass. The raw chromatograms were then aligned using the software SIEVE™ (*ThermoElectron*). The integration of the measured ion current over a metabolite's elution time and m/z interval is directly proportional to its absolute abundance in the solution. We manually removed from the SIEVE's output unspecific and misaligned peaks to eliminate the noise.

Isotope labeling

For labeling of cancer cells, cells were seeded ad allowed to attach overnight. Fresh unlabeled medium, with 100 µM glutamine, was added to the cells 2 hours before labeling. Labeled medium, with 100 µM of [U-$^{13}C_5$]-glutamine was then added to the cells, and cellular metabolites were extracted as described above at 24 or 4 hours.

3.10 BNIP3 silencing

Cells were plated in 12 well/plate and allowed to attach overnight. Transfection complex was prepared in FBS free-medium with esiRNA BNIP3 (*Mission esiRNA, Sigma)* and DharmaFECT transfection reagent (*Dharmacon-Ge Healthcare*), according to the manufacturers' instructions. The transfection mixture was dispensed at a concentration of 100nM/well for 48 hours.

3.11 Statistical analysis

All data were analyzed with GraphPad software and are expressed as mean ± SEM. Unpaired Students *t-tests* was used to analyze the results. Significance was considered at $p < 0.05$.

Multivariate analysis

A multivariate analysis has been performed to analyze the differences in the lipid fingerprint (Figure 16) and the metabolomic profile (Figure 48) of sensitive and resistant cells.

To identify the most significant differences between groups, univariate statistical analysis was used. Filtering procedures, such as fold-change analysis, *t-test* (for paired and unpaired data) and ANOVA were applied, as provided by MetaboAnalyst web-based software[160,161]. Significantly different data at the probability level of $p<0.05$ were used for further procedures of multivariate analysis, to obtain identification of relevant biomarkers. Tentatively, the entire data set was submitted to multivariate analysis by means of the procedures provided by MetaboAnalyst and meta-P server[162].

Principal Component Analysis (PCA). PCA is an unsupervised method to detect the directions which best explain the variance in a data set, transforming a number of possibly correlated variables into a smaller number of uncorrelated variables defined as principal components, which are linear combinations of the original variables. The first principal component explains as much of the variability in the data as possible, and each following component accounts for the remaining variability. The data are represented in a dimensional space of n variables, which are reduced into a few principal components; these are descriptive dimensions indicating the maximum variation 60 within the data. After the principal components scores have been obtained, they can be graphically plotted to observe any groupings in the data set. PCA computation was obtained with MetaboAnalyst based on R prcomp package, using singular value decomposition algorithm. The covariance matrix and standardized principal component score were selected. The scores of the first two principal components were graphically plotted to observe any groupings in the data set.

4 RESULTS

4.1 Cisplatin resistance

Cisplatin is known as one of the most effective chemotherapeutic agents used for the treatment of a wide variety of solid tumors; however, despite a consistent rate of initial responses, the treatment often results in onset of resistance leading to therapeutic failure[19].

In this project two different models of resistance, acquired and intrinsic, have been examined. Cisplatin sensitive and cisplatin-resistant ovarian cancer cells (2008-C13), and sensitive and resistant human cervix squamous carcinoma (A431-A431pt), have been characterized in order to define mechanisms of acquired resistance not yet fully understood. Moreover, in Toker's Laboratory (BIDMC, Harvard Medical School, Boston), the glutamine metabolic reprogramming in triple negative breast cancer cells that present an intrinsic resistance to cisplatin has been characterized.

The CDDP IC_{50} values for each cell line is reported in Table 2 which shows that wild type cells (2008 and A431) are more sensitive to cisplatin as compared to their resistant counterpart (C13 and A431pt).

	2008	**C13**	**A431**	**A431pt**
IC_{50}	1.376	10.44	7.019	20.88
CDDP (μM)	0.3854-4.910	1.555-70.16	2.789-17.76	13.29-32.81

Table 2: CDDP cytotoxic effect, expressed as IC_{50} of cisplatin-sensitive (2008, A431) and cisplatin-resistant cancer cells (C13, A431pt). Data are obtained from concentration-response curves after cisplatin treatment and represent 3-4 independent experiments.

Figure 15 shows that MDA-MB-468 present a higher sensitivity to cisplatin, while HCC1143 and HCC1937 are resistant to the treatment.

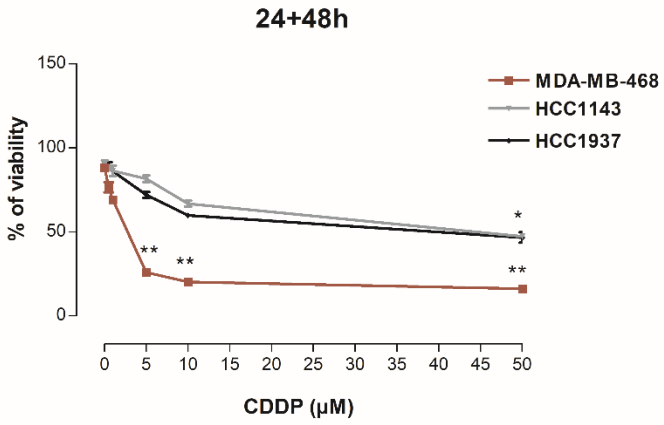

Figure 15: Effect of cisplatin (0.5-1-5-10-50µM) on MDA-MB-468, HCC1143, and HCC1937 cells viability after 24+48 hours of treatment, measured by Propidium Iodide Assay. Data are reported as % of vital cells related to control and are the mean of 3 experiment. *p<0.05; **p<0.01 treatment *vs* control.

The ability of certain cancers to shift their metabolism toward glycolysis even in the presence of adequate oxygen supply has been pioneered by Warburg[92]. Recently, besides several molecular alterations, a metabolic reprogramming involved in the faster growth, proliferation, and resistance of cancer cells to chemotherapeutic drugs have been demonstrated[14]. Herein, the metabolic profile of wild-type and cisplatin-resistant cancer cells has been investigated in different aspects. Specifically, the pathways involved in lipid metabolism, glutamine metabolism, and mitochondrial contribution to cells metabolism have been subjected to analysis.

4.1.1 Lipid profile in Sensitive (2008-A431) and Resistant (C13-A431pt) to cisplatin cancer cell lines

Besides the most known alteration in glycolytic pathway (Warburg effect), alterations in lipid and cholesterol associated pathways are now well recognized and largely describe in tumors[84,114]. Different studies have underlined that abnormalities in lipid metabolism promote cancer invasion and metastasis and are linked to more aggressive phenotypes also in response to chemotherapy[115]. Highly proliferative cancer cells show a strong lipid avidity which is satisfied by increasing the exogenous uptake or by over-activating the endogenous synthesis. The excess in lipid and cholesterol is stored in lipid droplets (LDs) and LDs content is now considered a hallmark of cancer aggressiveness[163].

^{1}H-NMR analysis of 2008 and C13 cells have revealed a significant higher content of mobile lipids (ML) in C13 resistant cells, in agreement with data reported for many cancer cells[156]. Thus, in order to deeply investigate this possible rewiring of resistant cells to a lipogenic phenotype, lipidomic analysis and evaluation of lipids content were performed.

4.1.1.1 Lipid fingerprint – MALDI-TOF spectrometry

The lipid profile of human cancer cell lines was delineated by MALDI-TOF spectrometry. The Multivariate analysis, Principal Component Analysis (PCA) was performed by Professor Ragazzi (University of Padova).

The PCA analysis reported in Figure 16 shows a clear separation in the lipid profile between sensitive and resistant cells (A) 2008-C13, B) A431-A431pt.

Data indicate that, in addition to an accumulation of lipids, the resistant cells also have a different lipid profile compared to the corresponding sensitive clones.

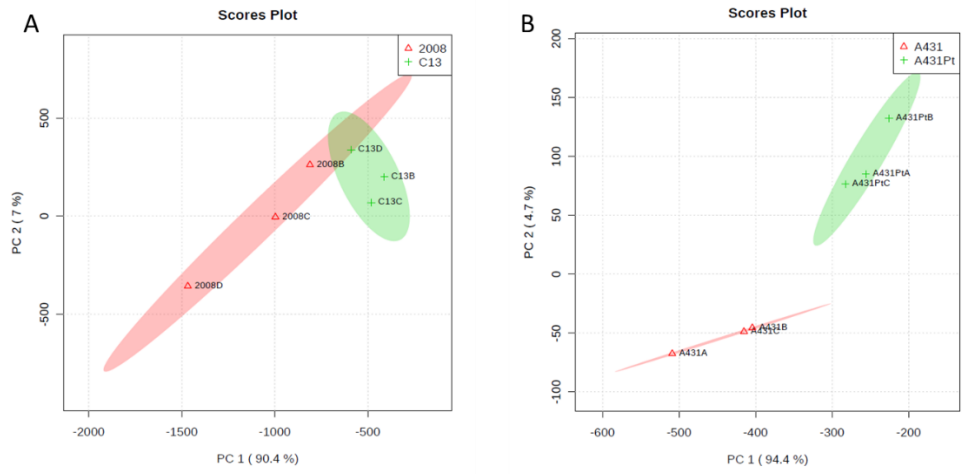

Figure 16: D scores plot between selected PCs. The PCA analysis is performed using the prcomp package.

4.1.1.2 Lipid droplets content

The intracellular lipid content was investigated by staining with Bodipy 493/503 neutral lipid dye, and the fluorescence was observed by confocal microscopy. Results in Figure 17 show a neutral lipid accumulation mainly in cytoplasmic droplets in all the cell lines, but more evident in resistant clones C13 and A431pt.

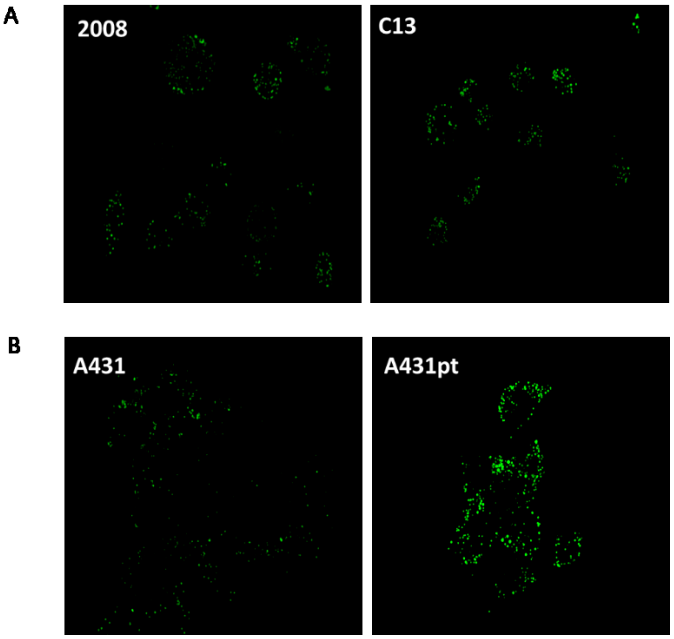

Figure 17: Bodipy 493/503 neutral lipid staining in 2008-C13 cells (A) and A431-A431pt cells (B). Images were acquired through confocal microscope LSM 800, software ZN 2.1 blue Edition. All images are representative of at least 4 different experiments.

The lipid droplets content was then analyzed using ImageJ software (1.45s free version), in order to obtain quantitative parameters. LDs' number per cell, dimensional distribution, and average diameters within the cell lines were obtained, and results are reported in Figure 18 and Figure 19.

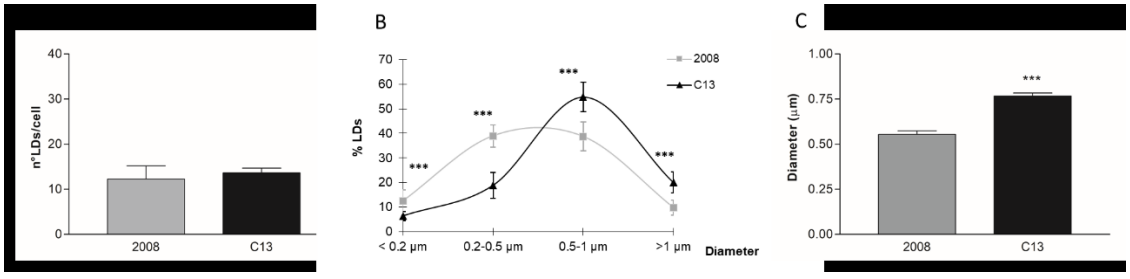

Figure 18: Quantitative parameters obtained by the analysis with ImageJ software (1.45s free version) of 2008-C13 cell's images acquired by confocal microscopy after Bodipy staining (at least 8 images/sample). Data are the mean±SEM of 3 different experiments; A) number of lipid droplets per cells; B) LDs dimensional distribution expressed as % of the total number; C) average of the diameters of lipid droplets. ***p<0.001 C13 *vs* 2008.

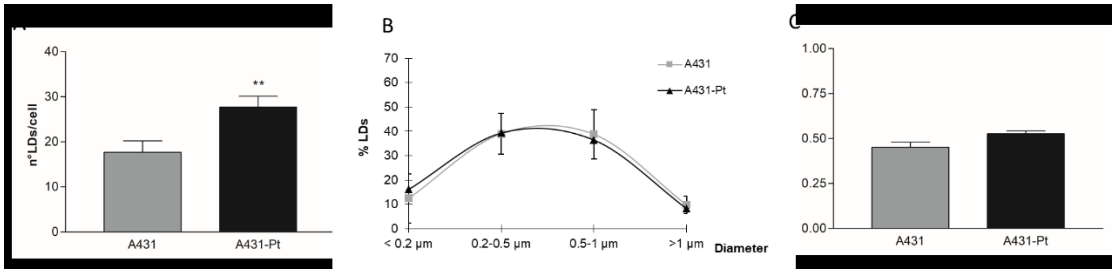

Figure 19: Quantitative parameters obtained by the analysis with ImageJ software (1.45s free version) of A431-A431pt cell's images acquired by confocal microscopy after Bodipy staining (at least 8 images/sample). Data are the mean±SEM of 3 different experiments; A) number of lipid droplets per cells; B) LDs dimensional distribution expressed as % of the total number; C) average of the diameters of lipid droplets. $^{**}p<0.01$ A431pt *vs* A431.

Results in Figure 18 show that there are no differences in the number of LDs per cell between 2008 and C13 cell lines (A), nevertheless the LDs' dimensional distribution (B) shows that C13 present lipid droplets of bigger dimension and the average of the diameter is significantly higher in resistant C13 clone. In Figure 19, results regarding A431-A431pt cell lines show that the dimension of LDs are the same between sensitive and resistant clones (B-C) but the resistant A431pt cells present a higher number of LDs per cell (A). So, results obtained show an increased accumulation of lipids in the resistant clones (C13 and A431pt) with respect to the sensitive counterparts (2008-A431).

Previous results have identified an accumulation of lipids in resistant clones. Thus, in order to understand the mechanisms that is mainly implicated in this store, the principal pathways involved in lipid metabolism have been analyzed.

4.1.1.3 Lipogenesis analysis

Lipogenesis or *de novo* fatty acid synthesis is a metabolic pathway that synthesizes fatty acids from carbohydrates. The up-regulated FA synthesis has been observed in several tumor cells which present a significant increase in expression and activity of various enzymes involved in lipogenesis pathway[128]. With the aim to understand if the observed lipid accumulation in resistant clones could be due to an increased *de novo* lipid synthesis, the mRNA levels of some key enzymes involved in this process (ACLY, FASN, GPAT1-3-4) have been analyzed by qRT-PCR.

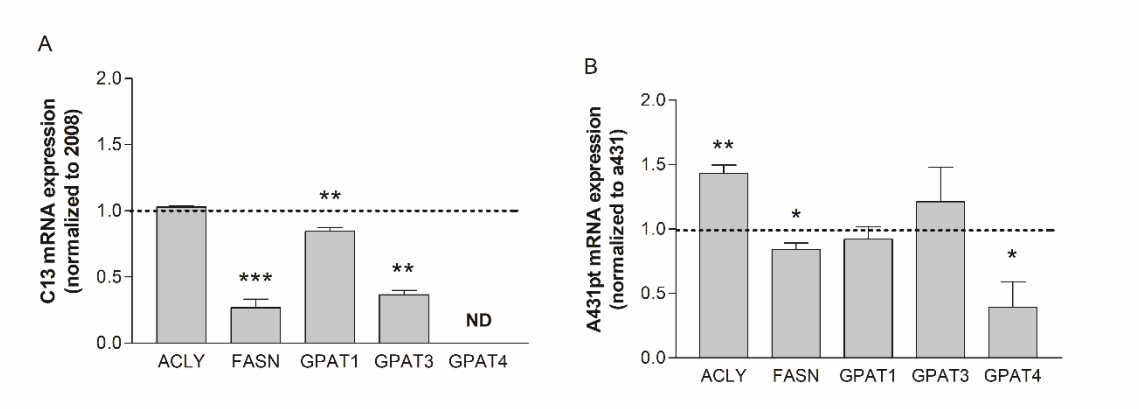

Figure 20: C13 (A) and A431pt (B) mRNA levels of ACLY, FASN, GPAT1, GPAT3, GPAT4 measured by qRT-PCR; Expression levels of the indicate genes were evaluated by the ΔΔCt method with β-actin as the reference gene. Data are the mean±SEM of 3-4 independent experiments and are normalized to the sensitive clones. **p*<0.05; ***p*<0.01; ****p*<0.001 resistant *vs* sensitive clone.

As reported in Figure 20 the levels of all the analyzed genes in resistant clones resulted to be decreased or equal to the sensitive counterpart. The only exception regards ACLY level, which is upregulated in A431pt with respect to A431 (this may suggest that A431pt cells can use Acetyl-CoA for cholesterol-esters synthesis, instead of using it for neutral fatty acid synthesis and storage in LDs). The absence of overexpression of genes coding for liponeogenesis-regulatory enzymes leads to excluding that the cause of the observed lipid accumulation may reside in a greater endogenous lipid synthesis by resistant cells.

4.1.1.4 Lipid uptake

Cytofluorimetric analysis

In order to examine if sensitive and resistant cells present differences in the uptake of exogenous free fatty acids, cells were treated with a Bodipy-labeled fluorescent fatty acid analog, Bodipy FL C_{16}, for 5 and 15 min and, after washing, intracellular fluorescence was measured by cytofluorimetric analysis (λec/em:488/525nm).

The uptake has been evaluated in basal conditions and in starvation induced by treatment with HBSS for 1 hour or with HBSS + 1% FBS for 16hours. Results in Figure 21A show that in basal condition and in short-term starvation there are no differences in the uptake between 2008 and C13 cell lines. The uptake of exogenous FFAs is increased in C13 resistant clones in long starvation (16h). A similar trend was also observed in A431pt cell line (Figure 21B); in basal condition, there are no differences between A431pt and A431 but in condition of starvation (both short and long period), the resistant clone presents a significant increase in the uptake, compared to the sensitive counterpart.

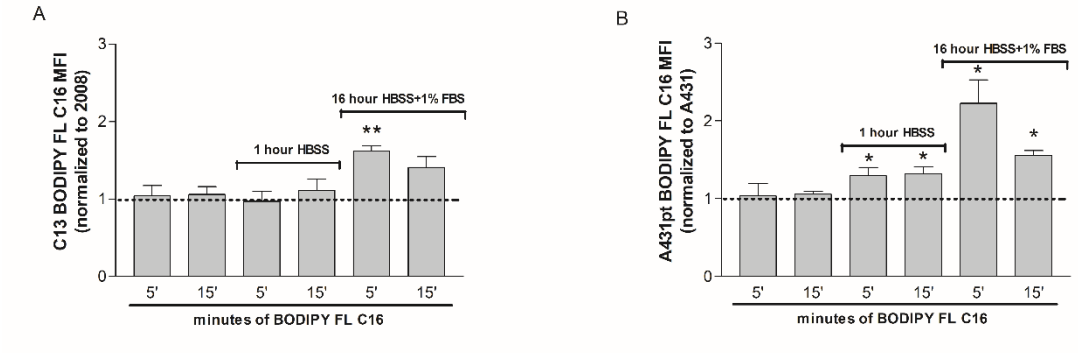

Figure 21: Bodipy FL C_{16} uptake in 2008-C13 (A) and A431-A431pt (B) cells measured by cytofluorimetry (λec/em:488/525nm). Data represent the mean of fluorescence intensity of resistant clones normalized to sensitive counterpart in basal conditions and in starvation (1hour and 16 hours), following 5 and 15 minutes of exposure to the probe. Data are the mean±SEM of at least 3 independent experiments. *p<0.05; **p<0.01 resistant *vs* sensitive clones.

Confocal Microscopy

The FFAs uptake has been also evaluated by confocal microscopy in basal condition and in16 hours of starvation (HBSS+1%FBS). Thus, cells were stained with Mitotracker Orange probe (mitochondrial staining) and with Bodipy FLC_{16}. Images in Figure 22 show that in basal condition resistant cells present a higher level of lipid accumulation; in condition of starvation both 2008 and C13 cell lines present an increase in exogenous lipid uptake.

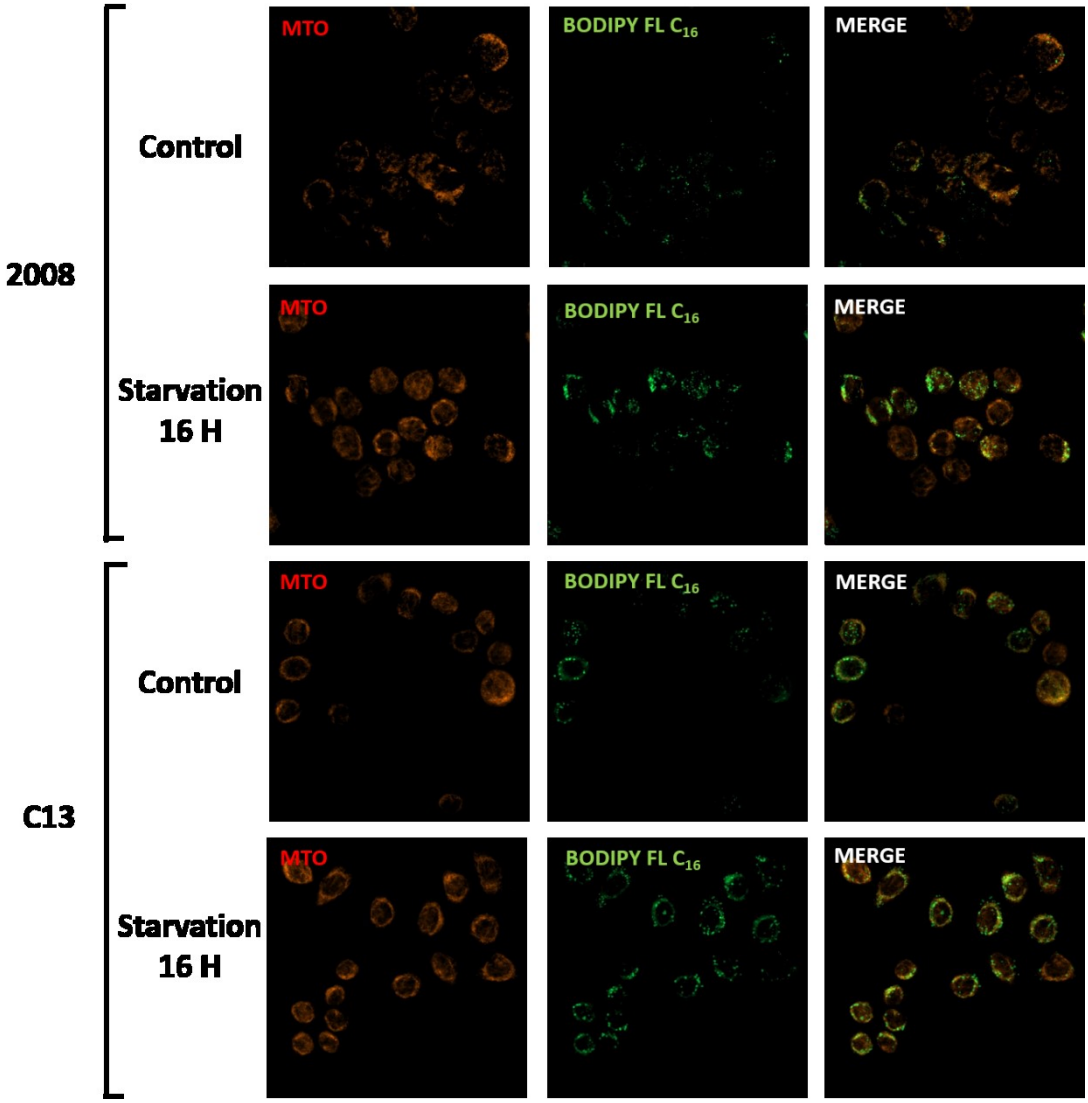

Figure 22: Images of 2008-C13 cells in basal condition and in 16 hours starvation. Cells stained with Mitotracker Orange and Bodipy FLC_{16} and images were acquired by confocal microscope LSM 800, magnification 60X, software ZN 2.1 blue Edition. Images are representative of 3 independent experiments.

Figure 23 reports the images related to A431 and A431pt staining. In these cell lines also, in starvation condition, there is an increase in the uptake, more evident in A431pt.

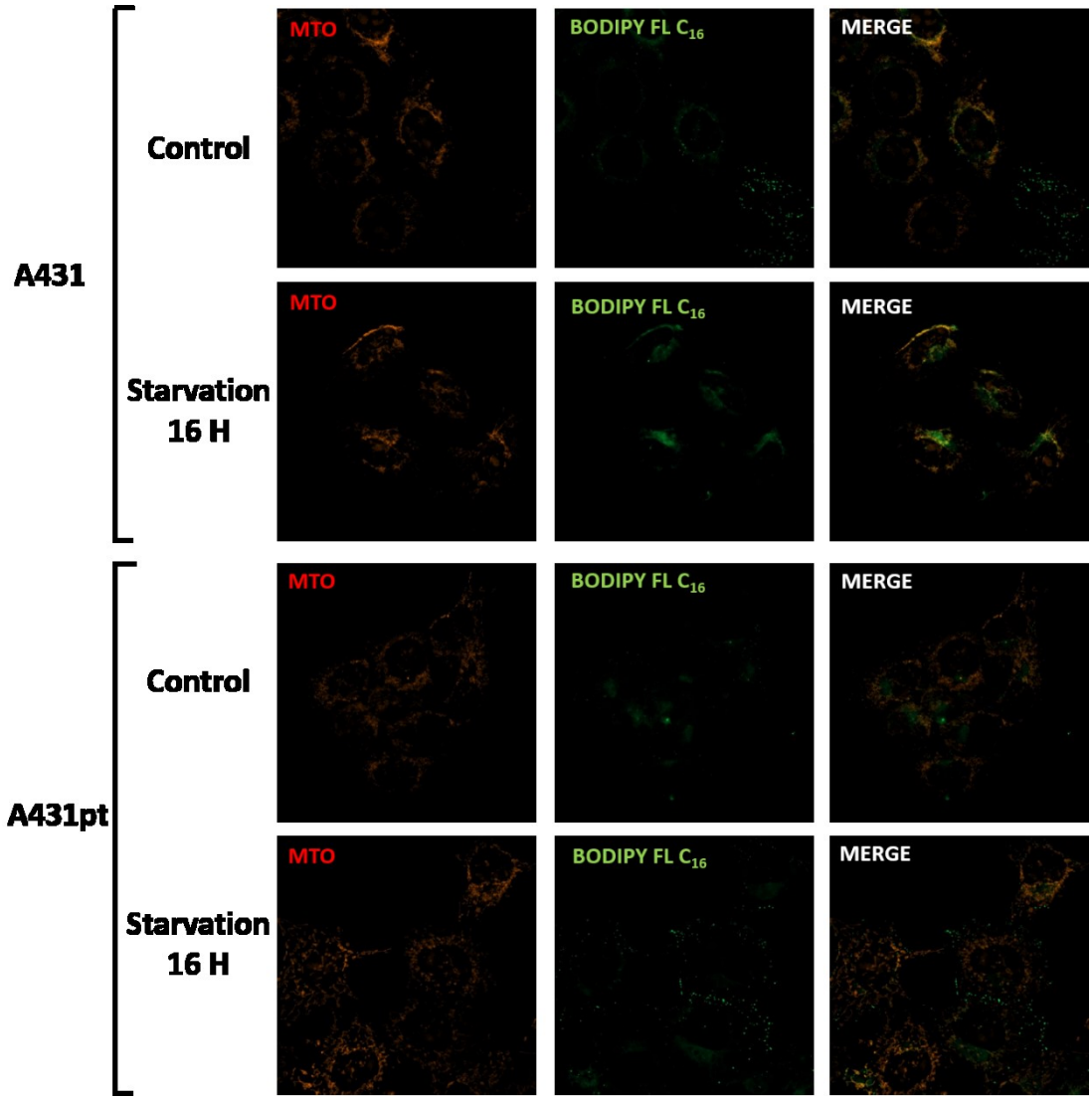

Figure 23: Images of A431-A431pt cells in basal condition and in 16hours starvation. Cells stained with Mitotracker Orange and Bodipy FL C_{16} and images were acquired by confocal microscope LSM 800, magnification 60X, software ZN 2.1 blue Edition. Images are representative of 3 independent experiments.

4.1.1.5 Lipid transporters

Having excluded the increased *de novo* lipid synthesis as a cause of lipid accumulation in cells, we moved the attention to the exogenous uptake. For a long time, it has been considered to occur by passive diffusion, but it is now well established that various membrane proteins act in this process. Thus, the expression of these transporters was analyzed at mRNA and protein levels in 2008-C13 and A431-A431pt cell lines.

Results in Figure 24 represent the mRNA levels of plasma membrane fatty acid-binding protein (FABPpm) in 2008-C13 and A431-A431pt. FABP is present in 10 different isoforms so the tissue-specific isoform has been analyzed. Results show an increased expression in FABP5 in A431pt with respect to A431 (B) while no difference has been revealed in FABP3 expression in C13 with respect to 2008(A).

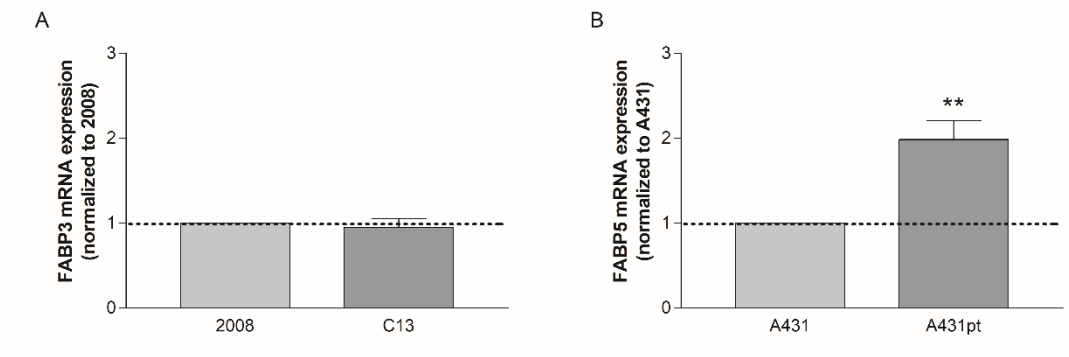

Figure 24: mRNA levels of fatty acid binding proteins. A) FABP3 level in C13 cell line, B) FABP5 level in A431pt cell line measured by RT-PCR. Data are reported as ratio to sensitive clone and are the mean±SEM of at least 3 independent experiments. ***p*<0,01 A431pt *vs* A431.

Figure 25 shows the protein levels of some mediators in lipid transport: C13 cell line presents higher levels of CD36, FATP2 and Caveolin-1 while lower levels of Low-density Lipoproteins (LDL) receptor and eFABP compared to 2008 sensitive clone. With the exception of LDL receptor, which is downregulated also in A431pt, in the cervix cell lines results are the opposite. A431pt cell line presents higher level of eFABP, lower Caveolin-1, and no differences in CD36 expression with respect to A431 sensitive clone.

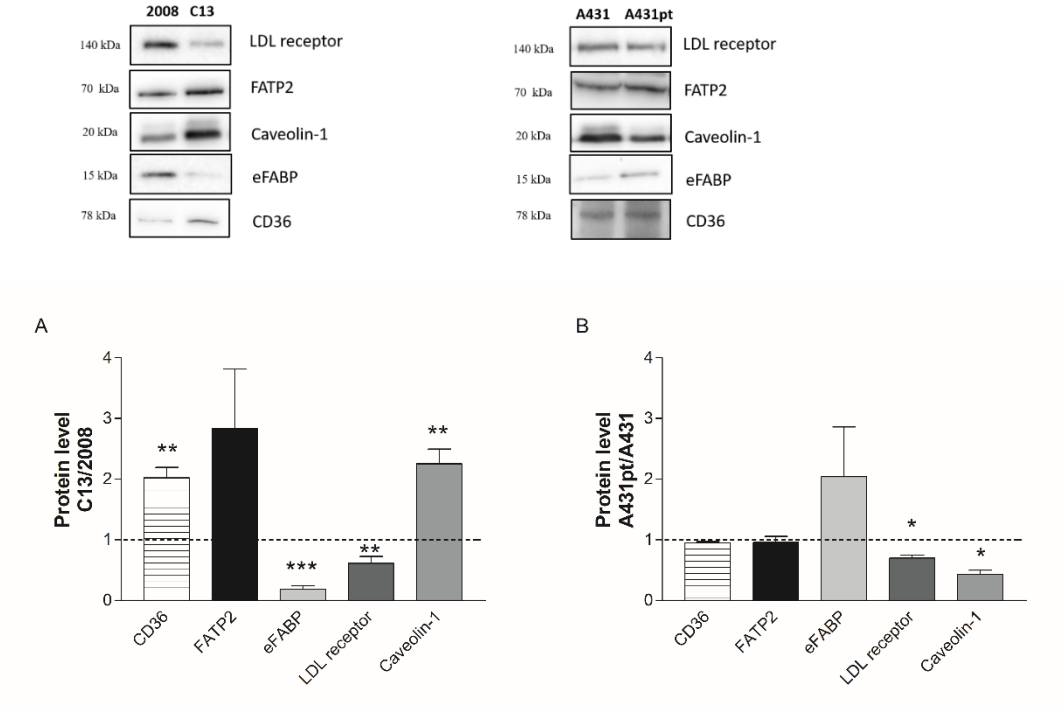

Figure 25: Protein expression of mediators of fatty acid transport. Protein level of CD36, FATP2, eFABP, LDL receptor, and Caveolin-1 in C13 (A) and A431pt (B) cell lines measured by Western blot assay. Data are expressed as ratio of resistant *vs* sensitive clones and are the mean±SEM of 3-4 independent experiments. *p<0.05; **p<0.01; ***p<0,001 resistant *vs* sensitive.

Results showed that resistant clones present a higher lipid uptake transport system but that the proteins involved in the uptake process possibly differ depending from the tissue origin of cell lines.

4.1.1.6 Lipolysis analysis

Lipolysis is the catabolic process of the FA cycle that provides FAs in conditions of metabolic needs and removes them when they are in excess. The hydrolysis of TGs to FAs and glycerol is catalyzed by three different lipases: adipose triglyceride lipase (ATGL), the hormone-sensitive lipase (HSL), and the monoglyceride lipase (MGL). The released FAs can be re-esterified in new TAG or can be shuttled to mitochondria for generation of energy via fatty acid oxidation or used for anabolic processes[139].

Always with a view to investigate the mechanisms involved in lipid accumulation, a reduction in the lipolytic process had been taken into consideration. For this reason, the activity of the lipases deputed to the catabolism of TGs has been evaluated in ovarian and cervix cancer cells. The analysis has been carried out using a Lipase Enzymatic Assay

Kit, (*Cayman*) both in basal conditions and after 4 hours of starvation (obtained incubating cells with HBSS +1%FBS) to force the lipolytic process. From the slope of the tangent line to the curves reporting the RFU's variation during the time, the RFU tendency, which corresponds to the quantity of substrate metabolized, was calculated. Graphs in Figure 26 show the Relative fluorescent intensity (RFU) tendency of cells normalized on protein content per samples. Results show that the resistant clones present no differences in lipases activity with respect to the sensitive counterpart. This result was observed both in basal conditions and in starvation, thus excluding an altered lipolytic activity at the base of the LDs accumulation observed in resistant clones.

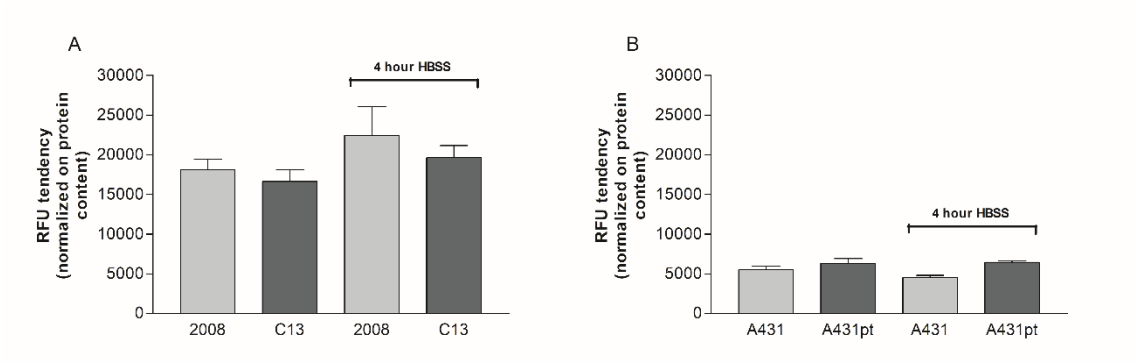

Figure 26: Lipases activity is measured by the quantity of metabolized substrate, expressed as relative fluorescence intensity tendency. Values are extrapolated from the slope of the curve describing the variation of RFU during the time. Results report the lipase activity of 2008-C13 (A) cell line and A431-A431pt (B) in basal condition and after 4 hours of starvation. Results are the mean±SEM of 3 independent experiments.

4.1.1.7 β-oxidation

Another pathway involved in lipid metabolism is β-oxidation. Through this pathway, cells metabolize fatty acids within mitochondria to generate energy. Thus, we analyzed by qRT-PCR the mRNA expression of some key factors in this process: PPARα (Peroxisome proliferator-activated receptor alpha), CPT1 (Carnitine palmitoyltransferase I) and CPT2 (Carnitine palmitoyltransferase II). Results in Figure 27 show that both C13 (A) and A431pt (B) resistant clones present a reduced level of PPARα with respect to the sensitive clones. The expression of CPT1 is unvaried in C13 line while decreased in A431pt compared to the corresponding 2008 and A431 sensitive cell line. Also, CPT2 expression is unvaried between sensitive and resistant clones. So, globally, the beta-oxidation pathway seems to be unaltered or decreased in resistant cells with respect to the sensitive cell lines.

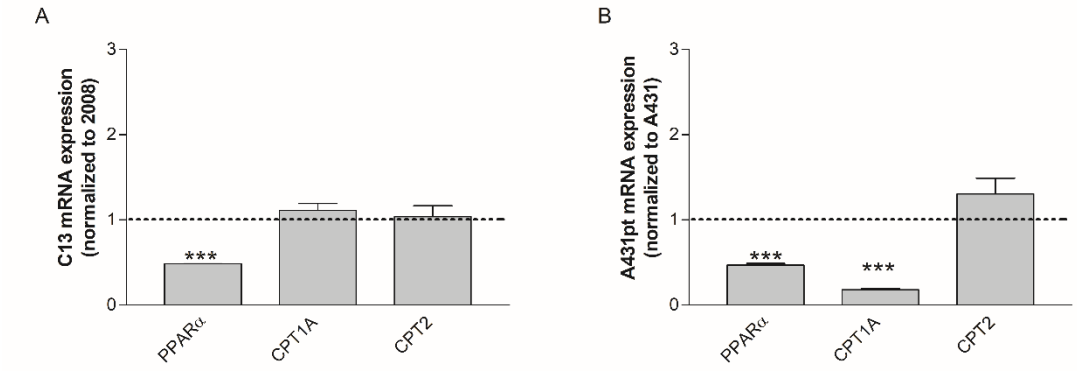

Figure 27: mRNA levels of PPARα, CPT1A and CPT2 genes in 2008-C13 (A) and A431-A431pt (B) cell lines, measured by qRT-PCR. Expression levels of the indicate genes were evaluated by the ΔΔCt method with β-actin as the reference gene. Data are the mean±SEM of 3-4 independent experiments and are normalized to the sensitive clones. ***$p<0.001$ resistant *vs* sensitive clone.

In order to investigate more in detail this pathway, cells were treated with Etomoxir (ETO), a widely used small-molecule inhibitor of fatty acid oxidation (FAO) through its irreversible inhibitory effects on the carnitine palmitoyl-transferase 1a (CPT1a). Cells viability and Lipid droplet content were evaluated in conditions of inhibition of β-oxidation. Results in Figure 28 show viability of 2008-C13 cell lines after treatment with Etomoxir. Treatment induces a slight reduction of both cell lines viability after 24(A) and 48hours (B) and there are no differences in the susceptibility of sensitive and resistant cells. The 24 hours treatment followed by 48 hours of recovery doesn't alter cells viability (C). A similar effect has been shown on A431-A431pt cell line (Figure 29) where the 24

and 48 hours treatment induces a slight reduction of viability of both cell lines (A-B), while the 24+48 hours treatment doesn't affect cell viability (C). No differences were observed between the sensitive and resistant clones.

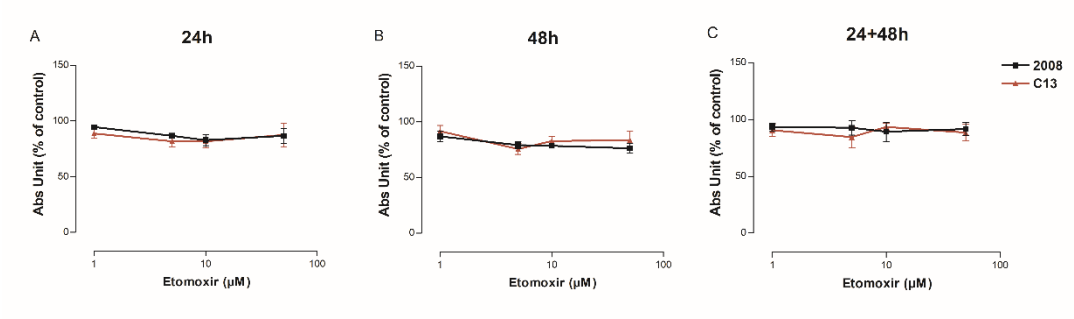

Figure 28: Effect of Etomoxir (1-5-10-50 µM) on 2008-C13 cells viability measured by SRB assay, after 24-48 and 24 hours + 48hours of recovery. Data are expressed as % of Absorbance of vital cells related to control and are the mean±SEM of 3 independent experiments.

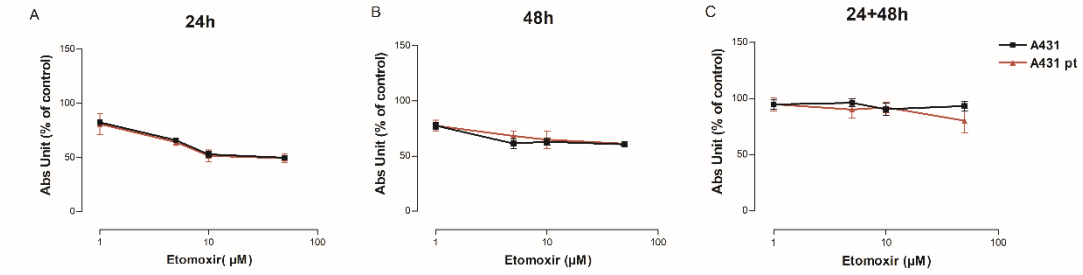

Figure 29: Effect of Etomoxir (1-5-10-50 µM) on A431-A431pt cells viability measured by SRB assay, after 24-48 and 24 hours + 48hours of recovery. Data are expressed as % of absorbance of vital cells related to control and are the mean±SEM of 3 independent experiments.

No significant differences in viability between sensitive and resistant clones have been observed in none of the analyzed conditions.

The effect of Etomoxir was also tested in lipid droplets accumulation. Cells were treated for 24 hours with Etomoxir and the LDs content was analyzed by confocal microscopy.

Figure 30 reports the images obtained from cells-staining with Mitotracker Orange and Bodipy in basal condition and after 24 hours of treatment with ETO 1 µM in 2008-C13. ETO treatment induces an increase in 2008 LDs content while no differences were observed in treated C13 respect the control.

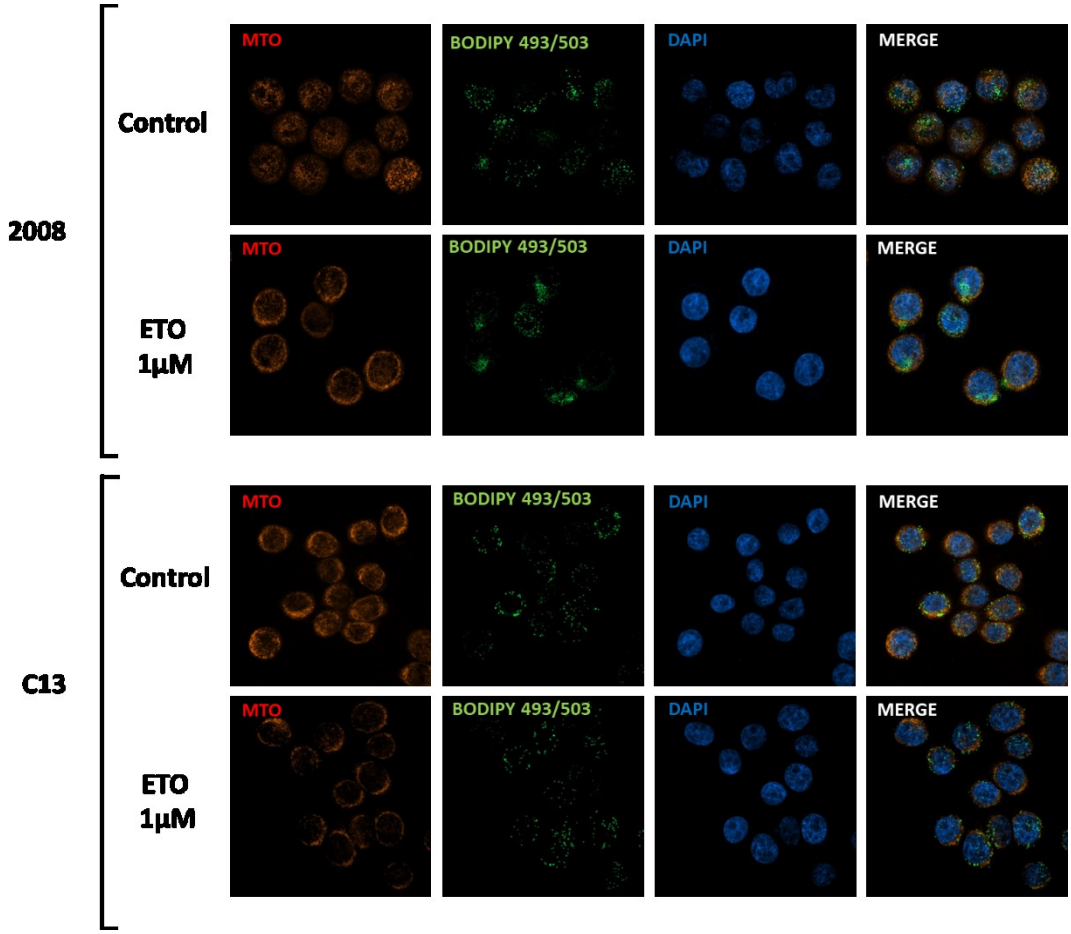

Figure 30: Representative images of the effect of Etomoxir (1µM) on Lipid droplet accumulation in 2008-C13. Cells were stained with Mitotracker orange (25 nM; λec/em:554/576nm), and Bodipy 486 (λec/em:493/503nm) and nuclei stained with DAPI. Images were acquired by confocal microscopy Zeiss LSM 800, analyzed with ZEN 2.0 imaging software and are representative of 3 different experiments.

The same experiment in A431-A431pt cell lines reveals that after ETO treatment there is a concentration dependent increase of LDs but no difference was observed between sensitive and resistant clones (Figure 31).

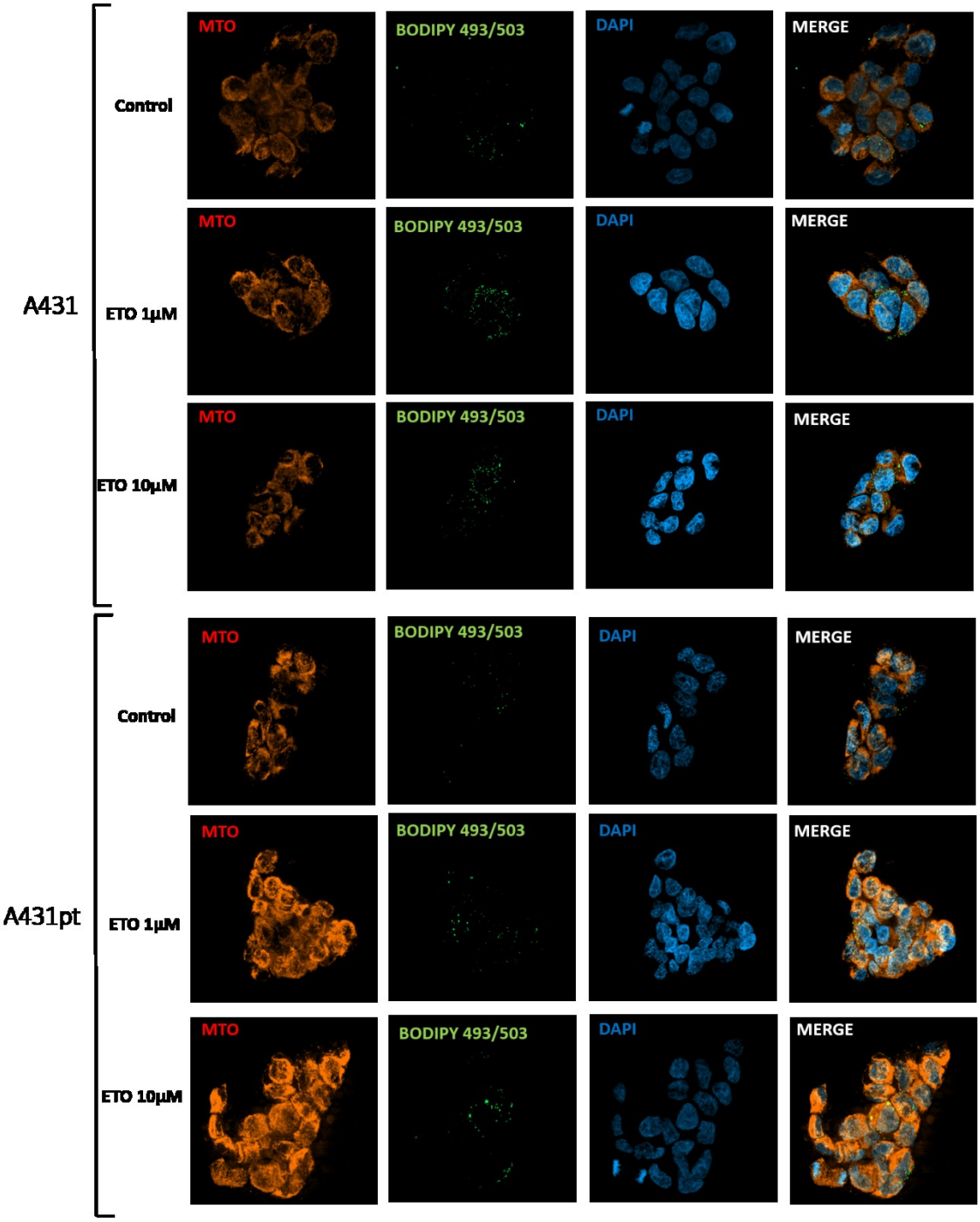

Figure 31: Representative images of the effect of Etomoxir (1-10µM) on Lipid droplets accumulation. Cells were stained with Mitotracker orange (25 nM; λec/em:554/576nm), and Bodipy 486 (λec/em:493/503nm) and nuclei stained with DAPI. Images were acquired by confocal microscopy Zeiss LSM 800 and analyzed with ZEN 2.0 imaging software and are representative of 3 different experiments.

The next strategy to better understand if there are differences in the β-oxidation pathway between sensitive and resistant cells has been to use an activator of this pathway. At this purpose, 2-[4-(5-chlorobenzothiazothiazol-2-yl) phenoxy]-2-methyl-propionic acid (MHY908), a synthetic novel PPARα/γ dual agonist, has been used. Firstly, MHY908 effect on cell viability was investigated by SBR assay.

Results in Figure 32 and Figure 33 show that treatment with MHY908 doesn't affect cell viability of 2008-C13 and of A431-A431pt in any considered concentration and time.

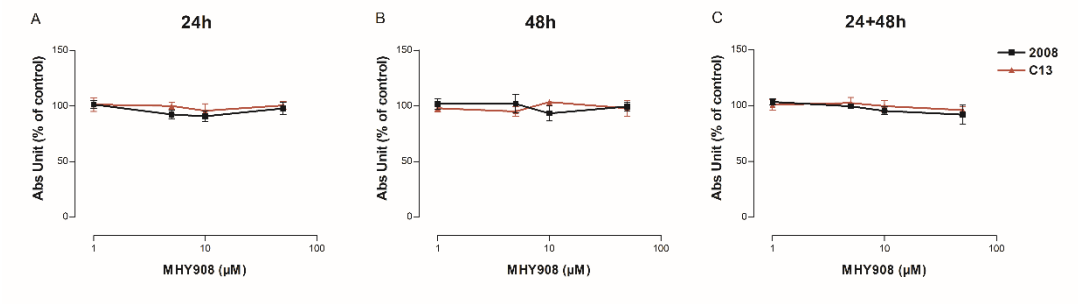

Figure 32: Effect of MHY908 (1-5-10-50 μM) on 2008-C13 cells viability measured by SRB assay, after 24 (A), 48(B) and 24+ 48hours of recovery (C). Data are expressed as % of absorbance of vital cells related to control and are the mean±SEM of 3 independent experiments.

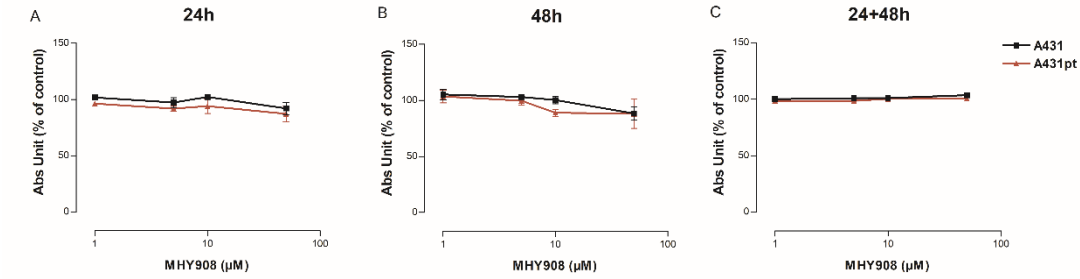

Figure 33: Effect of MHY908 (1-5-10-50 μM) on A431-A431pt cells viability measured by SRB assay, after 24 (A), 48(B) and 24+ 48hours of recovery (C). Data are expressed as % of absorbance of vital cells related to control and are the mean±SEM of 3 independent experiments.

The effect of the induction of β-oxidation on the accumulation of Lipid Droplets was then evaluated by confocal microscopy (Figure 34 and Figure 35). As it is possible to observe, in the presence of MHY908 there is a reduction of LDs in all the cell lines, more evident in resistant C13 and A431pt clones.

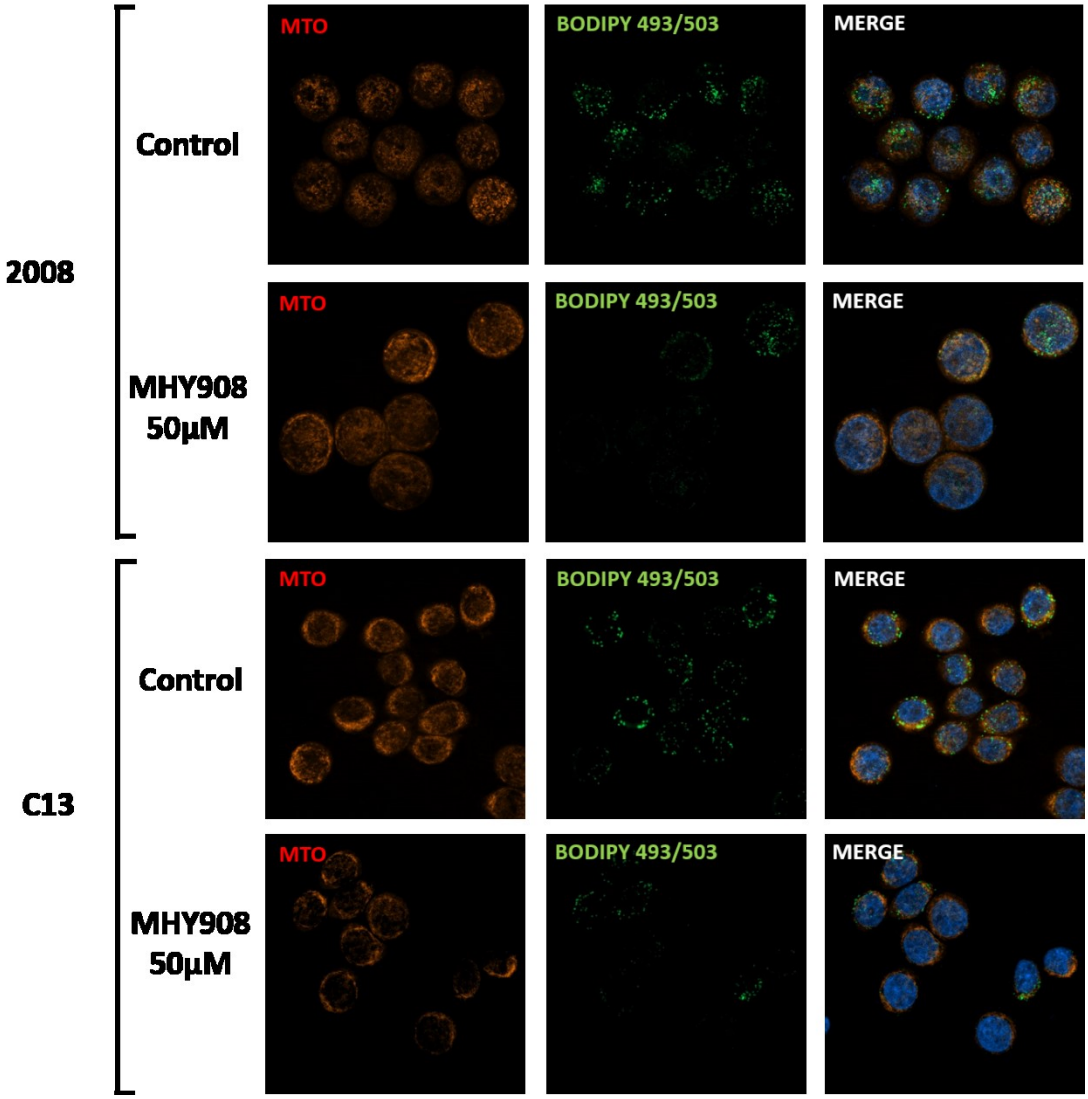

Figure 34: Representative images of the effect of MHY908 24 hours treatment (50 µM) on Lipid droplet accumulation in 2008-C13. Cells were stained with Mitotracker orange (25 nM; λec/em:554/576nm), and Bodipy 486 (λec/em:493/503nm). Images were acquired by confocal microscopy Zeiss LSM 800 and analyzed with ZEN 2.0 imaging software. Images are representative of 3 different experiments.

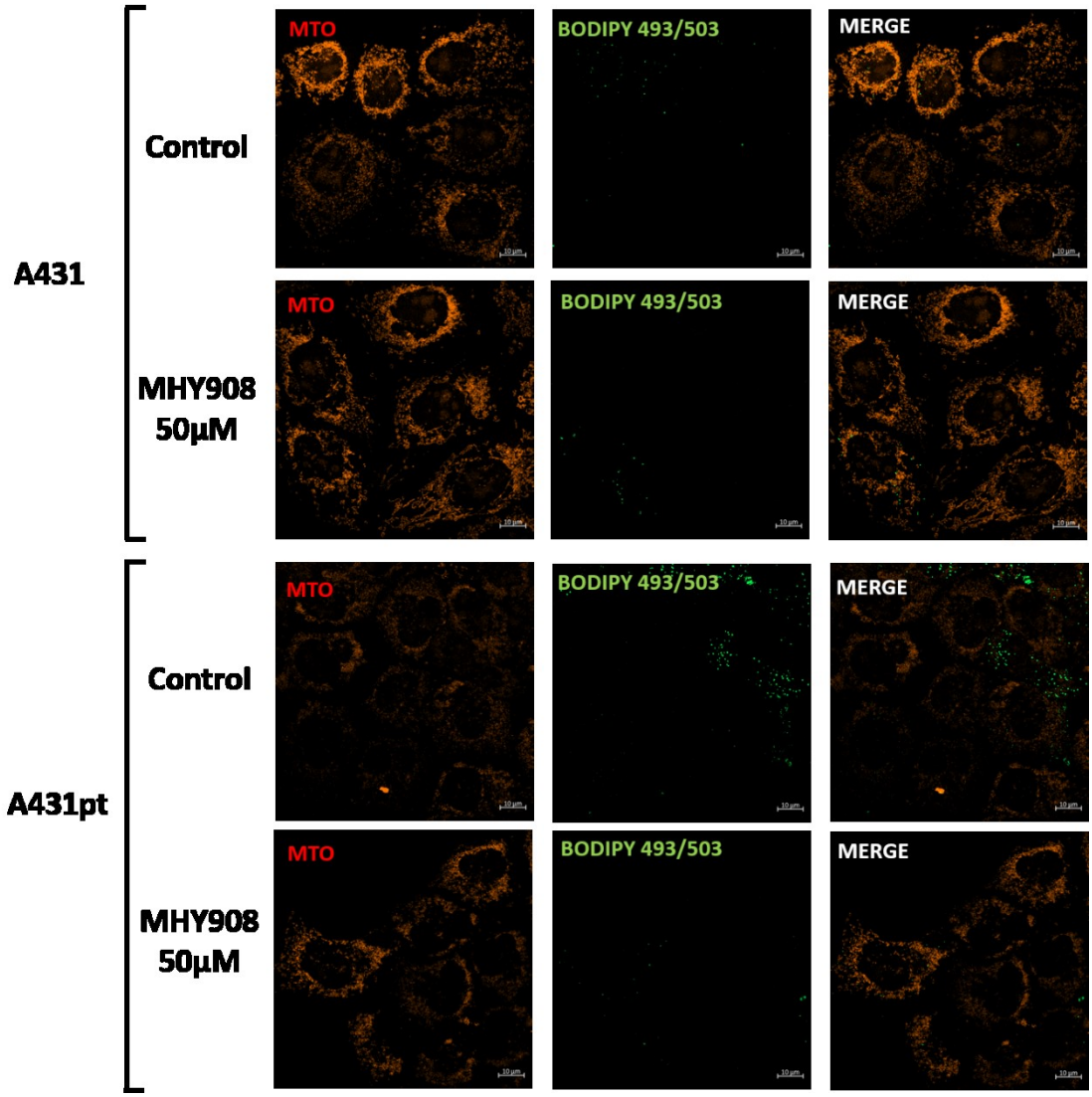

Figure 35: Representative images of the effect of MHY908 24 hours treatment (50 µM) on Lipid droplet accumulation in A431-A431pt. Cells were stained with Mitotracker orange (25 nM; λec/em:554/576nm), and Bodipy 486 (λec/em:493/503nm). Images were acquired by confocal microscopy Zeiss LSM 800 and analyzed with ZEN 2.0 imaging software. Images are representative of 3 different experiments.

4.1.2 **Glutamine metabolic profile in CDDP sensitive and resistant ovarian cancer cells (2008-C13) and in sensitive and resistant Triple Negative Breast Cancer cells (MDA-MB-468, HCC1143, HCC1937)**

Glutamine is the most abundant amino acid in blood and muscles, and is used as precursor of biomass and for energy production to sustain rapid proliferation[100]. Glutamine plays a pleiotropic role providing not only carbon but also nitrogen for nucleic acid synthesis and it is also involved in cellular redox homeostasis; so, it is important to consider both the catabolism and the anabolism of this amino acid in the context of diseases and cancer. Therefore, reduced glutamine metabolism may limit the proliferation of cancer cells and thereby serve as a metabolic checkpoint that becomes activated in response to genotoxic stress such as cisplatin [164].

4.1.2.1 Cells viability

Ovarian cancer cell lines

The effect of glutamine deprivation on cell proliferation has previously been evaluated in 2008-C13 cell lines. The growth curves (Figure 36) show that C13 resistant cells (B) present a marked proliferation decrease in glutamine-free media. This slowdown is not observed in 2008 sensitive cells (A) [157].

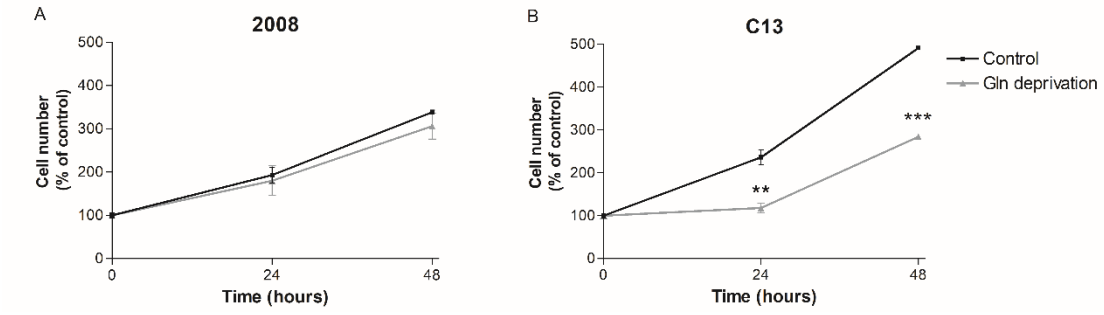

Figure 36: Effect of glutamine deprivation on 2008 (A) and C13(B) cell proliferation, after 24 and 48 hours of treatment, measured by Trypan Blue Exclusion assay. Results are reported as % of cell number related to control and are the mean±SEM of 3 independent experiments. ** $p<0.01$; *** $p<0.001$ glutamine deprivation *vs* control. (Data from [157])

In order to investigate if the glutamine depletion could modulate cells response to CDDP, the effect of the combined treatment on cells viability has been studied. Results in Figure 37 show that in 2008 sensitive cells there is no difference in the trend of the curves following treatment with CDDP or with the association. Instead, the association induce a marked effect in arresting cell proliferation with respect to cisplatin in C13 resistant cells (Figure 38). This suggests a possible effect of glutamine in modulating the cisplatin response.

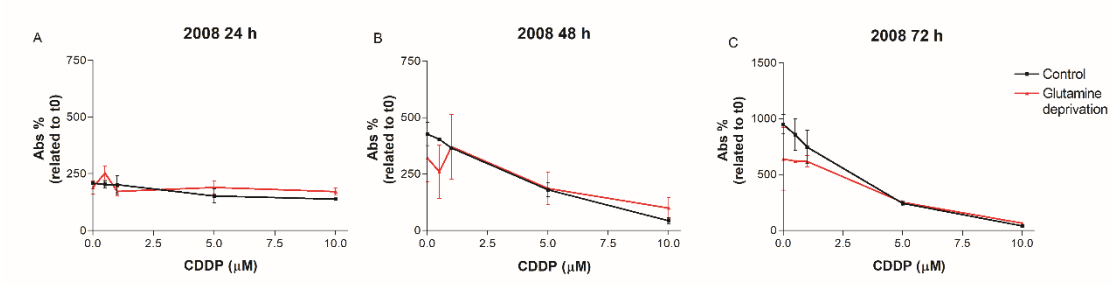

Figure 37: Effect of glutamine deprivation in association with cisplatin (0.5-1-5-10 μM) after 24-48-72 hours of treatment, measured by Crystal Violet Assay on 2008 cell lines. Data are expressed as Abs % related to time zero and are the mean±SEM of 2 independent experiments.

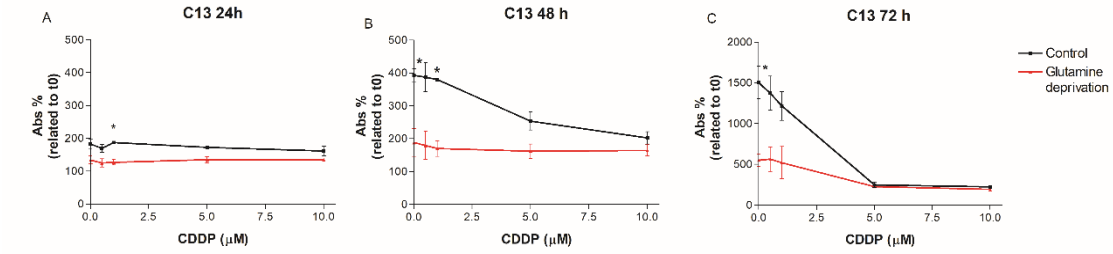

Figure 38: Effect of glutamine deprivation in association with cisplatin (0.5-1-5-10 μM) after 24-48-72 hours of treatment, measured by Crystal Violet Assay on C13 cell line. Data are expressed as Abs % related to time zero and are the mean±SEM of 2 independent experiments. *p<0.05 CDDP *vs* CDDP w-o glutamine.

The effect of glutamine deprivation on cell cycle was then analyzed by flow cytometry using Propidium Iodide Staining. Figure 39 shows that glutamine deprivation induces no alterations in sensitive 2008 cell line (A). The treatment, instead, induces a tendency to increase in S phase in C13 starved for 24 h (B). CDDP primary target is DNA, so an increase of the % of cell in the synthesis phase of the cycle can offer more target for CDDP action.

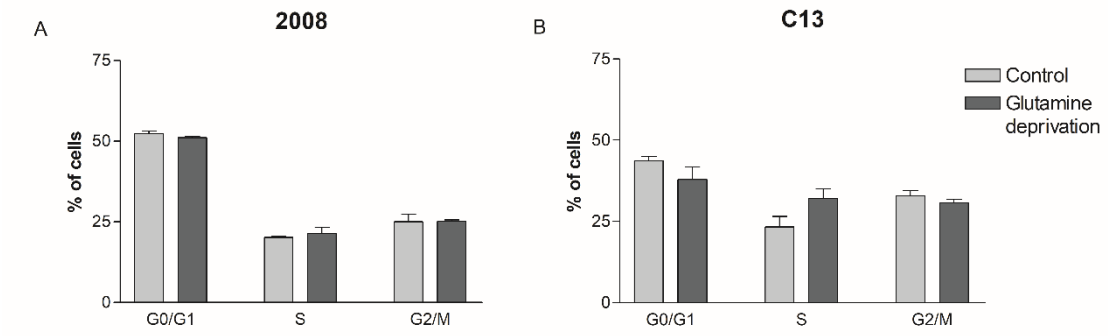

Figure 39: Effect of glutamine deprivation on 2008 (A) and C13 (B) cell cycle after 24 hours of treatment, measured by Flow cytometry using Propidium Iodide staining. Data are expressed as % of cells in each phase related to the total number of cells and are the mean±SEM of 3 independent experiments.

Triple negative breast cancer cell lines

The effect of glutamine deprivation on cells proliferation/viability in MDA-MB-468, HCC1143 and HCC1937 cell lines has been studied.

Figure 40 shows the effect of glutamine deprivation on cell proliferation in MDA-MB-468 (A), HCC1143 (B), and HCC1937 (C). Glutamine starvation induces growth arrest in all the cell lines, more significative in CDDP-resistant cells.

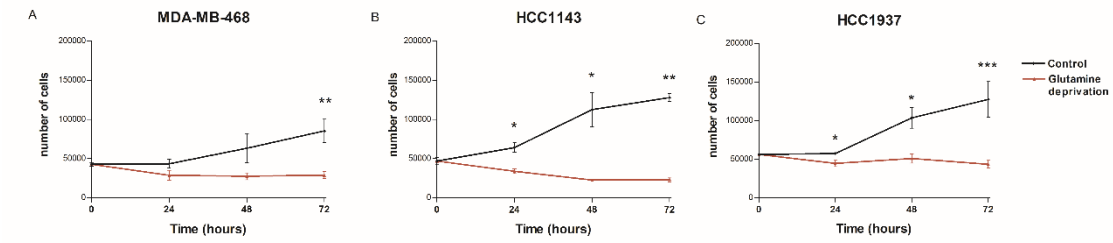

Figure 40: Effect of glutamine deprivation in MDA-MD-468 (A), HCC1143 (B), and HCC1937 (C) cells proliferation, after 24, 48 and 72 hours of treatment, measured by Trypan Blue Exclusion assay. Results are reported as cell number related to time zero and are the mean±SEM of 3 independent experiments. *$p<0.05$; **$p<0.01$; ***$p<0.001$ glutamine deprivation *vs* control.

The effect of glutamine deprivation was also investigated on cells viability by Propidium Iodide assay. Results in Figure 41 show that only the CDDP resistant cell line HCC1143 (B) presents a significant reduction of cells viability in glutamine starvation, especially in long term treatment.

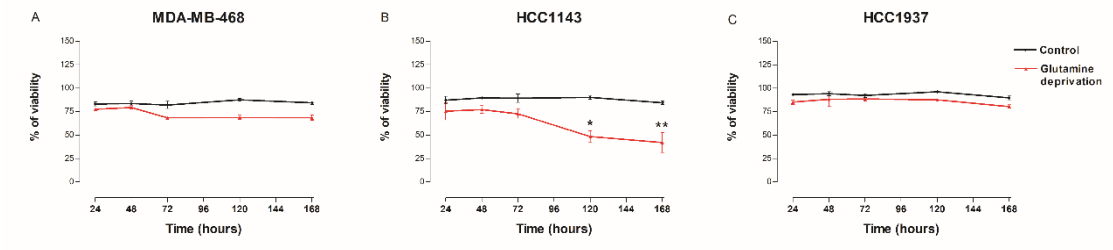

Figure 41: Effect of glutamine deprivation in MDA-MD-468 (A), HCC1143 (B), and HCC1937 (C) cells viability, after 24, 48,72,120,168 hours of treatment, measured by Propidium Iodide assay. Results are reported as % of vital cells related to control and are the mean±SEM of 3 independent experiments. *p<0.05 glutamine deprivation *vs* control.

The effect of the association treatment (CDDP 0.5-1-5- 10 µM + glutamine deprivation) on cell proliferation after 24, 48 and 72 hours was evaluated.

Results showed that the in MDA-MB-468, the sensitive clones, there is no difference in the trend of the curves following treatment with cisplatin alone or in combination with glutamine deprivation (Figure 42). In resistant lines, HCC114 and HCC1937 (Figure 43and Figure 44) especially at 72 hours of treatment (C), the association displays a marked effect in arresting cells proliferation with respect to the treatment with cisplatin alone, indicating a possible effect of glutamine in modulating the cisplatin response.

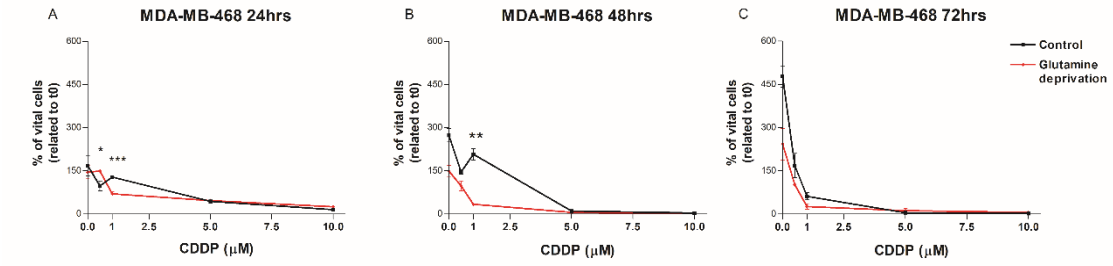

Figure 42: Effect of glutamine deprivation in association with cisplatin (0.5-1-5-10µM) after 24(A), 48(B), and 72 (C) hours of treatment, measured by Trypan Blue Exclusion assay on MDA-MB-468 cell line. Data are expressed as % of vital cells related to time zero and are the mean±SEM of 2-3 independent experiments. *p<0.05; **p<0.01; ***p<0.001 CDDP *vs* CDDP w-o glutamine

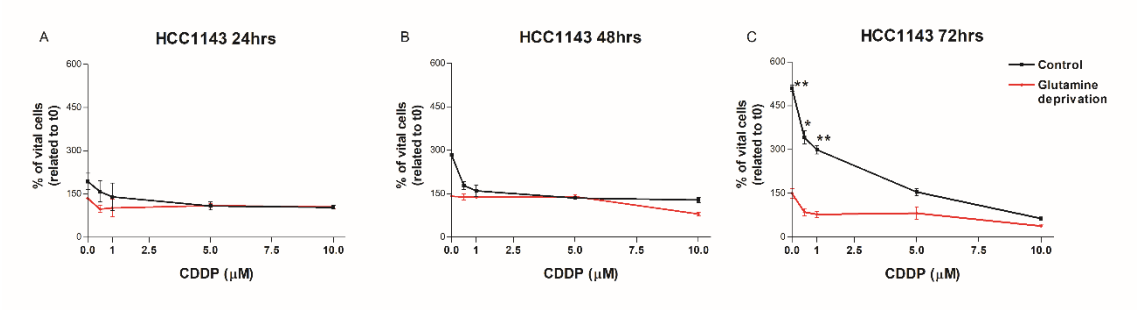

Figure 43: Effect of glutamine deprivation in association with cisplatin (0.5-1-5-10µM) after 24(A), 48(B), and 72 (C) hours of treatment, measured by Trypan Blue Exclusion assay on HCC1143 cell line. Data are expressed as % of vital cells related to time zero and are the mean±SEM of 2-3 independent experiments. **p*<0.05; ***p*<0.01; CDDP *vs* CDDP w-o glutamine

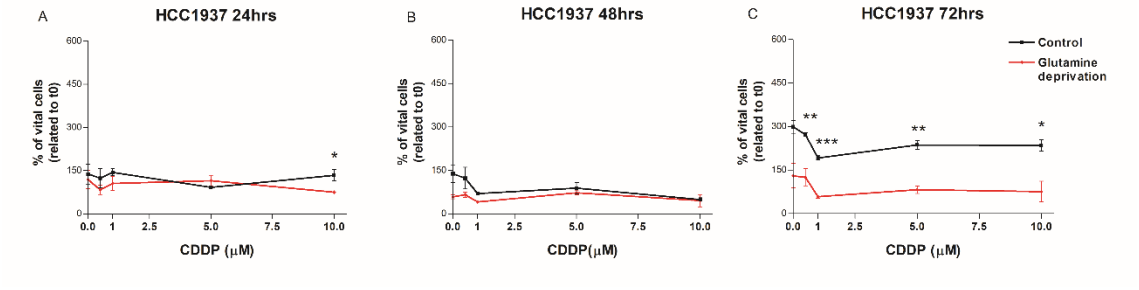

Figure 44: Effect of glutamine deprivation in association with cisplatin (0.5-1-5-10µM) after 24(A), 48(B), and 72 (C) hours of treatment, measured by Trypan Blue Exclusion assay on HCC1937 cell line. Data are expressed as % of vital cells related to time zero and are the mean±SEM of 2-3 independent experiments. **p*<0.05; ***p*<0.01; ****p*<0.001 CDDP *vs* CDDP w-o glutamine

4.1.2.2 Metabolomic Analysis

In order to understand which is the metabolic fate of glutamine in the different sensitive and CDDP-resistant cell lines, and if there are differences in the metabolic pathways of this amino acid between different clones, a metabolomic analysis using [U-^{13}C] glutamine has been performed.

Ovarian cancer cells

C13 and 2008 were incubated with [U-^{13}C] glutamine and the isotopologue distribution of tricarboxylic acid (TCA) cycle intermediates have been previously analyzed[157]. Results in Figure 45 show that the incorporation of glutamine-derived carbons into glutamate, succinate, fumarate, and malate was significantly higher in cisplatin-resistant cells. These results suggest that glutamine is a carbon source for resistant cells, which metabolize glutamine more and faster than sensitive clone.

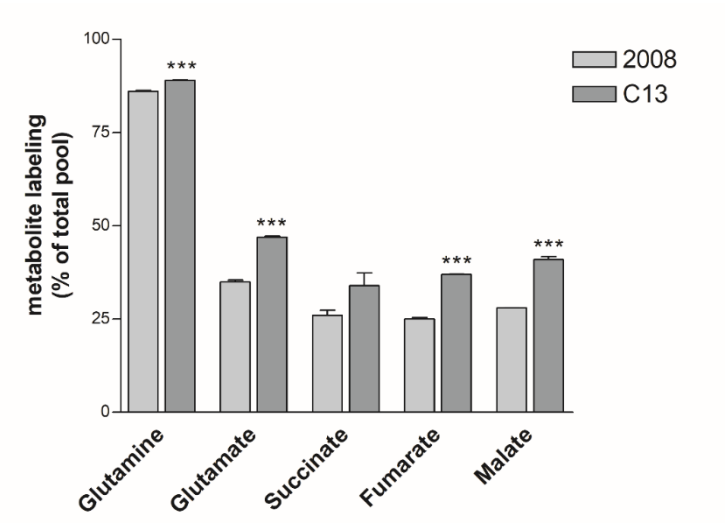

Figure 45: Incorporation of ^{13}C-labeled carbons into glutamate, succinate, fumarate, and malate after growing cells with [U-^{13}C] glutamine for 24hours. Results are obtained from at least three independent experiments ***$p < 0.001$; C13 *vs* 2008. (Data from [157])

Triple Negative Breast Cancer Cells

MDA-MB-468 and HCC1143 were incubated with [U-^{13}C] glutamine for 4 hours and the isotopologue distribution of tricarboxylic acid (TCA) cycle intermediates have been analyzed. Results in Figure 46 show that the incorporation of glutamine-derived carbons into glutamate, fumarate, malate, and citrate was higher in cisplatin-resistant HCC1143 cells. Even in this cell model of intrinsic resistance, these results suggest that glutamine is a carbon source for resistant cells, which metabolize glutamine more and faster than sensitive clone.

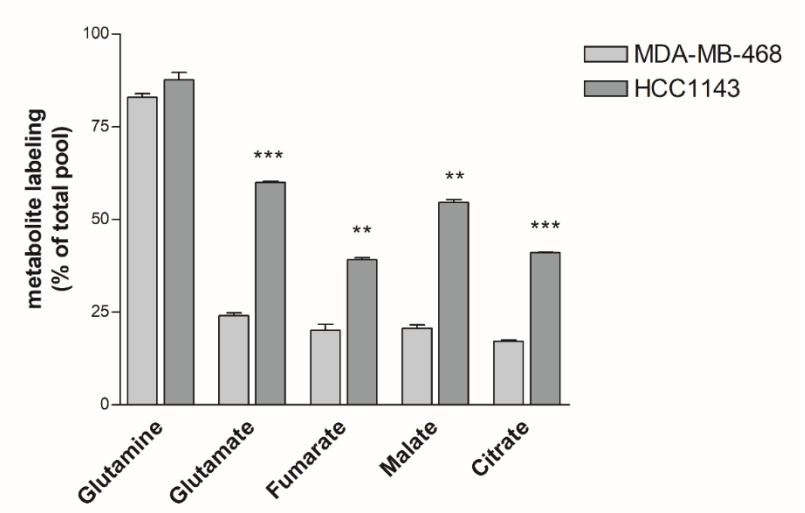

Figure 46: Incorporation of ^{13}C-labeled carbons into glutamate, fumarate, malate, and citrate after growing cells with [U-^{13}C] glutamine for 4hours. Data are expressed as % of labelling of total pool and are the mean±SEM of 2 different cultures. Data are normalized on protein content. **p<0.01; ***p<0.001 HCC1143 *vs* MDA-MB-468.

Besides being a carbon source for the TCA cycle, glutamine is a key precursor of glutamate, required, among many functions, for the biosynthesis of glutathione (GSH), a major redox buffer in the cells. GSH has been proposed as an important molecule to sustain cisplatin resistance. From the tracing of [U-^{13}C] glutamine it has been possible to verify that the contribution of glutamine to GSH (Figure 47) was increased in C13 (A) and HCC1143 (B) CDDP-resistant cells suggesting that a portion of glutamine is used by cisplatin-resistant cells to sustain GSH biosynthesis. These results indicate that the metabolic reprogramming of cisplatin resistant cells may contribute to redox buffering.

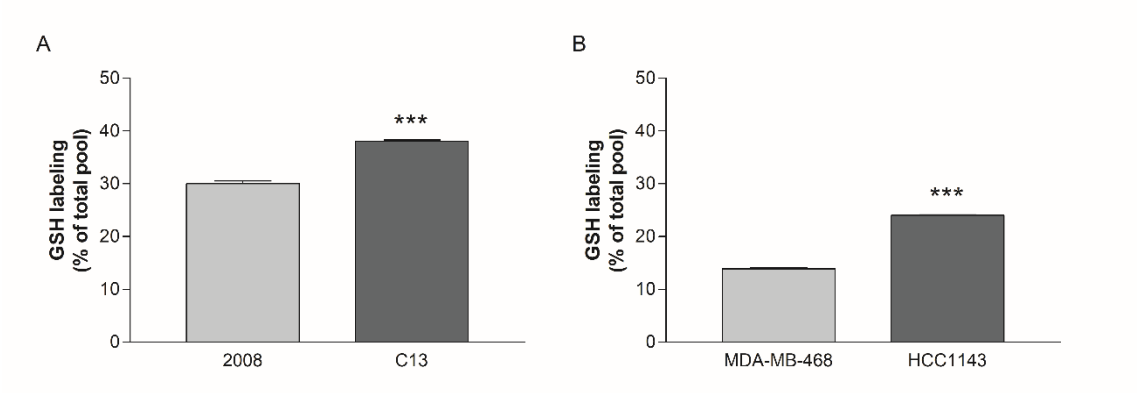

Figure 47: Intracellular levels of $^{13}C_5$-GSH after growing cell in presence of [U-^{13}C] glutamine. Data are represented as % of labeled GSH on total pool of intracellular GSH. (A) 2008-C13 ([157]); (B) MDA-MB-468-HCC1143. ***p<0.001 resistant *vs* sensitive clones. Results are expressed as mean±SEM of 2-3 experiments.

In order to evaluate how glutamine deprivation can rewire the metabolism of the cells, metabolomic analysis of sensitive MDA-MB-468 and resistant HCC1143 cells in basal condition and in glutamine starvation for 48 hours has been performed. As shown in Figure 48 (A) the principal component analysis indicates a distinct metabolic profile from sensitive and resistant cells. From the analysis performed, it has been observed that the resistant line presents, in glutamine deprivation, an increase of the Pentose Phosphate Pathway (PPP) intermediates which is not present in the sensitive cell line (B).

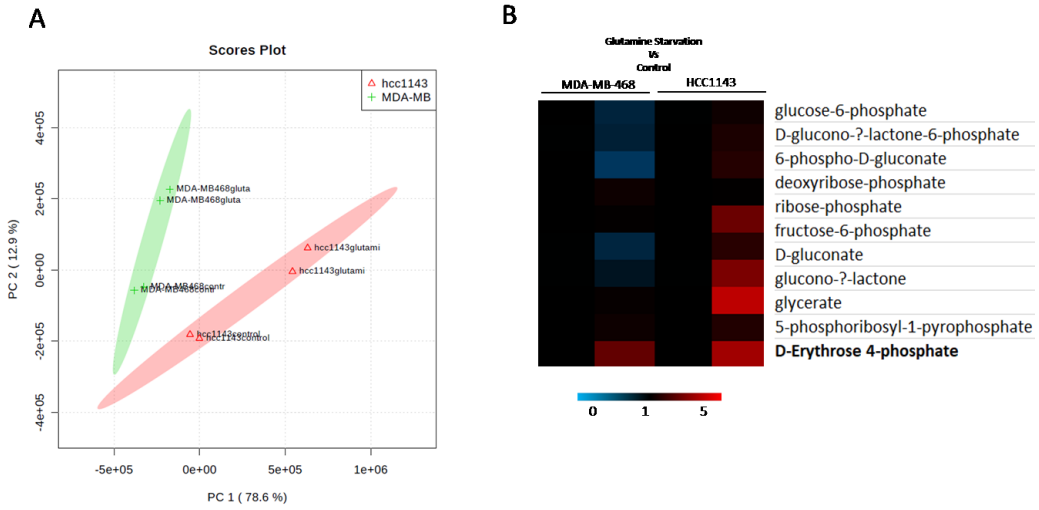

Figure 48: Metabolomics profiling in basal condition and in glutamine starvation for 48h measured by LC-ESI-QTOF MS/MS in MDA-MB-468 and HCC1143 cells. A) 2-D scores plot between selected PCs, the PCA analysis is performed using the prcomp package; B) Heatmap showing the fold change of indicated metabolites in MDA-MB-468 and HCC1143 after glutamine deprivation.

The pentose phosphate pathway (PPP) is thought to be the major source of NADPH produced at the levels of glucose-6-phosphate dehydrogenase (G6PDH) and 6-phosphogluconate dehydrogenase. Thus, it is possible that in the absence of glutamine, which is in part used for GSH production, resistant cells rewire their metabolism to PPP in order to maintain the redox homeostasis.

As a confirmation of this hypothesis, the mRNA expression of G6PDH, the key enzyme in the PPP pathway has been investigated in basal condition and in glutamine deprivation for 24 hours. Results in Figure 49 show that in basal conditions (A) resistant cells present lower levels of G6PDH respect the sensitive MDA-MB-468. When in glutamine deprivation (B) it is possible to observe an increase in mRNA levels in resistant HCC1143 and HCC1937 cell lines, that is not present in MDA-MB-468.

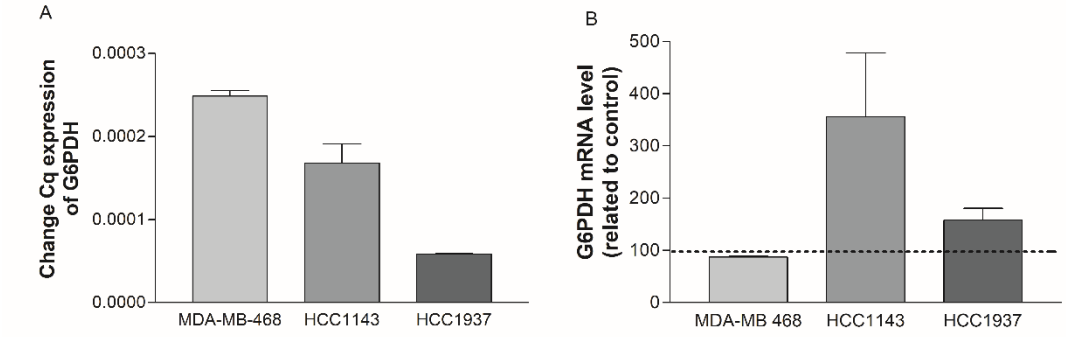

Figure 49: mRNA levels of G6PDH measured by RT-PCR in MDA-MB-468, HCC1143 and HCC1937 cells. (A) change in Cq expression of G6PDH in basal condition; (B) G6PDH mRNA level of cells in glutamine deprivation for 24hours. Data are the mean±SEM of 2 different experiments. Expression levels of the indicated genes were evaluated with the ΔΔCt method with 18S rRNA as reference gene.

4.2 Pharmacological targeting of metabolic reprogramming in CDDP-resistant cells

4.2.1 Targeting lipid metabolism

Results obtained regarding the characterization of the lipid-metabolic profile of resistant cells, has brought to light that the accumulation of Lipid droplets is not due to a dysregulation in the new lipid-synthesis pathway or in lipid-degradation pathways but it seems to be mainly due to an increase in the uptake of free fatty acids from the extracellular environment.

Thus, different strategies able to modulate lipid metabolism have been tested in order to better understand the lipid accumulation involvement in cisplatin resistance.

4.2.1.1 Lipid uptake impairment

The analysis of the principal pathways involved in lipid metabolism leads to excluding any increase in liponeogenesis or a decrease in the pathways involved in degradation of lipids (lipolysis and β-oxidation process) as causes of the accumulation of lipid droplets observed in CDDP-resistant clones. Intriguingly, results obtained so far indicate an increase in the uptake of exogenous lipids in resistant cells with respect to the sensitive counterpart. Thus, the effect of lipid deprivation for the culture media has been tested.

Firstly, the lipid depletion has been addressed by removing the Fetal Bovine serum from the culture media.

Figure 50 shows the effect of 24 hours of serum deprivation on cells viability. It is possible to observe that C13 line is more susceptible to serum starvation compared to 2008, which is not affected by the FBS deprivation (A). Results regarding A431-A431pt cell lines (B) indicate that both sensitive and resistant clones present a reduction in cells viability after FBS deprivation, more significant for A431pt.

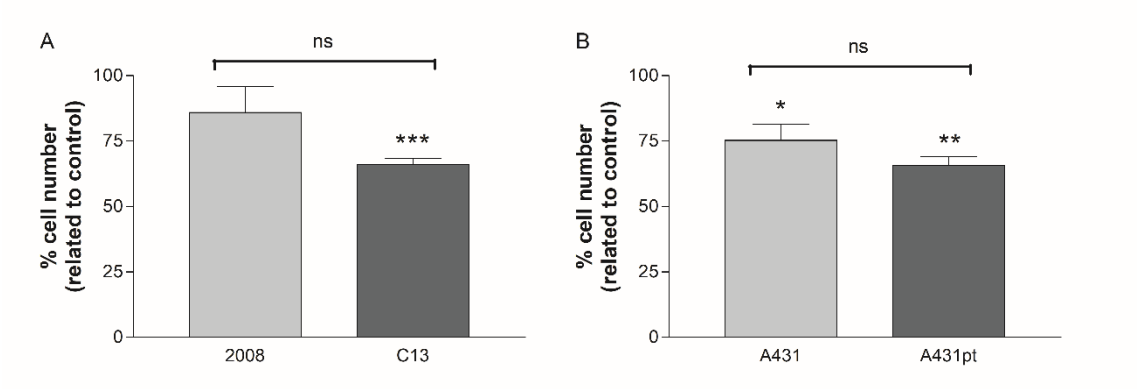

Figure 50: Effect of 24 hours of Fetal Bovine Serum deprivation on 2008-C13 (A) and A431-A431pt (B) cells viability, measured by Trypan Blue Exclusion Assay. Data are expressed of % of cell number related to control and are the mean±SEM of 4 independent experiments. *p<0.05; **p<0.01; ***p<0.001 treatment *vs* control.

Beside lipids, serum contains a large number of nutritional and macromolecular factors essential for cell growth (like amino acids, sugars, hormones, etc.) so its removal from the cell culture media could affect cells viability by deprivation of a large number of factors.

Thus, a Lipid-depleted Fetal Bovine serum (*Biowest*) was used to better address the purpose of testing the lipid involvement in cells viability and cisplatin resistance.

Figure 51 shows the effect of the treatment with Lipid-depleted FBS for 24 hours on 2008-C13 (A) and A431-A431pt (B) cells viability. Results show that the treatment affects CDDP-resistant and CDDP-sensitive cells in the same fashion, reducing cells viability of about 20% in all the cell lines.

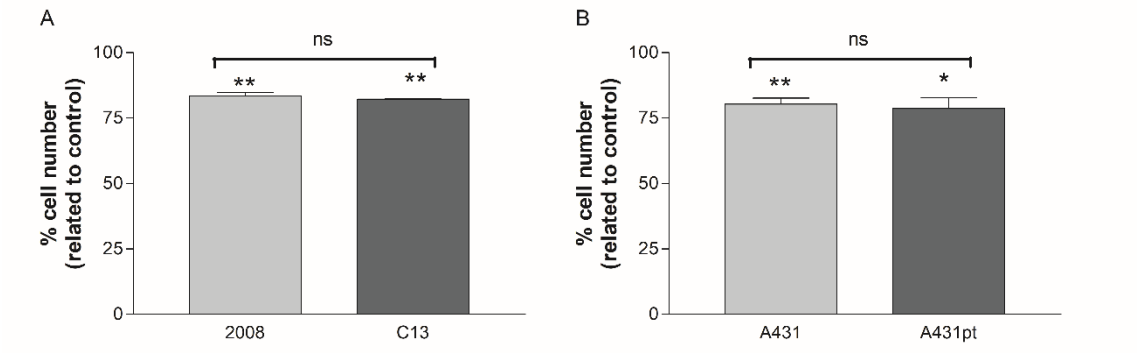

Figure 51: Effect of 24 hours of Lipid-depleted FBS on 2008-C13 (A) and A431-A431pt (B) cells viability, measured by Trypan Blue Exclusion Assay. Data are expressed as % of cell number related to control and are the mean±SEM of .4 independent experiments. *p<0.05; **p<0.01 treatment *vs* control.

The effect of lipid starvation on LD accumulation has thus been evaluated. Figure 52 and Figure 53 report representative images of the staining of the lipid droplet content in 2008-C13 (Figure 52) and A431-A431pt (Figure 53) cell lines. The results after 24 hours of depletion of lipids show that treatment induces a decrease in the LDs abundance. This effect is notably seen in all sensitive and resistant clones.

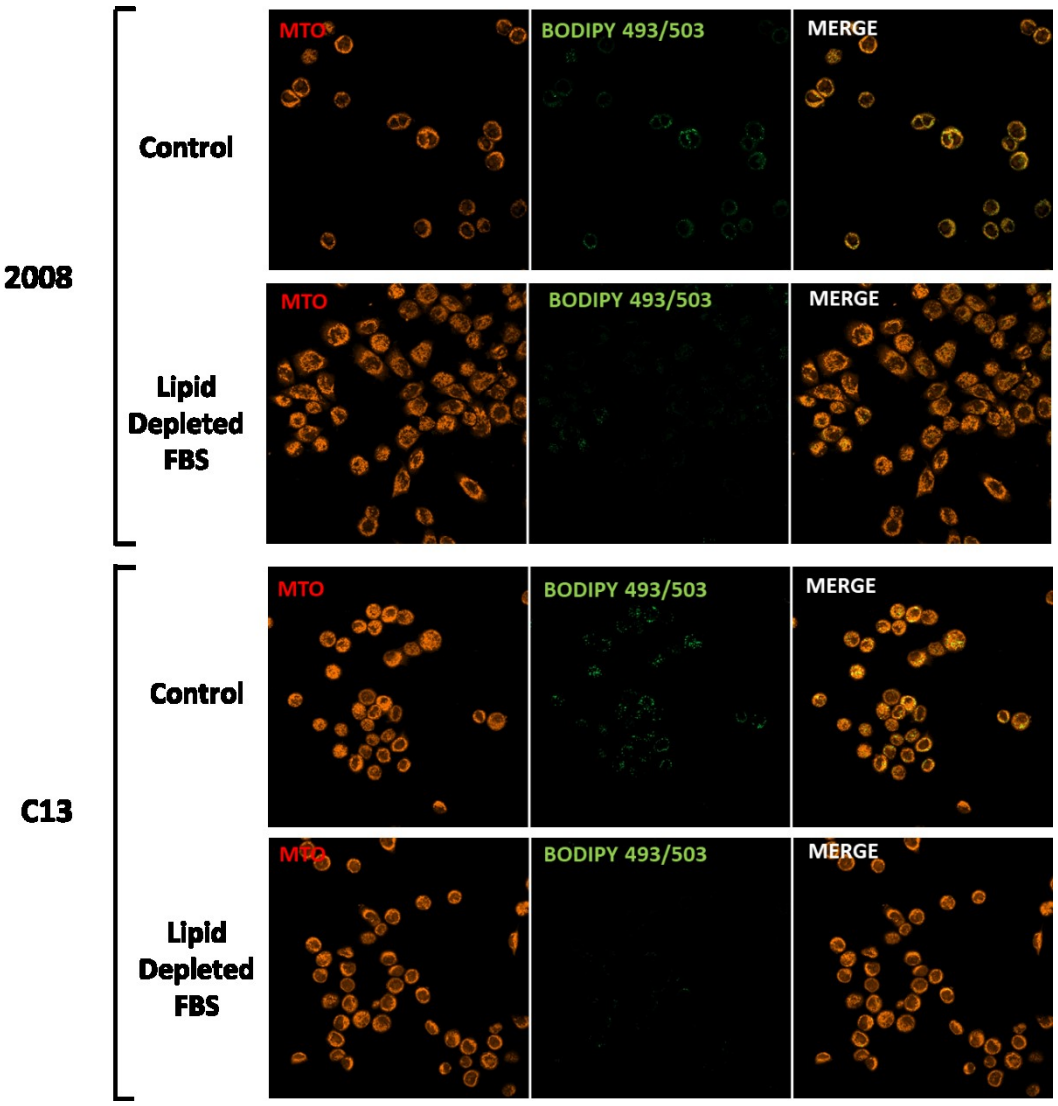

Figure 52: Representative images of the effect of 24 hours of lipid depletion on Lipid droplets accumulation. 2008 and C13 were stained with Mitotracker orange (25 nM; λec/em:554/576nm), and Bodipy 486 (λec/em:493/503nm). Images were acquired by confocal microscopy Zeiss LSM 800, analyzed with ZEN 2.0 imaging software and are representative of 3 different experiments.

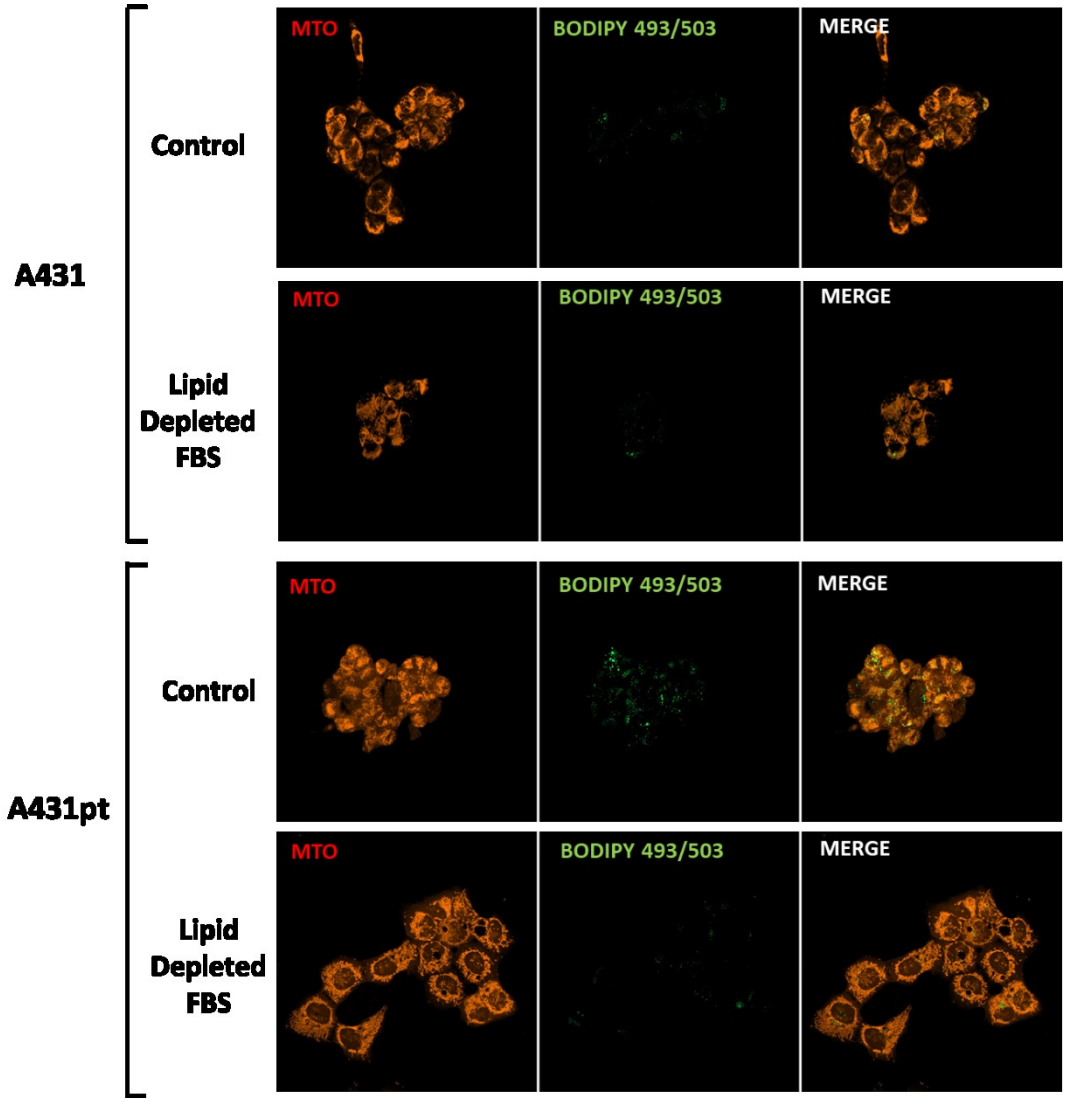

Figure 53: Representative images of the effect of 24 hours of lipid depletion on Lipid droplets accumulation. A431 and A431pt were stained with Mitotracker orange (25 nM; λec/em:554/576nm), and Bodipy 486 (λec/em:493/503nm). Images were acquired by confocal microscopy Zeiss LSM 800, analyzed with ZEN 2.0 imaging software and are representative of 3 different experiments.

Having verified that the serum lipid depletion induces a slight reduction of cell viability (without differences between sensitive and resistant clones) and a reduction in lipid droplet accumulation, the effect of its combination with cisplatin has been investigated.

Results in Figure 54 show that in 2008 cell line (B) the lipid deprivation does not alter cells viability with respect to cisplatin treatment. Interestingly, in the resistant C13 clone (C), the association between cisplatin and lipid depletion induced a significant decrease in cell viability with respect to cisplatin alone.

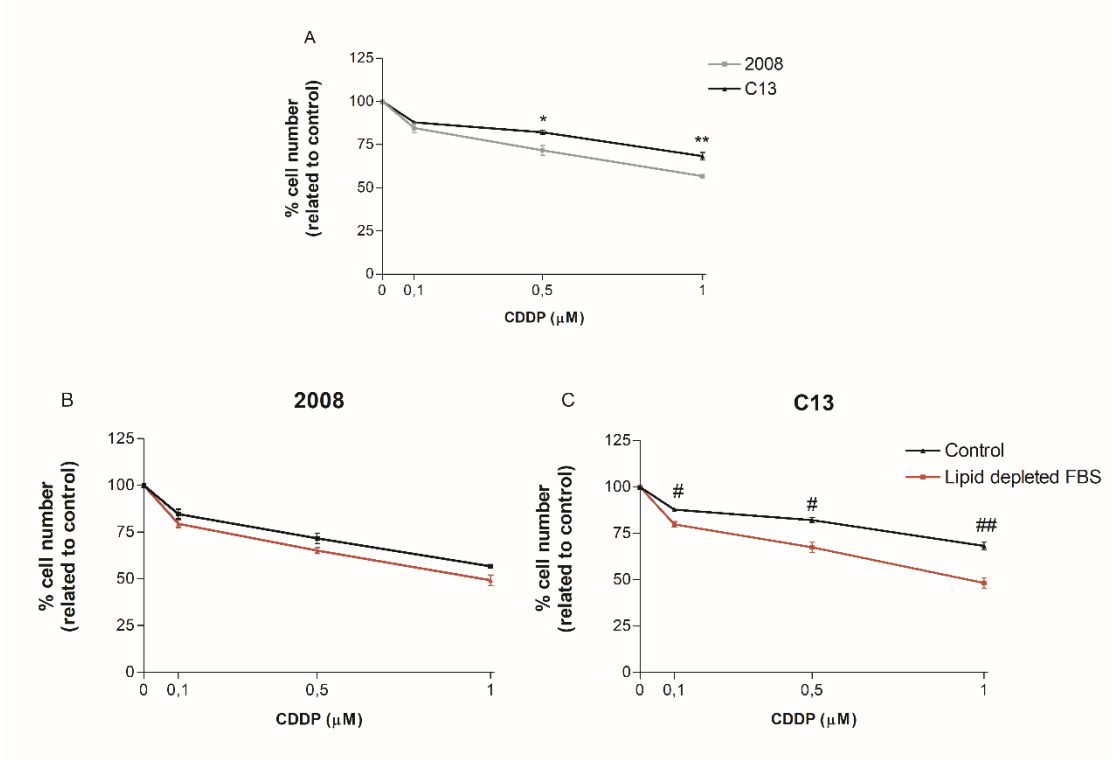

Figure 54: Effect of 24 hours of CDDP treatment (A) or combined treatment with CDDP and Lipid depleted FBS on 2008 (B) and C13 (C) cells viability measured by Trypan Blue Exclusion Assay. Data are expressed as %of cell number related to control and are the mean±SEM of 3 independent experiments. *p<0.05; **p<0.01 Resistant *vs* sensitive cells, # p<0.05; ##p<0.01 lipid depletion *vs* control.

Similar trend has been observed for A431-A431pt cell lines (Figure 55). In fact, the association has no different effect with respect to the cisplatin in the sensitive A431 line (B) but it induces a significant decrease in cell viability of CDDP-resistant A431pt (C).

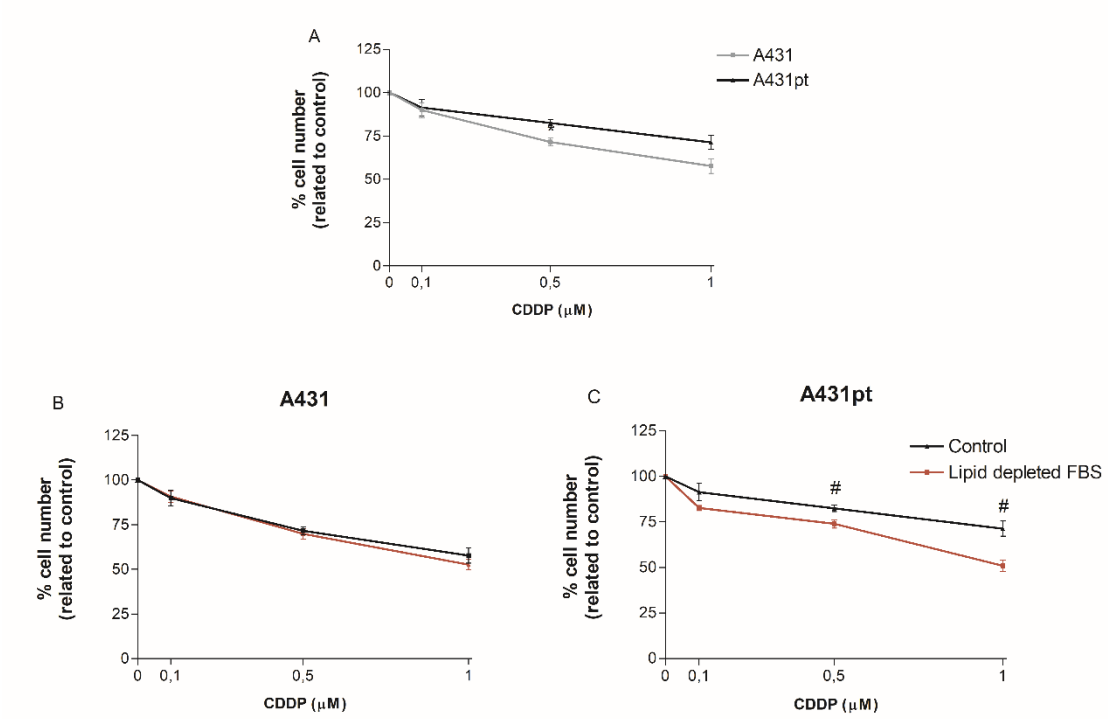

Figure 55: Effect of 24 hours of CDDP treatment (A) or combined treatment with CDDP and Lipid depleted FBS on A431 (B) and A431pt (C) cells viability measured by Trypan Blue Exclusion Assay. Data are expressed as % of cell number related to control and are the mean±SEM of 3 independent experiments. # $p<0.05$ lipid depletion *vs* control.

4.2.1.2 Pharmacological modulation of lipid metabolism

Results showed that all the resistant clones (C13 and A431pt) present a downregulation of PPARα gene-level compared to the sensitive clones (2008 and A431). Thus, the effect of a well-known drug, an agonist of PPARα, has been tested. Fenofibrate (FF; propan-2-yl 2-{4-[(4-chlorophenyl) carbonyl]phenoxy}-2-methylpropanoate) is a well-tolerated, FDA-approved anti-hyperlipidemic and vasoactive drug, which lowers serum levels of triglycerides and cholesterol, and improves the low-density lipoprotein[165]. PPARα-dependent and PPARα-independent signaling are involved in cancer cell reactions to FF. The effect of this modulator of the lipid metabolism has been tested in order to study if the perturbation of the lipid homeostasis can alter the cellular response to the chemotherapeutic drug.

Cell viability

The effect of 24 hours treatment with fenofibrate on cell viability has been tested.

Results in Figure 56(A-B) show that cell viability is not significantly altered in none of the cell lines under study. Only the highest concentration of FF induces a decrease in cells viability.

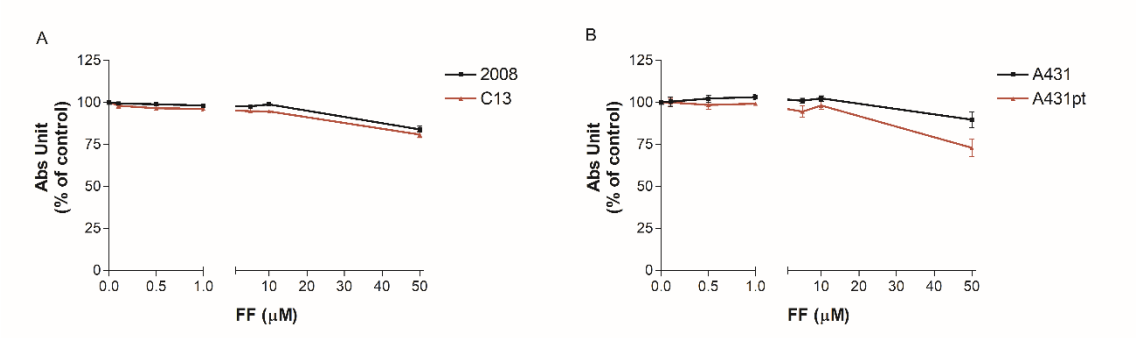

Figure 56: Effect of fenofibrate (0,1-0,5-1-5-10 μM) on cell viability after 24 hours treatment. (A) 2008-C13 cell lines, (B) A431-A431pt cell lines. Results are expressed as % of cells related to control and are the mean±SEM of at least 3 independent experiments.

Having verified that treatment with FF does not affect cell viability in all the cell lines, the effect of the combinatory treatment of FF and CDDP has been tested. Two concentrations of FF have been used for the experiments, 0.1 and 0.5 μM, and results are reported in Figure 57 (2008-C13) and Figure 58 (A431-A431pt). The two sensitive and the two resistant clones present a similar trend of response to the treatment. In the 2008 and A431 sensitive cell line the association of CDDP with FF 0.1 μM is more effective in reducing cells viability respect the CDDP alone (Figure 57 and Figure 58 (A)). The association with FF 0.5 μM seems to have no different effect respect the CDDP alone (Figure 57 and Figure 58 (C)). Data regarding the CDDP resistant clones show that the association of CDDP with FF 0.1 μM induces a significant reduction in cell viability compared to CDDP alone (Figure 57 and Figure 58 (B)). Interestingly, the higher concentration of FF (0.5 μM) sensitizes C13 and A431pt cells to low CDDP concentrations while increasing the CDDP concentration this combinatory effect is reduced (Figure 57 and Figure 58 (D)).

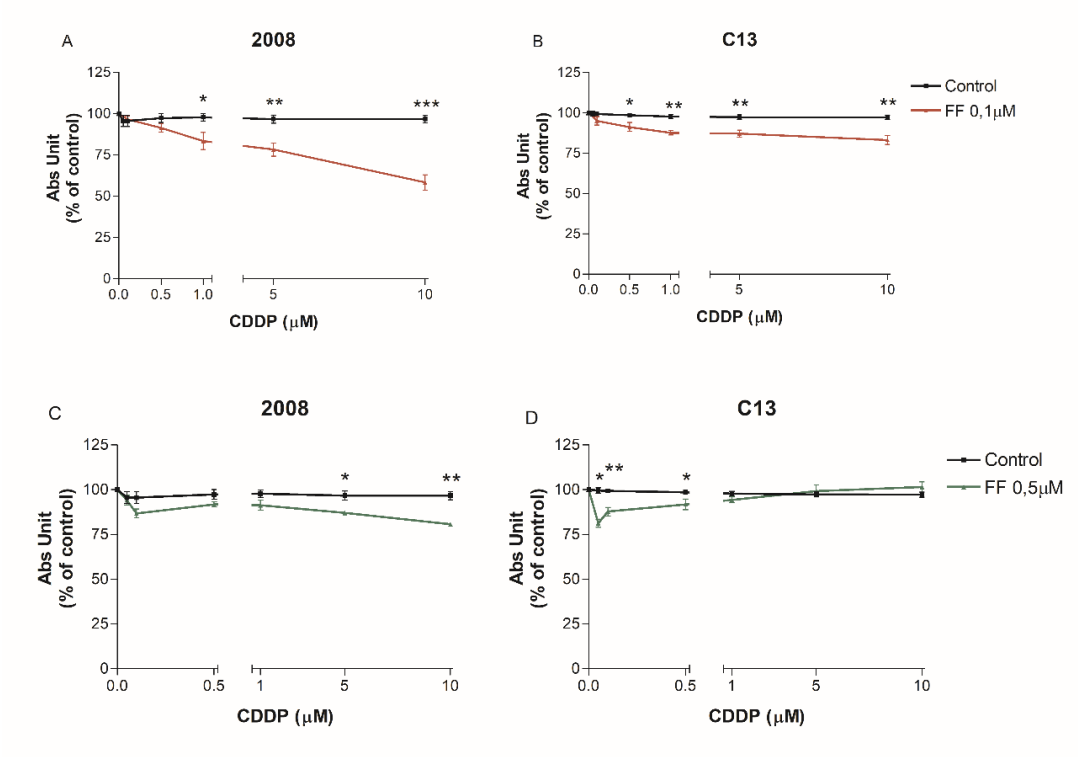

Figure 57: Effect of 24 hours of co-treatment with CDDP and FF 0.1 µM (A-B) and 0.5 µM (C-D) on 2008 and C13 cell viability measured by SRB assay. Results are expressed as % of vital cells related to control and are the mean±SEM of at least 3 independent experiments. *p<0.05; **p<0.01; ***p<0.001 FF *vs* Control.

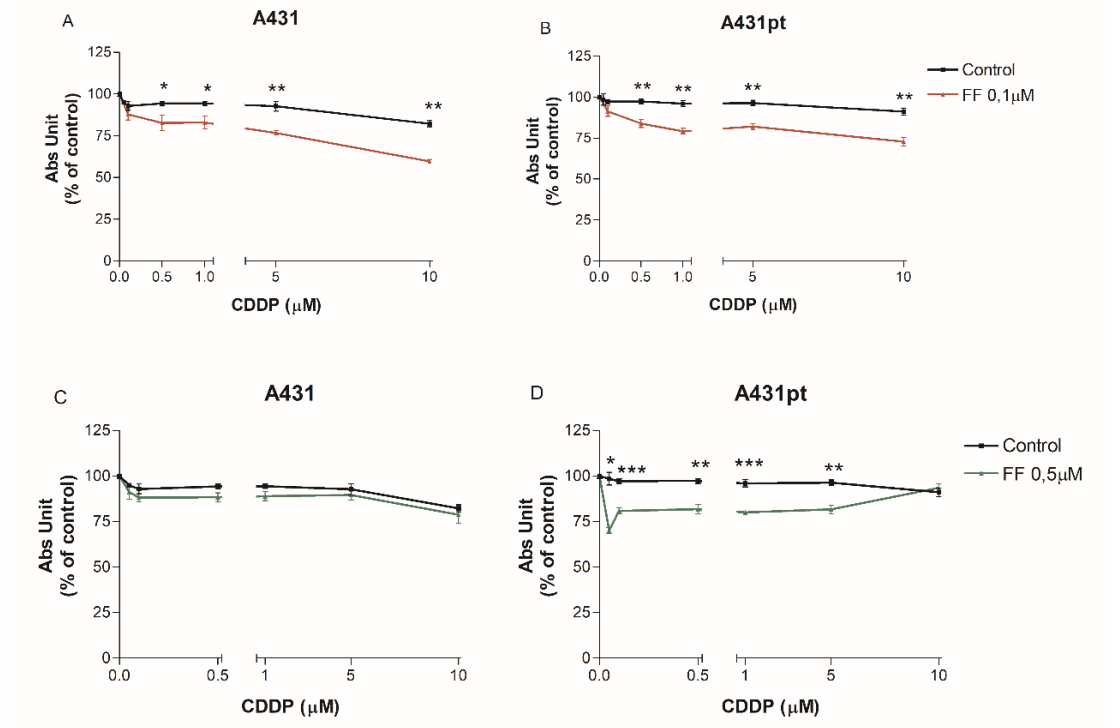

Figure 58: Effect of 24 hours of co-treatment with CDDP and FF 0,1 µM (A-B) and 0,5 µM (C-D) on A431 and A431pt cells viability measured by SRB assay. Results are expressed as % of vital cells related to control and are the mean±SEM of at least 3 independent experiments. *p<0.05; **p<0.01; ***p<0.001 FF *vs* Control.

Fatty acid uptake -Cytofluorimetric analysis

In order to analyze the effect of fenofibrate on the uptake of lipids, this process has been analyzed by flow cytometry using Bodipy FL C_{16} as fluorescent palmitic acid analogous. Cells were treated with fenofibrate (0.5 and 10 μM) and incubated with the probe for 15 minutes. Results in Figure 59 shows that FF 10 μM induces a tendency to an increased uptake in both the ovarian cancer cell lines (2008-C13 (A)) and a significant increase in the uptake in the A431-A431pt cell lines. The lower FF concentration instead, induces a significant reduction in the uptake of lipids in 2008 and C13 (A) and a significant increase in A431pt resistant cell line (B).

Results suggest that the higher concentration of FF induces an increase of uptake while lower concentration displays different effect in the different cell models.

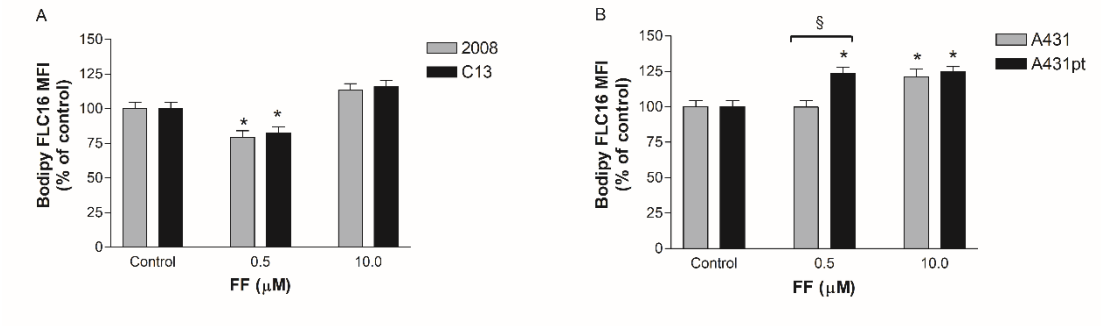

Figure 59: Bodipy FL C16 uptake in 2008-C13 (A) and A431-A431pt (B) cell lines, measured by cytofluorimetry (λec/em:488/525nm). Cells were treated for 24 hours with fenofibrate 0.5 and 10 mM. Data represent the mean of fluorescence intensity normalized to control, following 15 minutes of exposure to the probe. Data are the mean±SEM of 3 independent experiments. *p<0.05 treatment *vs* control; §p<0.05 resistant clones *vs* sensitive clones.

Fatty acid uptake - Confocal Microscopy

The effect of fenofibrate on the modulation of the cellular lipid content has been also evaluated by Confocal Microscopy and the Lipid Droplets content was displayed with Bodipy 493/503 staining.

In line with the results obtained from the cytofluorimetric analysis of the lipid uptake (Figure 59), the low concentration of fenofibrate (0.5μM) induces a decrease in the LDs content both in 2008 and in C13 cell lines. Treatment with fenofibrate at 5 and 50 μM induces a concentration-dependent increase of LDs in both cell lines (Figure 60 and Figure 61).

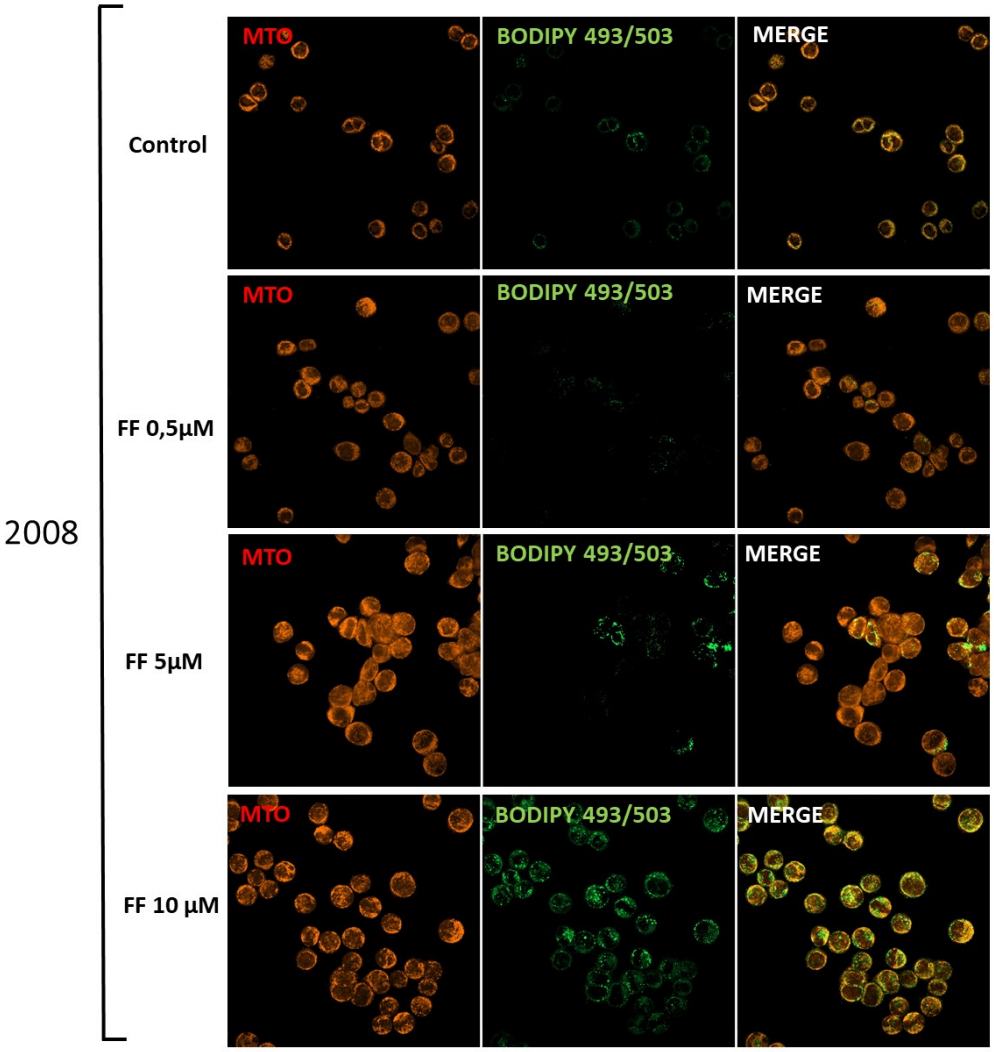

Figure 60: Representative images of the effect of fenofibrate (0.5-5-10 µM) on Lipid droplet accumulation in 2008 cells. Cells were stained with Mitotracker orange (25 nM; λec/em:554/576nm), and Bodipy 486 (λec/em:493/503nm); Images were acquired by confocal microscopy Zeiss LSM 800 and analyzed with ZEN 2.0 imaging software. Images are representative of 3 different experiments.

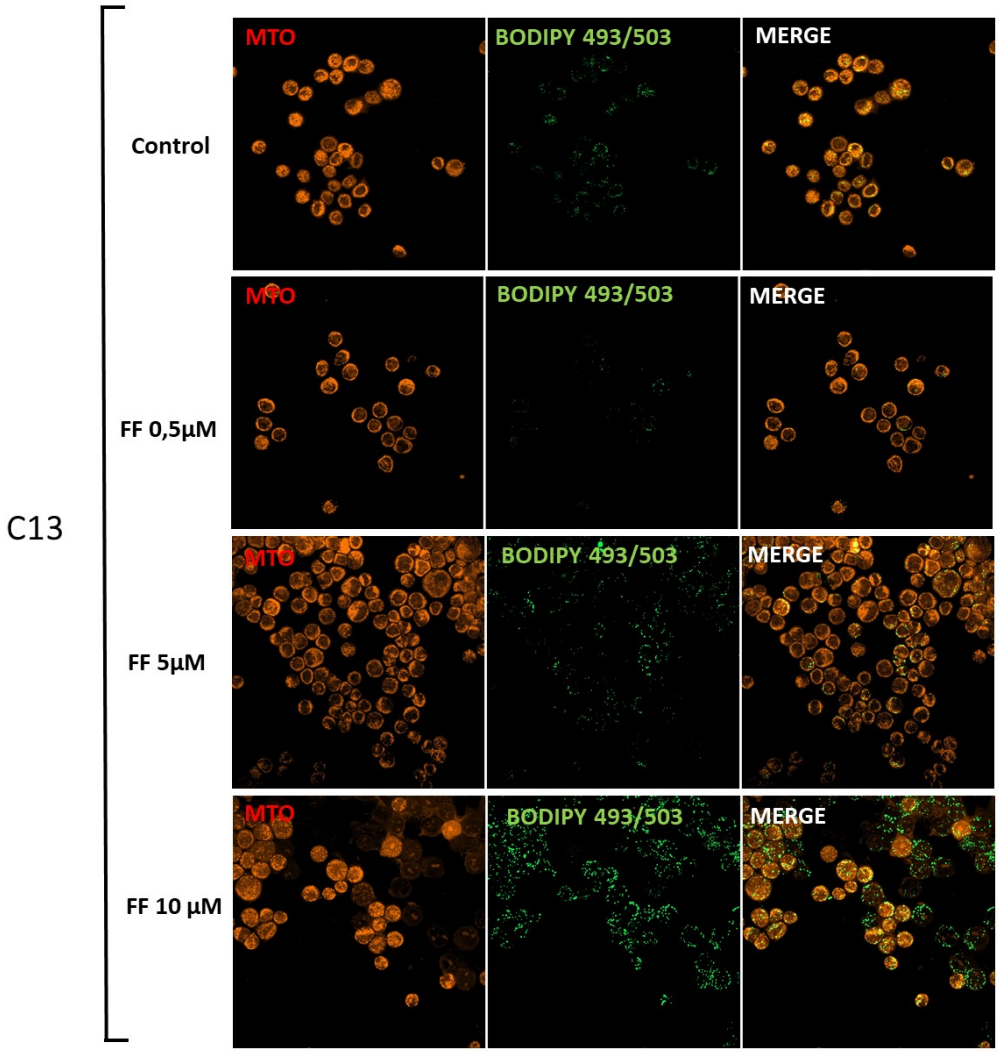

Figure 61: Representative images of the effect of fenofibrate (0.5-5-10 µM) on Lipid droplet accumulation in C13 cells. Cells were stained with Mitotracker orange (25 nM λec/em:554/576nm), and Bodipy 486 (λec/em:493/503nm); Images were acquired by confocal microscopy Zeiss LSM 800 and analyzed with ZEN 2.0 imaging software. Images are representative of 3 different experiments.

Figure 62 and Figure 63show the images acquired for A431 and A31pt respectively. In this case also, results appear in line with the data obtained by the fatty acid-uptake. In fact, the lowest concentration of fenofibrate induces a decrease in the LDs amount in A431 and a moderate increase in the resistant A431pt clone. As for the 2008-C13 lines, fenofibrate 5 µM and 50 µM induces a concentration-dependent increase in the LDs content.

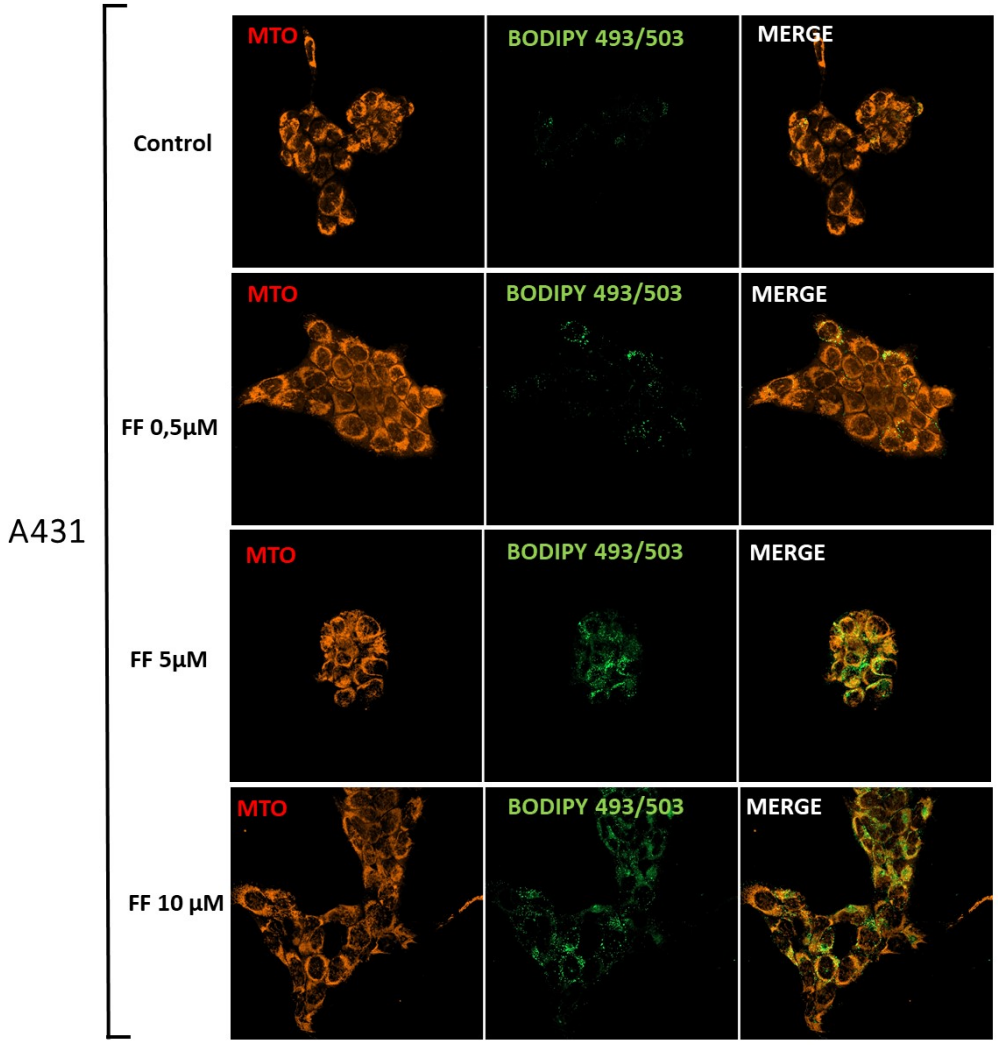

Figure 62: Representative images of the effect of fenofibrate (0.5-5-10 µM) on Lipid droplet accumulation in A431 cells. Cells were stained with Mitotracker orange (25 nM; λec/em:554/576nm), and Bodipy 486 (λec/em:493/503nm); Images were acquired by confocal microscopy Zeiss LSM 800 and analyzed with ZEN 2.0 imaging software. Images are representative of 3 different experiments.

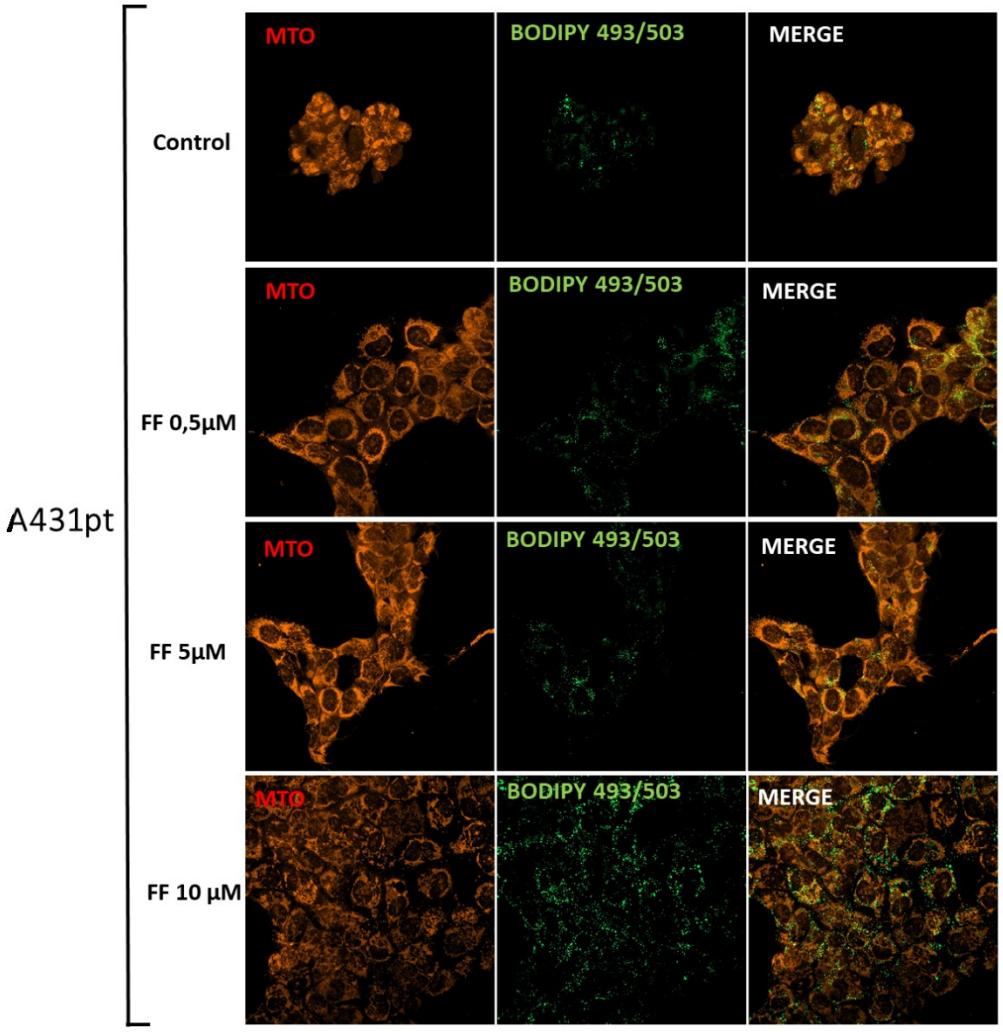

Figure 63: Representative images of the effect of fenofibrate (0.5-5-10 µM) on Lipid droplet accumulation in A431pt cells. Cells were stained with Mitotracker orange (25 nM; λec/em:554/576nm), and Bodipy 486 (λec/em:493/503nm); Images were acquired by confocal microscopy Zeiss LSM 800 and analyzed with ZEN 2.0 imaging software. Images are representative of 3 different experiments.

4.2.2 **Targeting mitochondria Remodeling**

Previous studies in Montopoli's Lab, had already demonstrated that cisplatin-resistant ovarian cancer cells (C13), present altered mitochondrial functions with respect to the sensitive 2008 clone. C13 cells present a reduction in mitochondrial potential and mass, in oxygen consumption, a reduction in the respiratory chain activity and are more susceptible to metabolic stress conditions such as galactose and rotenone incubation[156,157]. Moreover, recent unpublished data of the lab identify a mitochondrial network remodeling shifted toward the fission process in C13 resistant cells suggesting a possible implication of mitochondria remodeling in cisplatin resistance. The mitochondria fragmentation, which leads to smaller mitochondria, is correlated with mitophagy (the mitochondria-selective autophagy), facilitating the engulfment by autophagosomes[166,167].

The investigations regarding the autophagy process, and more specifically the mitophagy process, suggested that the cisplatin resistant cells present faster mitochondria turnover and that mitophagy might be a mitochondria quality control mechanism. Indeed, the mitophagy process could avoid the mtDNA damage caused by cisplatin allowing cells to survive.

Results in Figure 64 show the expression of BNIP3 (BCL2/adenovirus E1B 19 kDa protein-interacting protein 3), one of the main mitophagic regulators which act as receptor for autophagic machinery at the surface of mitochondria. C13 cells present a significantly higher level of BNIP3 both in gene expression[157] (A) and in protein level (B) with respect to the parental cells.

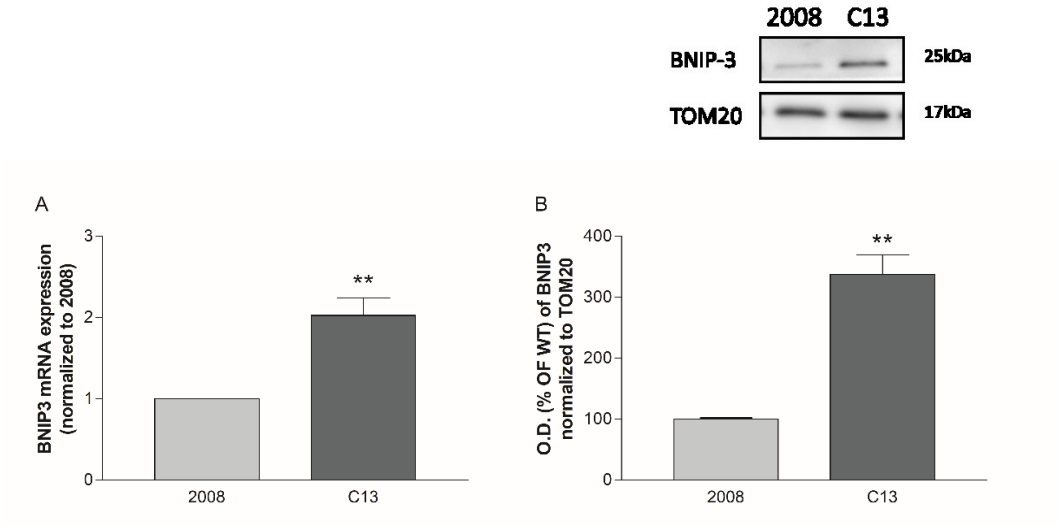

Figure 64: BNIP3 levels in 2008-C13 cells. (A) BNIP3 mRNA levels of C13 related to 2008 cells, measured by qRT-PCR assay[157]. B) BNIP3 C13 protein level measured by Western Blot assay. Data are reported as % of BNIP3 levels, normalized on TOM20. All the data are the mean±SEM of 3 independent experiments. ** $p<0.01$ C13 *vs* 2008.

In order to understand if the upregulation of mitophagy is linked to cells survival to CDDP, BNIP3 has been silenced (Figure 65 A).

BNIP3 knocked-down cells have been treated with cisplatin to verify whether a reduction of mitophagy levels induced by BNIP3 ablation could restore sensitivity to cisplatin. Figure 65(C) shows similar cell viability curves after cisplatin treatment in resistant and sensitive cell lines, treated with BNIP3 esiRNA as compared to the scrambled lines (B). These results suggest a possible role of mitophagy in giving an advantage in survival after cisplatin treatment.

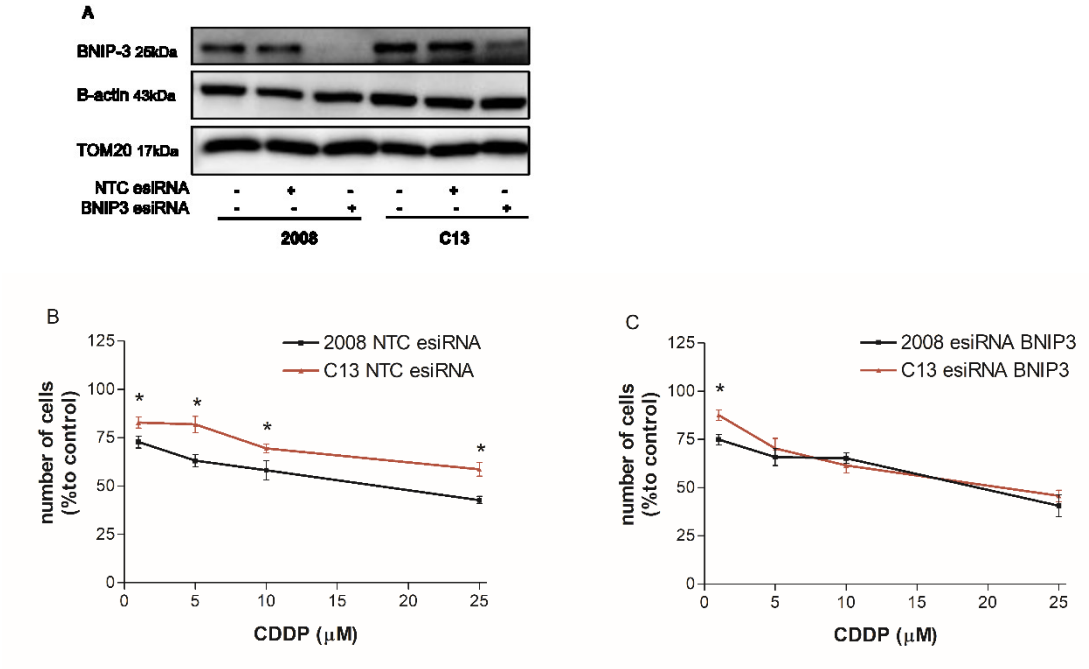

Figure 65: (A) 2008-C13 were transfected with a control NTC esiRNA (scramble esiRNA) or esiRNA targeting BNIP3 (esiBNIP3) and analyzed for BNIP3 protein expression, normalized to TOM20 and beta-actin. B-C) Effect of 24 h treatment with CDDP (1-5-10-25 μM) on cell viability of 2008-C13 scramble (B) or BNIP3 silenced cells (C). Data are expressed as % of cell number of treated cells compared to the untreated controls. Data are the mean ±SEM of 3 different experiments. *$p<0.05$, C13 *vs* 2008.

Specific inhibitors of mitophagy are not currently in commerce. Therefore, with a view to a pharmacological approach to reduce cisplatin resistance, we corroborated our data using two highly specific small molecules inhibitors of the autophagic process. PIK-III and SAR-405[168169] are two specific inhibitors of the Vacuolar protein sorting 34 (Vps34) that plays a role in intracellular vesicular trafficking and autophagosome formation during autophagy[170]. Previous studies of our lab have already demonstrated that resistant C13 cells present an increased autophagic rate with respect to the 2008[157]. Thus, the effect of autophagy inhibitors combined with cisplatin has been tested in our cancer cell model. Results in Figure 66 show that both the inhibitors are more effective in reducing C13 cells viability with respect to 2008.

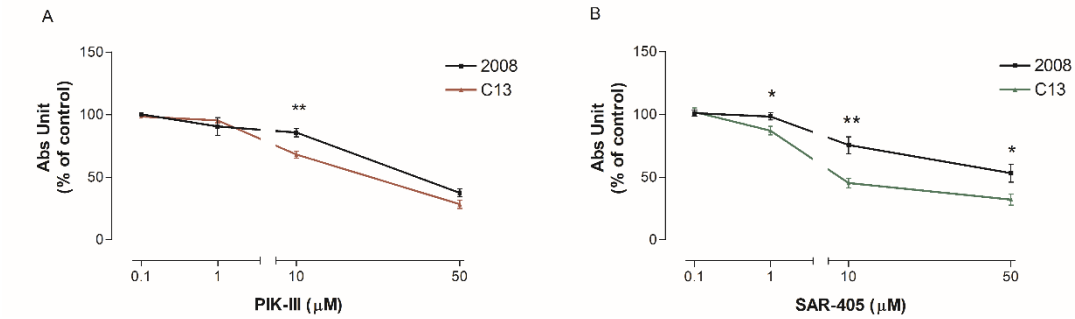

Figure 66: Effect of 24 hours treatment with PIK-III(A) and SAR-405 (B) (0.1-1-10-50 μM) on cells viability measured by SRB assay. Results are expressed as %Abs related to control and are the mean±SEM of at least 3 independent experiments. *p<0.05; **p<0.01 C13 *vs* 2008.

Results in Figure 67 show that the association with of the inhibitors with cisplatin has no effect on 2008 cell viability (A-C) while it induces a significant decrease in resistant cell viability respect the cisplatin treatment (B-D).

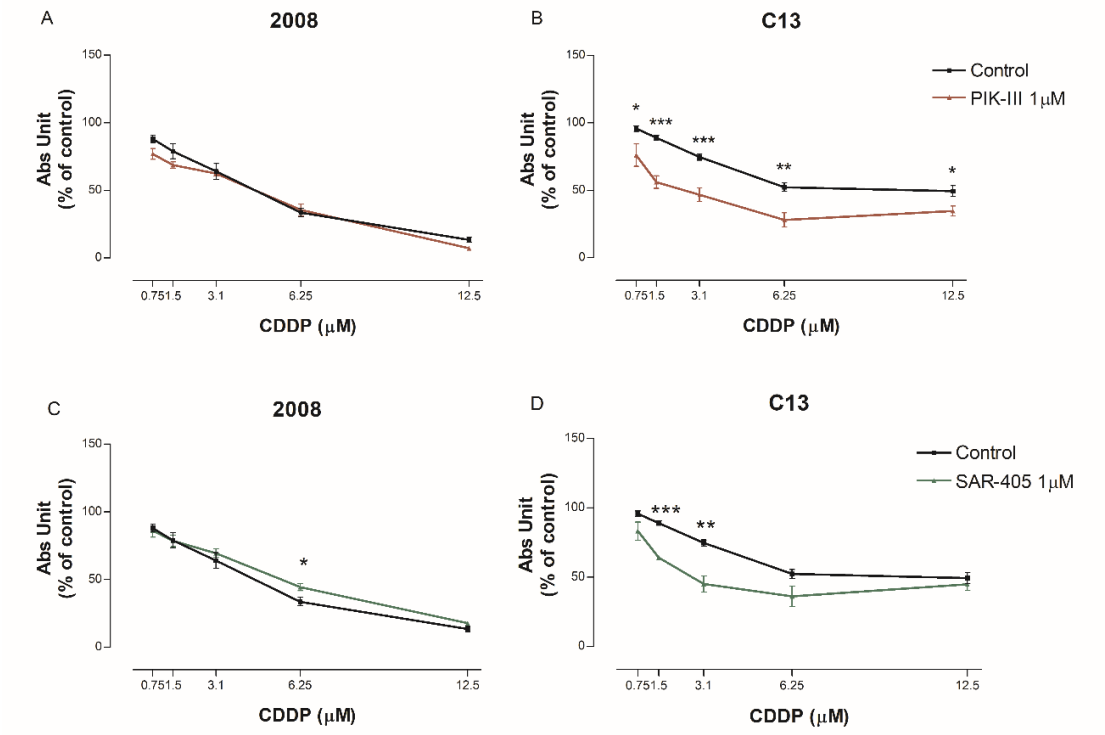

Figure 67: Effect of 24 hours combination of autophagy inhibitors and CDDP (0.75-1.5-3.1-6.25-12.5 M) on 2008-C13 cell viability measured by SRB assay. (A-B) PIK-III (1μM)); (C-D) SAR-405 (1μM). Data are expressed as Abs % related to control and are the mean±SEM of at least 3 independent experiments. *p<0.05; **p<0.01; ***p<0.0001 association *vs* CDDP.

These data confirm that targeting autophagy can be a valid strategy in order to restore cisplatin sensitivity in resistant cells.

5 DISCUSSION

Cancer metabolic reprogramming is firmly established as one of the cancer hallmarks. In order to support rapid proliferation, survival in severe microenvironment, invasion, and metastasis, cancer cells need to reprogram their catabolic and anabolic processes; the rewiring concerns all the four major classes of macromolecules (carbohydrates, proteins, lipids, and nucleic acids[88]) and allows cells to adjust the energy metabolism, in order to dispose of the necessary large amount of energy and biomass[171].

cis-diamminedichloroplatinum (II) (best known as cisplatin), is one of the most potent and most employed alkylating chemotherapeutic agents in the treatment of several solid malignancies (including ovarian, testicular, colorectal, bladder, lung, and head and neck, cancers)[19]. Despite a consistent rate of initial responses, cisplatin treatment often results in therapeutic failure, due to the development of chemoresistance. Resistance is a multifactorial event, whose mechanism has been investigated for the past 30 years. Besides the most known mechanisms of resistance (which include decreased drug uptake, increased export, increased levels of intracellular glutathione and DNA repair mechanisms, or a decreased apoptosis), findings of last years have highlighted a prominent role of cancer metabolic reprogramming in cisplatin-resistance phenomena[28].

Previous studies of our laboratory have already demonstrated that cisplatin-resistant ovarian cancer cells (C13) present a higher dependency on glucose[122] and impaired mitochondrial parameters with respect to the sensitive cells (2008). Mitochondrial potential and mass are reduced, as well as oxygen consumption; moreover, C13 cells viability is reduced in metabolic stress conditions such as rotenone and galactose. Furthermore, we have also demonstrated that cisplatin-resistant cancer cells rely on the PPP pathway to overcome drug toxicity by upregulation of G6PDH enzyme[157]. The combined treatment with G6PDH inhibitors such as 6-AN and cisplatin, showed an addictive effect in C13 cell lines, suggesting G6PDH as a potentially targetable enzyme to increase drug efficacy.

H-NMR spectroscopy analysis has also shown a higher basal content of mobile lipids (MLs) in C13 cells as compared to 2008 cells, with higher lipid accumulation mainly within cytoplasmic droplets of the C13 cells[156]. These findings allow us to propose a

"metabolic remodeling" of cisplatin-resistant ovarian carcinoma cells to a lipogenic phenotype.

On the wave of these observations, the purpose of this work has been the evaluation of the metabolic alterations in lipid metabolism and glutamine pathway in different cisplatin-resistant cancer cells, with the final aim of identifying specific metabolic liabilities and specific targets of resistant cells exploitable to overcome the resistance. Future perspective will be the extension of the current studies to other platinum drugs currently used in clinical therapy, like oxaliplatin or carboplatin.

Results of this work, in line with the recent literature[116,117], show a strong lipid avidity in the analyzed cancer cell lines, more significant in the CDDP-resistant clones (C13 and A431pt).

Numerous studies have shown that many human cancer cells present high *de novo* lipogenesis mediated by high activities of FASN enzyme. Moreover, inhibition of FASN has been shown to sensitize ovarian cancer cells to cisplatin treatment[172,173]. In our cell models, results underline that lipid accumulation is due to an increased exogenous fatty acids uptake rather than to alterations in the synthesis or degradation pathways. Even if the results of this work did not allow the identification of a resistant cell-specific active mechanism of lipid transport, the availability of fatty acids in the microenvironment has been shown to influence cancer cells response to cisplatin treatment. In fact, the deprivation of lipids from the culture media, besides inducing a reduction in lipid droplet accumulation, sensitizes resistant cells to cisplatin treatment. Some studies revealed that the uptake of exogenous lipids promotes the pathogenesis of prostate cancer and that adipocytes promote tumorigenesis and metastasis by providing free FAs to ovarian cancer and breast cancer cells[142,174,175]. So, our observations fit in the literature contest, supporting the idea of an involvement of the lipid accumulation in the capacity of resistant cells to escape drug toxicity.

Results indicate also a common reduction in Peroxisome proliferator-activated receptor-alpha (PPARα) gene expression in resistant cancer cells. PPARα is activated by a variety of endogenous molecules (including FAs and FA derivatives) that make it an intracellular lipid sensor. Its activation, especially during fasting, promotes processes such as FAO and ketogenesis, fatty acids uptake, and triglycerides metabolism and storage[176].

Fenofibrate is a fibric acid derivative commonly used in the clinic for dyslipidemia treatment[177], which presents lipid-modifying effects mediated by the activation of PPARα.

Several recent studies provide evidence that fenofibrate also exerts anticancer effect in different tumor cell lines (prostate, liver, breast, lung, glioma, and pancreas) via a variety of pathways involved in cell-cycle arrest, apoptosis and migration[178].

In this scenario, we tested the effect of fenofibrate in our cell models in order to verify if the fibrate properties can modulate cells response to cisplatin treatment. Results showed that fenofibrate sensitizes both sensitive and resistant clones to CDDP. Data also show that low concentration of fenofibrate induces a slight reduction in lipid accumulation while higher doses induce a concentration-dependent increase in LDs within the cells. These results open up the possibility that fenofibrate determines an imbalance in the lipid metabolic pathways, which may lead to excess amounts of free FAs in cells inducing to lipotoxicity[179]. Moreover, also the "lipid quality" within the LDs is an important factor to be considered in the lipotoxicity phenomena[117].

Clinical evidence has already suggested a role of excess adipose tissue as a causal fact for the development of chemotherapeutic drug resistance[180–182]. Obesity can, in fact, modify the pharmacokinetics of the drug, induce chronic inflammations, and can alter tumor-associated adipocyte adipokine secretion[180–182]. Especially for tumors which microenvironment is rich in adipose tissue, like breast and gynecological cancers, this aspect plays an important role. Different *in vitro* studies have demonstrated that adipocytes enhance ovarian cancer cell chemoresistance supporting these observations[126,183]. In line with these facts, results obtained in this work show a connection between lipid profile and cisplatin resistance. A deep understanding of this aspect could help in the identification of specific metabolic targets exploitable for combinatory therapy. Moreover, new insights in this aspect could help in the development of new therapeutic approaches, aimed at targeting energy pathways, through a combination of lifestyle (especially diet and physical activity) and pharmacological approaches.

Always with regard to the investigation in the different cells' metabolic pathways, previous unpublished data of our laboratory have identified an imbalance in

mitochondria-dynamic in CDDP-resistant cells toward the fission process. Fission is closely linked to mitophagy, the selective autophagy of damaged mitochondria[166] and several studies have previously shown that induction of autophagy causes drug resistance[184]. The selective autophagy of mitochondria promotes cell survival by removing damaged mitochondria sparing cells from apoptosis. Results obtained in this work support this idea; in fact, the silencing of BNIP3 sensitizes cisplatin-resistant cancer cells to the drug. Moreover, since in commerce there are not mitophagy specific inhibitors, our results were confirmed using two autophagy inhibitors; PIK-III and SAR-405 are well-known small molecules inhibitors of Vps34[168] [169], mediators of the autophagic process. Results show that both are able to sensitize resistant cells to cisplatin. Other recent works highlighted the role of mitophagy/ autophagy in the survival of cancer cells to chemotherapy suggesting that a combination of inhibitors of these pathways with the conventional chemotherapy could be a novel therapeutic strategy for different cancer types[167,185,186].

In addition, in this work preliminary studies of glutamine implication in cisplatin resistance have been performed. In collaboration with Professor Toker (BIDMC -Harvard Medical School- Boston) the implication of the remodeling of glutamine metabolism in drug resistance has been evaluated in breast cancer cells (model of innate cisplatin resistance) and ovarian cancer cells (acquired resistance). Amino acids metabolism may also offer promising targets to cancer treatment and even if their role in chemotherapy resistance is still in exploration, some studies highlight that amino acid availability might be important in the development of drug resistance. In fact, cancer cells may show great dependency on a specific amino acid[187–189].

A better understanding of metabolic alterations in different drug-resistant cancers is desirable in order to improve cancer therapy. This work takes place in the panorama of research aimed at better characterize the metabolic alteration in cancers and specifically on the research aimed at the identification of specific metabolic liabilities in cisplatin-resistant cancer cells. Metabolism is a complex of intricate and interconnected pathways that cooperate to sustain cell proliferation allowing cells to survive in a challenging environment. A systematic characterization of the main metabolic pathways of transformed cells, (which include glycolysis, oxidative phosphorylation, glutaminolysis, and mitochondria metabolism), and of the interconnection between them and the

microenvironment, can provide new hints for cancer therapy. Better knowledge about metabolic reprogramming will help to identify new prognostic biomarkers and new metabolic targets useful for innovative pharmacological approaches to overcome drug toxicity or to enhance the efficacy of the current chemotherapy.

6 REFERENCES

1. Bray F, Ferlay J, Soerjomataram I, Siegel RL, Torre LA, Jemal A. Global cancer statistics 2018: GLOBOCAN estimates of incidence and mortality worldwide for 36 cancers in 185 countries. *CA Cancer J Clin*. 2018;68(6):394-424. doi:10.3322/caac.21492

2. Omran AR. The Epidemiologic Transition: A Theory of the Epidemiology of Population Change. *Milbank Q*. 2005;83(4):731-757. doi:10.1111/j.1468-0009.2005.00398.x

3. Ortega ÁD, Sánchez-Aragó M, Giner-Sánchez D, Sánchez-Cenizo L, Willers I, Cuezva JM. Glucose avidity of carcinomas. *Cancer Lett*. 2009;276(2):125-135. doi:10.1016/j.canlet.2008.08.007

4. Lee EYHP, Muller WJ. Oncogenes and Tumor Suppressor Genes. *Cold Spring Harb Perspect Biol*. 2010;2(10). doi:10.1101/cshperspect.a003236

5. Liu F, Lei W, O'Rourke JP, Ness SA. Oncogenic mutations cause dramatic, qualitative changes in the transcriptional activity of c-Myb. *Oncogene*. 2006;25(5):795-805. doi:10.1038/sj.onc.1209105

6. Osada H, Takahashi T. Genetic alterations of multiple tumor suppressors and oncogenes in the carcinogenesis and progression of lung cancer. *Oncogene*. 2002;21(48):7421-7434. doi:10.1038/sj.onc.1205802

7. Levine AJ, Puzio-Kuter AM. The Control of the Metabolic Switch in Cancers by Oncogenes and Tumor Suppressor Genes. *Science*. 2010;330(6009):1340-1344. doi:10.1126/science.1193494

8. Turley SJ, Cremasco V, Astarita JL. Immunological hallmarks of stromal cells in the tumour microenvironment. *Nat Rev Immunol*. 2015;15(11):669-682. doi:10.1038/nri3902

9. Abbas Z, Rehman S. An Overview of Cancer Treatment Modalities. *Neoplasm*. September 2018. doi:10.5772/intechopen.76558

10. Vasey PA. Resistance to chemotherapy in advanced ovarian cancer: mechanisms and current strategies. *Br J Cancer*. 2003;89(3):S23-S28. doi:10.1038/sj.bjc.6601497

11. Luqmani YA. Mechanisms of Drug Resistance in Cancer Chemotherapy. *Med Princ Pract*. 2005;14(Suppl. 1):35-48. doi:10.1159/000086183

12. Shi W-J, Gao J-B. Molecular mechanisms of chemoresistance in gastric cancer. *World J Gastrointest Oncol*. 2016;8(9):673-681. doi:10.4251/wjgo.v8.i9.673

13. Swanton C. Intratumor heterogeneity: evolution through space and time. *Cancer Res*. 2012;72(19):4875-4882. doi:10.1158/0008-5472.CAN-12-2217

14. Zaal EA, Berkers CR. The Influence of Metabolism on Drug Response in Cancer. *Front Oncol*. 2018;8. doi:10.3389/fonc.2018.00500

15. Division C, Products E, Electrode P. Inhibition of Cell Division in Escherichia coli by Electrolysis Products from a Platinum Electrode. *Nature*. 1965;20:698-699.

16. Icrf W, Harris C. O 4·4 9'8 •. 1969;222:385-386.

17. Coluccia M, Natile G. Trans-platinum complexes in cancer therapy. *Anticancer Agents Med Chem*. 2007;7(1):111-123. doi:10.2174/187152007779314080

18. Monneret C. Platinum anticancer drugs. From serendipity to rational design. *Ann Pharm Fr*. 2011;69(6):286-295. doi:10.1016/j.pharma.2011.10.001

19. Ho GY, Woodward N, Coward JIG. Cisplatin versus carboplatin: comparative review of therapeutic management in solid malignancies. *Crit Rev Oncol Hematol*. 2016;102:37-46. doi:10.1016/j.critrevonc.2016.03.014

20. Florea AM, Büsselberg D. Cisplatin as an anti-tumor drug: Cellular mechanisms of activity, drug resistance and induced side effects. *Cancers*. 2011;3(1):1351-1371. doi:10.3390/cancers3011351

21. Ghosh S. Cisplatin: The first metal based anticancer drug. *Bioorganic Chem*. 2019;88:102925. doi:10.1016/j.bioorg.2019.102925

22. Kartalou M, Essigmann JM. Recognition of cisplatin adducts by cellular proteins. *Mutat Res Mol Mech Mutagen*. 2001;478(1):1-21. doi:10.1016/S0027-5107(01)00142-7

23. More SS, Akil O, Ianculescu AG, Geier EG, Lustig LR, Giacomini KM. Role of the Copper Transporter, CTR1, in Platinum-Induced Ototoxicity. *J Neurosci*. 2010;30(28):9500-9509. doi:10.1523/JNEUROSCI.1544-10.2010

24. Fichtinger-Schepman AMJ, Van der Veer JL, Den Hartog JHJ, Lohman PHM, Reedijk J. Adducts of the antitumor drug cis-diamminedichloroplatinum(II) with DNA: formation, identification, and quantitation. *Biochemistry*. 1985;24(3):707-713. doi:10.1021/bi00324a025

25. Florea A-M, Büsselberg D. Cisplatin as an anti-tumor drug: cellular mechanisms of activity, drug resistance and induced side effects. *Cancers*. 2011;3(1):1351-1371. doi:10.3390/cancers3011351

26. Brozovic A, Ambriović-Ristov A, Osmak M. The relationship between cisplatin-induced reactive oxygen species, glutathione, and BCL-2 and resistance to cisplatin. *Crit Rev Toxicol*. 2010;40(4):347-359. doi:10.3109/10408441003601836

27. Siddik ZH. Cisplatin: mode of cytotoxic action and molecular basis of resistance. *Oncogene*. 2003;22(47):7265-7279. doi:10.1038/sj.onc.1206933

28. Galluzzi L, Vitale I, Michels J, et al. Systems biology of cisplatin resistance: past, present and future. *Cell Death Dis*. 2014;5(5):e1257. doi:10.1038/cddis.2013.428

29. Judson I, Kelland LR. New Developments and Approaches in the Platinum Arena. *Drugs*. 2000;59(4):29-36. doi:10.2165/00003495-200059004-00004

30. Gullo JJ, Litterst CL, Maguire PJ, Sikic BI, Hoth DF, Woolley PV. Pharmacokinetics and protein binding of cis-dichlorodiammine platinum (II) administered as a one hour or as a twenty hour infusion. *Cancer Chemother Pharmacol*. 1980;5(1):21-26. doi:10.1007/BF00578558

31. Binks SP, Dobrota M. Kinetics and mechanism of uptake of platinum-based pharmaceuticals by the rat small intestine. *Biochem Pharmacol*. 1990;40(6):1329-1336. doi:10.1016/0006-2952(90)90400-F

32. Kilari D, Guancial E, Kim ES. Role of copper transporters in platinum resistance. *World J Clin Oncol*. 2016;7(1):106-113. doi:10.5306/wjco.v7.i1.106

33. Palm ME, Weise CF, Lundin C, et al. Cisplatin binds human copper chaperone Atox1 and promotes unfolding in vitro. *Proc Natl Acad Sci U S A*. 2011;108(17):6951-6956. doi:10.1073/pnas.1012899108

34. Köberle B, Tomicic MT, Usanova S, Kaina B. Cisplatin resistance: Preclinical findings and clinical implications. *Biochim Biophys Acta BBA - Rev Cancer*. 2010;1806(2):172-182. doi:10.1016/j.bbcan.2010.07.004

35. Zhu X, Zhu H, Luo H, Zhang W, Shen Z, Hu X. Molecular mechanisms of cisplatin resistance in cervical cancer. *Drug Des Devel Ther*. June 2016:1885. doi:10.2147/DDDT.S106412

36. Amable L. Cisplatin resistance and opportunities for precision medicine. *Pharmacol Res*. 2016;106:27-36. doi:10.1016/j.phrs.2016.01.001

37. Higashimoto M, Kanzaki A, Shimakawa T, et al. Expression of copper-transporting P-type adenosine triphosphatase in human esophageal carcinoma. https://www.ingentaconnect.com/content/sp/ijmm/2003/00000011/00000003/art00010%3bjsessionid=ecdgtmh7rhbcd.x-ic-live-03. Published March 1, 2003. Accessed September 11, 2019.

38. Miyashita H, Nitta Y, Mori S, et al. Expression of copper-transporting P-type adenosine triphosphatase (ATP7B) as a chemoresistance marker in human oral squamous cell carcinoma treated with cisplatin. *Oral Oncol*. 2003;39(2):157-162.

39. Gottesman MM, Ling V. The molecular basis of multidrug resistance in cancer: The early years of P-glycoprotein research. *FEBS Lett*. 2006;580(4):998-1009. doi:10.1016/j.febslet.2005.12.060

40. Hoffmann U, Kroemer HK. The ABC transporters MDR1 and MRP2: multiple functions in disposition of xenobiotics and drug resistance. *Drug Metab Rev*. 2004;36(3-4):669-701. doi:10.1081/DMR-200033473

41. Lewis AD, Hayes JD, Wolf CR. Glutathione and glutathione-dependent enzymes in ovarian adenocarcinoma cell lines derived from a patient before and after the onset of drug resistance: intrinsic differences and cell cycle effects. *Carcinogenesis*. 1988;9(7):1283-1287. doi:10.1093/carcin/9.7.1283

42. Toyoda H, Mizushima T, Satoh M, et al. HeLa Cell Transformants Overproducing Mouse Metallothionein Show in vivo Resistance to cis-Platinum in Nude Mice. *Jpn J Cancer Res*. 2000;91(1):91-98. doi:10.1111/j.1349-7006.2000.tb00864.x

43. Kasahara K, Fujiwara Y, Nishio K, et al. Metallothionein Content Correlates with the Sensitivity of Human Small Cell Lung Cancer Cell Lines to Cisplatin. *Cancer Res*. 1991;51(12):3237-3242.

44. Schilder RJ, Hall L, Monks A, et al. Metallothionein gene expression and resistance to cisplatin in human ovarian cancer. *Int J Cancer*. 1990;45(3):416-422. doi:10.1002/ijc.2910450306

45. Lu J, Holmgren A. Thioredoxin system in cell death progression. *Antioxid Redox Signal*. 2012;17(12):1738-1747. doi:10.1089/ars.2012.4650

46. Wangpaichitr M, Sullivan EJ, Theodoropoulos G, et al. The Relationship of Thioredoxin-1 and Cisplatin Resistance: Its Impact on ROS and Oxidative Metabolism in Lung Cancer Cells. *Mol Cancer Ther*. 2012;11(3):604-615. doi:10.1158/1535-7163.MCT-11-0599

47. Arnér ESJ, Nakamura H, Sasada T, Yodoi J, Holmgren A, Spyrou G. Analysis of the inhibition of mammalian thioredoxin, thioredoxin reductase, and glutaredoxin by cis-diamminedichloroplatinum (II) and its major metabolite, the glutathione-platinum complex. *Free Radic Biol Med*. 2001;31(10):1170-1178. doi:10.1016/S0891-5849(01)00698-0

48. Cobo M, Isla D, Massuti B, et al. Customizing Cisplatin Based on Quantitative Excision Repair Cross-Complementing 1 mRNA Expression: A Phase III Trial in Non–Small-Cell Lung Cancer. *J Clin Oncol*. September 2016. doi:10.1200/JCO.2006.09.7915

49. Guo H, Liu H, Wu H, et al. Nickel Carcinogenesis Mechanism: DNA Damage. *Int J Mol Sci*. 2019;20(19):4690. doi:10.3390/ijms20194690

50. Furuta T, Ueda T, Aune G, Sarasin A, Kraemer KH, Pommier Y. Transcription-coupled nucleotide excision repair as a determinant of cisplatin sensitivity of human cells. *Cancer Res*. 2002;62(17):4899-4902.

51. Kunkel TA, Erie DA. DNA mismatch repair. *Annu Rev Biochem*. 2005;74:681-710. doi:10.1146/annurev.biochem.74.082803.133243

52. Britten RA, Liu D, Tessier A, Hutchison MJ, Murray D. ERCC1 expression as a molecular marker of cisplatin resistance in human cervical tumor cells. *Int J Cancer*. 2000;89(5):453-457.

53. Selvakumaran M, Pisarcik DA, Bao R, Yeung AT, Hamilton TC. Enhanced cisplatin cytotoxicity by disturbing the nucleotide excision repair pathway in ovarian cancer cell lines. *Cancer Res*. 2003;63(6):1311-1316.

54. Du P, Wang Y, Chen L, Gan Y, Wu Q. High ERCC1 expression is associated with platinum-resistance, but not survival in patients with epithelial ovarian cancer. *Oncol Lett*. 2016;12(2):857-862. doi:10.3892/ol.2016.4732

55. Yin M, Yan J, Martinez-Balibrea E, et al. ERCC1 and ERCC2 polymorphisms predict clinical outcomes of oxaliplatin-based chemotherapies in gastric and colorectal cancer: a systemic review and meta-analysis. *Clin Cancer Res Off J Am Assoc Cancer Res*. 2011;17(6):1632-1640. doi:10.1158/1078-0432.CCR-10-2169

56. Vaisman A, Varchenko M, Umar A, et al. The role of hMLH1, hMSH3, and hMSH6 defects in cisplatin and oxaliplatin resistance: correlation with replicative bypass of platinum-DNA adducts. *Cancer Res*. 1998;58(16):3579-3585.

57. Fink D, Aebi S, Howell SB. The role of DNA mismatch repair in drug resistance. *Clin Cancer Res Off J Am Assoc Cancer Res*. 1998;4(1):1-6.

58. Drummond JT, Anthoney A, Brown R, Modrich P. Cisplatin and adriamycin resistance are associated with MutLalpha and mismatch repair deficiency in an ovarian tumor cell line. *J Biol Chem*. 1996;271(33):19645-19648. doi:10.1074/jbc.271.33.19645

59. Papouli E, Cejka P, Jiricny J. Dependence of the Cytotoxicity of DNA-Damaging Agents on the Mismatch Repair Status of Human Cells. *Cancer Res*. 2004;64(10):3391-3394. doi:10.1158/0008-5472.CAN-04-0513

60. Goodspeed A, Jean A, Costello JC. A Whole-genome CRISPR Screen Identifies a Role of MSH2 in Cisplatin-mediated Cell Death in Muscle-invasive Bladder Cancer. *Eur Urol*. 2019;75(2):242-250. doi:10.1016/j.eururo.2018.10.040

61. Peltomäki P. Role of DNA mismatch repair defects in the pathogenesis of human cancer. *J Clin Oncol Off J Am Soc Clin Oncol*. 2003;21(6):1174-1179. doi:10.1200/JCO.2003.04.060

62. Kartalou M, Essigmann JM. Mechanisms of resistance to cisplatin. *Mutat Res Mol Mech Mutagen*. 2001;478(1):23-43. doi:10.1016/S0027-5107(01)00141-5

63. Kim CW, Lu JN, Go S-I, et al. p53 restoration can overcome cisplatin resistance through inhibition of Akt as well as induction of Bax. *Int J Oncol*. 2013;43(5):1495-1502. doi:10.3892/ijo.2013.2070

64. Kigawa J, Sato S, Shimada M, et al. p53 gene status and chemosensitivity in ovarian cancer. *Hum Cell*. 2001;14(3):165-171.

65. Huang W-C, Hung M-C. Induction of Akt Activity by Chemotherapy Confers Acquired Resistance. *J Formos Med Assoc*. 2009;108(3):180-194. doi:10.1016/S0929-6646(09)60051-6

66. Zhang Y, Bao C, Mu Q, et al. Reversal of cisplatin resistance by inhibiting PI3K/Akt signal pathway in human lung cancer cells. *Neoplasma*. 2016;63(3):362-370. doi:10.4149/304_150806N433

67. Gohr K, Hamacher A, Engelke LH, Kassack MU. Inhibition of PI3K/Akt/mTOR overcomes cisplatin resistance in the triple negative breast cancer cell line HCC38. *BMC Cancer*. 2017;17(1):711. doi:10.1186/s12885-017-3695-5

68. Hata AN, Engelman JA, Faber AC. The BCL-2 family: key mediators of the apoptotic response to targeted anti-cancer therapeutics. *Cancer Discov*. 2015;5(5):475-487. doi:10.1158/2159-8290.CD-15-0011

69. Han J-Y, Hong EK, Choi BG, et al. Death receptor 5 and Bcl-2 protein expression as predictors of tumor response to gemcitabine and cisplatin in patients with advanced non-small-cell lung cancer. *Med Oncol*. 2003;20(4):355-362. doi:10.1385/MO:20:4:355

70. Brozovic A, Fritz G, Christmann M, et al. Long-term activation of SAPK/JNK, p38 kinase and fas-L expression by cisplatin is attenuated in human carcinoma cells that acquired drug resistance. *Int J Cancer*. 2004;112(6):974-985. doi:10.1002/ijc.20522

71. Mansouri A, Ridgway LD, Korapati AL, et al. Sustained activation of JNK/p38 MAPK pathways in response to cisplatin leads to Fas ligand induction and cell death in ovarian carcinoma cells. *J Biol Chem*. 2003;278(21):19245-19256. doi:10.1074/jbc.M208134200

72. Basu A, Tu H. Activation of ERK during DNA damage-induced apoptosis involves protein kinase Cdelta. *Biochem Biophys Res Commun*. 2005;334(4):1068-1073. doi:10.1016/j.bbrc.2005.06.199

73. Godwin P, Baird AM, Heavey S, Barr MP, O'Byrne KJ, Gately K. Targeting Nuclear Factor-Kappa B to Overcome Resistance to Chemotherapy. *Front Oncol*. 2013;3. doi:10.3389/fonc.2013.00120

74. Venkatraman M, Anto RJ, Nair A, Varghese M, Karunagaran D. Biological and chemical inhibitors of NF-kappaB sensitize SiHa cells to cisplatin-induced apoptosis. *Mol Carcinog*. 2005;44(1):51-59. doi:10.1002/mc.20116

75. Yun J, Finkel T. Mitohormesis. *Cell Metab*. 2014;19(5):757-766. doi:10.1016/j.cmet.2014.01.011

76. Riera CE, Merkwirth C, De Magalhaes Filho CD, Dillin A. Signaling Networks Determining Life Span. *Annu Rev Biochem*. 2016;85:35-64. doi:10.1146/annurev-biochem-060815-014451

77. DeBerardinis RJ, Chandel NS. Fundamentals of cancer metabolism. *Sci Adv*. 2016;2(5). doi:10.1126/sciadv.1600200

78. Qian X, Xu W, Xu J, et al. Enolase 1 stimulates glycolysis to promote chemoresistance in gastric cancer. *Oncotarget*. 2017;8(29):47691-47708. doi:10.18632/oncotarget.17868

79. Akram M. Mini-review on Glycolysis and Cancer. *J Cancer Educ*. 2013;28(3):454-457. doi:10.1007/s13187-013-0486-9

80. Jin L, Zhou Y. Crucial role of the pentose phosphate pathway in malignant tumors (Review). *Oncol Lett*. 2019;17(5):4213-4221. doi:10.3892/ol.2019.10112

81. Patra KC, Hay N. The pentose phosphate pathway and cancer. *Trends Biochem Sci*. 2014;39(8):347-354. doi:10.1016/j.tibs.2014.06.005

82. Wang D, Dubois RN. Eicosanoids and cancer. *Nat Rev Cancer*. 2010;10(3):181-193. doi:10.1038/nrc2809

83. Rysman E, Brusselmans K, Scheys K, et al. De novo lipogenesis protects cancer cells from free radicals and chemotherapeutics by promoting membrane lipid saturation. *Cancer Res*. 2010;70(20):8117-8126. doi:10.1158/0008-5472.CAN-09-3871

84. Baenke F, Peck B, Miess H, Schulze A. Hooked on fat: the role of lipid synthesis in cancer metabolism and tumour development. *Dis Model Mech*. 2013;6(6):1353-1363. doi:10.1242/dmm.011338

85. Hanahan D, Weinberg RA. Hallmarks of cancer: the next generation. *Cell*. 2011;144(5):646-674. doi:10.1016/j.cell.2011.02.013

86. Menendez JA. Fine-tuning the lipogenic/lipolytic balance to optimize the metabolic requirements of cancer cell growth: molecular mechanisms and therapeutic perspectives. *Biochim Biophys Acta*. 2010;1801(3):381-391. doi:10.1016/j.bbalip.2009.09.005

87. Phan LM, Yeung S-CJ, Lee M-H. Cancer metabolic reprogramming: importance, main features, and potentials for precise targeted anti-cancer therapies. *Cancer Biol Med*. 2014;11(1):1-19. doi:10.7497/j.issn.2095-3941.2014.01.001

88. Cairns RA, Harris IS, Mak TW. Regulation of cancer cell metabolism. *Nat Rev Cancer*. 2011;11(2):85-95. doi:10.1038/nrc2981

89. DeBerardinis RJ, Chandel NS. Fundamentals of cancer metabolism. *Sci Adv*. 2016;2(5):e1600200. doi:10.1126/sciadv.1600200

90. Ward PS, Thompson CB. Metabolic Reprogramming: A Cancer Hallmark Even Warburg Did Not Anticipate. *Cancer Cell*. 2012;21(3):297-308. doi:10.1016/j.ccr.2012.02.014

91. Obre E, Rossignol R. Emerging concepts in bioenergetics and cancer research: Metabolic flexibility, coupling, symbiosis, switch, oxidative tumors, metabolic remodeling, signaling and bioenergetic therapy. *Int J Biochem Cell Biol*. 2015;59:167-181. doi:10.1016/j.biocel.2014.12.008

92. Warburg O, Wind F, Negelein E. THE METABOLISM OF TUMORS IN THE BODY. *J Gen Physiol*. 1927;8(6):519-530. doi:10.1085/jgp.8.6.519

93. Hay N. Reprogramming glucose metabolism in cancer: can it be exploited for cancer therapy? *Nat Rev Cancer*. 2016;16:635.

94. Kroemer G, Pouyssegur J. Tumor Cell Metabolism: Cancer's Achilles' Heel. *Cancer Cell*. 2008;13(6):472-482. doi:10.1016/j.ccr.2008.05.005

95. Gatenby RA, Gillies RJ. Why do cancers have high aerobic glycolysis? *Nat Rev Cancer*. 2004;4(11):891-899. doi:10.1038/nrc1478

96. Pouysségur J, Dayan F, Mazure NM. Hypoxia signalling in cancer and approaches to enforce tumour regression. *Nature*. 2006;441(7092):437-443. doi:10.1038/nature04871

97. Koukourakis MI, Giatromanolaki A, Harris AL, Sivridis E. Comparison of metabolic pathways between cancer cells and stromal cells in colorectal carcinomas: a metabolic survival role for tumor-associated stroma. *Cancer Res*. 2006;66(2):632-637. doi:10.1158/0008-5472.CAN-05-3260

98. Swietach P, Vaughan-Jones RD, Harris AL. Regulation of tumor pH and the role of carbonic anhydrase 9. *Cancer Metastasis Rev*. 2007;26(2):299-310. doi:10.1007/s10555-007-9064-0

99. Berardi MJ, Fantin VR. Survival of the fittest: metabolic adaptations in cancer. *Curr Opin Genet Dev*. 2011;21(1):59-66. doi:10.1016/j.gde.2010.10.001

100. Windmueller HG, Spaeth AE. Uptake and metabolism of plasma glutamine by the small intestine. *J Biol Chem*. 1974;249(16):5070-5079.

101. Timmerman LA, Holton T, Yuneva M, et al. Glutamine sensitivity analysis identifies the xCT antiporter as a common triple-negative breast tumor therapeutic target. *Cancer Cell*. 2013;24(4):450-465. doi:10.1016/j.ccr.2013.08.020

102. Cluntun AA, Lukey MJ, Cerione RA, Locasale JW. Glutamine Metabolism in Cancer: Understanding the Heterogeneity. *Trends Cancer*. 2017;3(3):169-180. doi:10.1016/j.trecan.2017.01.005

103. Yang L, Venneti S, Nagrath D. Glutaminolysis: A Hallmark of Cancer Metabolism. *Annu Rev Biomed Eng*. 2017;19(1):163-194. doi:10.1146/annurev-bioeng-071516-044546

104. Cormerais Y, Massard PA, Vucetic M, et al. The glutamine transporter ASCT2 (SLC1A5) promotes tumor growth independently of the amino acid transporter LAT1 (SLC7A5). *J Biol Chem*. 2018;293(8):2877-2887. doi:10.1074/jbc.RA117.001342

105. White MA, Lin C, Rajapakshe K, et al. Glutamine Transporters Are Targets of Multiple Oncogenic Signaling Pathways in Prostate Cancer. *Mol Cancer Res MCR*. 2017;15(8):1017-1028. doi:10.1158/1541-7786.MCR-16-0480

106. Gao P, Tchernyshyov I, Chang T-C, et al. c-Myc suppression of miR-23a/b enhances mitochondrial glutaminase expression and glutamine metabolism. *Nature*. 2009;458(7239):762-765. doi:10.1038/nature07823

107. Bott AJ, Maimouni S, Zong W-X. The Pleiotropic Effects of Glutamine Metabolism in Cancer. *Cancers*. 2019;11(6):770. doi:10.3390/cancers11060770

108. Chan WK, Lorenzi PL, Anishkin A, et al. The glutaminase activity of l-asparaginase is not required for anticancer activity against ASNS-negative cells. *Blood*. 2014;123(23):3596-3606. doi:10.1182/blood-2013-10-535112

109. Li T, Le A. Glutamine Metabolism in Cancer. In: Le A, ed. *The Heterogeneity of Cancer Metabolism*. Advances in Experimental Medicine and Biology. Cham: Springer International Publishing; 2018:13-32. doi:10.1007/978-3-319-77736-8_2

110. Cannino G, Ciscato F, Masgras I, Sánchez-Martín C, Rasola A. Metabolic Plasticity of Tumor Cell Mitochondria. *Front Oncol*. 2018;8. doi:10.3389/fonc.2018.00333

111. Carracedo A, Cantley LC, Pandolfi PP. Cancer metabolism: fatty acid oxidation in the limelight. *Nat Rev Cancer*. 2013;13(4):227-232. doi:10.1038/nrc3483

112. Westermann B. Mitochondrial fusion and fission in cell life and death. *Nat Rev Mol Cell Biol*. 2010;11(12):872-884. doi:10.1038/nrm3013

113. Cocetta V, Ragazzi E, Montopoli M. Mitochondrial Involvement in Cisplatin Resistance. *Int J Mol Sci*. 2019;20(14). doi:10.3390/ijms20143384

114. Ackerman D, Simon MC. Hypoxia, lipids, and cancer: surviving the harsh tumor microenvironment. *Trends Cell Biol*. 2014;24(8):472-478. doi:10.1016/j.tcb.2014.06.001

115. Long J, Zhang C-J, Zhu N, et al. Lipid metabolism and carcinogenesis, cancer development. *Am J Cancer Res*. 2018;8(5):778-791.

116. Cao Y. Adipocyte and lipid metabolism in cancer drug resistance. *J Clin Invest*. 2019;129(8):3006-3017. doi:10.1172/JCI127201

117. Petan T, Jarc E, Jusović M. Lipid Droplets in Cancer: Guardians of Fat in a Stressful World. *Mol Basel Switz*. 2018;23(8). doi:10.3390/molecules23081941

118. Qiu B, Ackerman D, Sanchez DJ, et al. HIF2α-Dependent Lipid Storage Promotes Endoplasmic Reticulum Homeostasis in Clear-Cell Renal Cell Carcinoma. *Cancer Discov*. 2015;5(6):652-667. doi:10.1158/2159-8290.CD-14-1507

119. Mentoor I, Engelbrecht A-M, Nell T. Fatty acids: Adiposity and breast cancer chemotherapy, a bad synergy? *Prostaglandins Leukot Essent Fatty Acids*. 2019;140:18-33. doi:10.1016/j.plefa.2018.11.009

120. Glatz JFC, Luiken JJFP, Bonen A. Membrane Fatty Acid Transporters as Regulators of Lipid Metabolism: Implications for Metabolic Disease. *Physiol Rev*. 2010;90(1):367-417. doi:10.1152/physrev.00003.2009

121. Anderson CM, Stahl A. SLC27 fatty acid transport proteins. *Mol Aspects Med*. 2013;34(2-3):516-528. doi:10.1016/j.mam.2012.07.010

122. Wang J, Li Y. CD36 tango in cancer: signaling pathways and functions. *Theranostics*. 2019;9(17):4893-4908. doi:10.7150/thno.36037

123. Enciu A-M, Radu E, Popescu ID, Hinescu ME, Ceafalan LC. Targeting CD36 as Biomarker for Metastasis Prognostic: How Far from Translation into Clinical Practice? BioMed Research International. doi:10.1155/2018/7801202

124. Jia Z, Pei Z, Maiguel D, Toomer CJ, Watkins PA. The fatty acid transport protein (FATP) family: very long chain acyl-CoA synthetases or solute carriers? *J Mol Neurosci MN*. 2007;33(1):25-31.

125. Smathers RL, Petersen DR. The human fatty acid-binding protein family: Evolutionary divergences and functions. *Hum Genomics*. 2011;5(3):170-191. doi:10.1186/1479-7364-5-3-170

126. Amiri M, Yousefnia S, Seyed Forootan F, Peymani M, Ghaedi K, Nasr Esfahani MH. Diverse roles of fatty acid binding proteins (FABPs) in development and pathogenesis of cancers. *Gene*. 2018;676:171-183. doi:10.1016/j.gene.2018.07.035

127. Gimeno RE, Cao J. *Thematic Review Series: Glycerolipids.* Mammalian glycerol-3-phosphate acyltransferases: new genes for an old activity. *J Lipid Res*. 2008;49(10):2079-2088. doi:10.1194/jlr.R800013-JLR200

128. Abramson HN. The Lipogenesis Pathway as a Cancer Target. *J Med Chem*. 2011;54(16):5615-5638. doi:10.1021/jm2005805

129. Kuhajda FP. Fatty-acid synthase and human cancer: new perspectives on its role in tumor biology. *Nutr Burbank Los Angel Cty Calif*. 2000;16(3):202-208.

130. Kuhajda FP. Fatty acid synthase and cancer: new application of an old pathway. *Cancer Res*. 2006;66(12):5977-5980. doi:10.1158/0008-5472.CAN-05-4673

131. Menendez JA, Lupu R. Fatty acid synthase and the lipogenic phenotype in cancer pathogenesis. *Nat Rev Cancer*. 2007;7(10):763-777. doi:10.1038/nrc2222

132. Zaidi N, Swinnen JV, Smans K. ATP-Citrate Lyase: A Key Player in Cancer Metabolism. *Cancer Res*. 2012;72(15):3709-3714. doi:10.1158/0008-5472.CAN-11-4112

133. Milgraum LZ, Witters LA, Pasternack GR, Kuhajda FP. Enzymes of the fatty acid synthesis pathway are highly expressed in in situ breast carcinoma. *Clin Cancer Res Off J Am Assoc Cancer Res*. 1997;3(11):2115-2120.

134. Wilfling F, Haas JT, Walther TC, Farese RV. Lipid droplet biogenesis. *Curr Opin Cell Biol*. 2014;29:39-45. doi:10.1016/j.ceb.2014.03.008

135. Bensaad K, Favaro E, Lewis CA, et al. Fatty acid uptake and lipid storage induced by HIF-1α contribute to cell growth and survival after hypoxia-reoxygenation. *Cell Rep*. 2014;9(1):349-365. doi:10.1016/j.celrep.2014.08.056

136. Rambold AS, Cohen S, Lippincott-Schwartz J. Fatty acid trafficking in starved cells: regulation by lipid droplet lipolysis, autophagy, and mitochondrial fusion dynamics. *Dev Cell*. 2015;32(6):678-692. doi:10.1016/j.devcel.2015.01.029

137. Nguyen TB, Olzmann JA. Lipid droplets and lipotoxicity during autophagy. *Autophagy*. 2017;13(11):2002-2003. doi:10.1080/15548627.2017.1359451

138. Welte MA, Gould AP. Lipid droplet functions beyond energy storage. *Biochim Biophys Acta Mol Cell Biol Lipids*. 2017;1862(10 Pt B):1260-1272. doi:10.1016/j.bbalip.2017.07.006

139. Zechner R, Zimmermann R, Eichmann TO, et al. FAT SIGNALS - Lipases and Lipolysis in Lipid Metabolism and Signaling. *Cell Metab*. 2012;15(3):279-291. doi:10.1016/j.cmet.2011.12.018

140. Schulze RJ, Sathyanarayan A, Mashek DG. Breaking fat: The regulation and mechanisms of lipophagy. *Biochim Biophys Acta BBA - Mol Cell Biol Lipids*. 2017;1862(10, Part B):1178-1187. doi:10.1016/j.bbalip.2017.06.008

141. Zagani R, El-Assaad W, Gamache I, Teodoro JG. Inhibition of adipose triglyceride lipase (ATGL) by the putative tumor suppressor G0S2 or a small molecule inhibitor attenuates the growth of cancer cells. *Oncotarget*. 2015;6(29):28282-28295. doi:10.18632/oncotarget.5061

142. Wang YY, Attané C, Milhas D, et al. Mammary adipocytes stimulate breast cancer invasion through metabolic remodeling of tumor cells. *JCI Insight*. 2017;2(4):e87489. doi:10.1172/jci.insight.87489

143. Grace SA, Meeks MW, Chen Y, et al. Adipose Triglyceride Lipase (ATGL) Expression Is Associated with Adiposity and Tumor Stromal Proliferation in Patients with Pancreatic Ductal Adenocarcinoma. *Anticancer Res*. 2017;37(2):699-703. doi:10.21873/anticanres.11366

144. Al-Zoughbi W, Pichler M, Gorkiewicz G, et al. Loss of adipose triglyceride lipase is associated with human cancer and induces mouse pulmonary neoplasia. *Oncotarget*. 2016;7(23):33832-33840. doi:10.18632/oncotarget.9418

145. Wu JW, Preuss C, Wang SP, et al. Epistatic interaction between the lipase-encoding genes Pnpla2 and Lipe causes liposarcoma in mice. *PLoS Genet*. 2017;13(5):e1006716. doi:10.1371/journal.pgen.1006716

146. Singh R, Kaushik S, Wang Y, et al. Autophagy regulates lipid metabolism. *Nature*. 2009;458(7242):1131-1135. doi:10.1038/nature07976

147. Singh R, Cuervo AM. Lipophagy: Connecting Autophagy and Lipid Metabolism. International Journal of Cell Biology. doi:10.1155/2012/282041

148. Kaur J, Debnath J. Autophagy at the crossroads of catabolism and anabolism. *Nat Rev Mol Cell Biol*. 2015;16(8):461-472. doi:10.1038/nrm4024

149. Kaini RR, Sillerud LO, Zhaorigetu S, Hu C-AA. Autophagy regulates lipolysis and cell survival through lipid droplet degradation in androgen-sensitive prostate cancer cells. *The Prostate*. 2012;72(13):1412-1422. doi:10.1002/pros.22489

150. Du H, Zhao T, Ding X, Yan C. Hepatocyte-Specific Expression of Human Lysosome Acid Lipase Corrects Liver Inflammation and Tumor Metastasis in lal−/− Mice. *Am J Pathol*. 2015;185(9):2379-2389. doi:10.1016/j.ajpath.2015.05.021

151. Schlaepfer IR, Rider L, Rodrigues LU, et al. Lipid catabolism via CPT1 as a therapeutic target for prostate cancer. *Mol Cancer Ther*. 2014;13(10):2361-2371. doi:10.1158/1535-7163.MCT-14-0183

152. Pucci S, Zonetti MJ, Fisco T, et al. Carnitine palmitoyl transferase-1A (CPT1A): a new tumor specific target in human breast cancer. *Oncotarget*. 2016;7(15):19982-19996. doi:10.18632/oncotarget.6964

153. Samudio I, Harmancey R, Fiegl M, et al. Pharmacologic inhibition of fatty acid oxidation sensitizes human leukemia cells to apoptosis induction. *J Clin Invest*. 2010;120(1):142-156. doi:10.1172/JCI38942

154. Qu Q, Zeng F, Liu X, Wang QJ, Deng F. Fatty acid oxidation and carnitine palmitoyltransferase I: emerging therapeutic targets in cancer. *Cell Death Dis*. 2016;7:e2226. doi:10.1038/cddis.2016.132

155. Begriche K, Massart J, Robin M-A, Borgne-Sanchez A, Fromenty B. Drug-induced toxicity on mitochondria and lipid metabolism: Mechanistic diversity and deleterious consequences for the liver. *J Hepatol*. 2011;54(4):773-794. doi:10.1016/j.jhep.2010.11.006

156. Montopoli M, Bellanda M, Lonardoni F, et al. "Metabolic reprogramming" in ovarian cancer cells resistant to cisplatin. *Curr Cancer Drug Targets*. 2011;11(2):226-235.

157. Catanzaro D, Gaude E, Orso G, et al. Inhibition of glucose-6-phosphate dehydrogenase sensitizes cisplatin-resistant cells to death. *Oncotarget*. 2015;6(30):30102-30114. doi:10.18632/oncotarget.4945

158. Strober W. Trypan blue exclusion test of cell viability. *Curr Protoc Immunol*. 2001;Appendix 3:Appendix 3B. doi:10.1002/0471142735.ima03bs21

159. Zhang L, Mizumoto K, Sato N, et al. Quantitative determination of apoptotic death in cultured human pancreatic cancer cells by propidium iodide and digitonin. *Cancer Lett*. 1999;142(2):129-137. doi:10.1016/s0304-3835(99)00107-x

160. Xia J, Psychogios N, Young N, Wishart DS. MetaboAnalyst: a web server for metabolomic data analysis and interpretation. *Nucleic Acids Res*. 2009;37(Web Server issue):W652-660. doi:10.1093/nar/gkp356

161. Xia J, Wishart DS. Metabolomic data processing, analysis, and interpretation using MetaboAnalyst. *Curr Protoc Bioinforma*. 2011;Chapter 14:Unit 14.10. doi:10.1002/0471250953.bi1410s34

162. Suhre K, Shin S-Y, Petersen A-K, et al. Human metabolic individuality in biomedical and pharmaceutical research. *Nature*. 2011;477(7362):54-60. doi:10.1038/nature10354

163. Beloribi-Djefaflia S, Vasseur S, Guillaumond F. Lipid metabolic reprogramming in cancer cells. *Oncogenesis*. 2016;5(1):e189. doi:10.1038/oncsis.2015.49

164. Jeong SM, Xiao C, Finley LWS, et al. SIRT4 Has Tumor-Suppressive Activity and Regulates the Cellular Metabolic Response to DNA Damage by Inhibiting Mitochondrial Glutamine Metabolism. *Cancer Cell*. 2013;23(4):450-463. doi:10.1016/j.ccr.2013.02.024

165. McKeage K, Keating GM. Fenofibrate: a review of its use in dyslipidaemia. *Drugs*. 2011;71(14):1917-1946. doi:10.2165/11208090-000000000-00000

166. Shirihai O, Song M, Dorn GW. How mitochondrial dynamism orchestrates mitophagy. *Circ Res*. 2015;116(11):1835-1849. doi:10.1161/CIRCRESAHA.116.306374

167. Abdrakhmanov A, Kulikov AV, Luchkina EA, Zhivotovsky B, Gogvadze V. Involvement of mitophagy in cisplatin-induced cell death regulation. *Biol Chem*. 2019;400(2):161-170. doi:10.1515/hsz-2018-0210

168. Dowdle WE, Nyfeler B, Nagel J, et al. Selective VPS34 inhibitor blocks autophagy and uncovers a role for NCOA4 in ferritin degradation and iron homeostasis in vivo. *Nat Cell Biol*. 2014;16(11):1069-1079. doi:10.1038/ncb3053

169. Ronan B, Flamand O, Vescovi L, et al. A highly potent and selective Vps34 inhibitor alters vesicle trafficking and autophagy. *Nat Chem Biol*. 2014;10(12):1013-1019. doi:10.1038/nchembio.1681

170. Backer JM. The regulation and function of Class III PI3Ks: novel roles for Vps34. *Biochem J*. 2008;410(1):1-17. doi:10.1042/BJ20071427

171. Menendez JA. Fine-tuning the lipogenic/lipolytic balance to optimize the metabolic requirements of cancer cell growth: Molecular mechanisms and therapeutic perspectives. *Biochim Biophys Acta BBA - Mol Cell Biol Lipids*. 2010;1801(3):381-391. doi:10.1016/j.bbalip.2009.09.005

172. Ueda SM, Yap KL, Davidson B, et al. Expression of Fatty Acid Synthase Depends on NAC1 and Is Associated with Recurrent Ovarian Serous Carcinomas. *J Oncol*. 2010;2010:285191. doi:10.1155/2010/285191

173. Bauerschlag DO, Maass N, Leonhardt P, et al. Fatty acid synthase overexpression: target for therapy and reversal of chemoresistance in ovarian cancer. *J Transl Med*. 2015;13(1):146. doi:10.1186/s12967-015-0511-3

174. Nieman KM, Kenny HA, Penicka CV, et al. Adipocytes promote ovarian cancer metastasis and provide energy for rapid tumor growth. *Nat Med*. 2011;17(11):1498-1503. doi:10.1038/nm.2492

175. Huang C-K, Chang P-H, Kuo W-H, et al. Adipocytes promote malignant growth of breast tumours with monocarboxylate transporter 2 expression via β-hydroxybutyrate. *Nat Commun*. 2017;8(1):1-13. doi:10.1038/ncomms14706

176. Bougarne N, Weyers B, Desmet SJ, et al. Molecular Actions of PPARα in Lipid Metabolism and Inflammation. *Endocr Rev*. 2018;39(5):760-802. doi:10.1210/er.2018-00064

177. Keating GM. Fenofibrate: a review of its lipid-modifying effects in dyslipidemia and its vascular effects in type 2 diabetes mellitus. *Am J Cardiovasc Drugs Drugs Devices Interv*. 2011;11(4):227-247. doi:10.2165/11207690-000000000-00000

178. Lian X, Wang G, Zhou H, Zheng Z, Fu Y, Cai L. Anticancer Properties of Fenofibrate: A Repurposing Use. *J Cancer*. 2018;9(9):1527-1537. doi:10.7150/jca.24488

179. Ertunc ME, Hotamisligil GS. Lipid signaling and lipotoxicity in metaflammation: indications for metabolic disease pathogenesis and treatment. *J Lipid Res*. 2016;57(12):2099-2114. doi:10.1194/jlr.R066514

180. Elwood JM, Tin Tin S, Kuper-Hommel M, Lawrenson R, Campbell I. Obesity and breast cancer outcomes in chemotherapy patients in New Zealand – a population-based cohort study. *BMC Cancer*. 2018;18(1):76. doi:10.1186/s12885-017-3971-4

181. Horowitz NS, Wright AA. Impact of obesity on chemotherapy management and outcomes in women with gynecologic malignancies. *Gynecol Oncol*. 2015;138(1):201-206. doi:10.1016/j.ygyno.2015.04.002

182. Yang J, Zaman MM, Vlasakov I, et al. Adipocytes promote ovarian cancer chemoresistance. *Sci Rep*. 2019;9(1):1-12. doi:10.1038/s41598-019-49649-1

183. Cardenas C, Montagna MK, Pitruzzello M, Lima E, Mor G, Alvero AB. Adipocyte microenvironment promotes Bclxl expression and confers chemoresistance in ovarian cancer cells. *Apoptosis*. 2017;22(4):558-569. doi:10.1007/s10495-016-1339-x

184. Sui X, Chen R, Wang Z, et al. Autophagy and chemotherapy resistance: a promising therapeutic target for cancer treatment. *Cell Death Dis*. 2013;4:e838. doi:10.1038/cddis.2013.350

185. Zhou J, Li G, Zheng Y, et al. A novel autophagy/mitophagy inhibitor liensinine sensitizes breast cancer cells to chemotherapy through DNM1L-mediated

mitochondrial fission. *Autophagy*. 2015;11(8):1259-1279. doi:10.1080/15548627.2015.1056970

186. Schlütermann D, Skowron MA, Berleth N, et al. Targeting urothelial carcinoma cells by combining cisplatin with a specific inhibitor of the autophagy-inducing class III PtdIns3K complex. *Urol Oncol*. 2018;36(4):160.e1-160.e13. doi:10.1016/j.urolonc.2017.11.021

187. Maddocks ODK, Berkers CR, Mason SM, et al. Serine starvation induces stress and p53-dependent metabolic remodelling in cancer cells. *Nature*. 2013;493(7433):542-546. doi:10.1038/nature11743

188. Krishnan N, Dickman MB, Becker DF. Proline modulates the intracellular redox environment and protects mammalian cells against oxidative stress. *Free Radic Biol Med*. 2008;44(4):671-681. doi:10.1016/j.freeradbiomed.2007.10.054

189. Kremer JC, Prudner BC, Lange SES, et al. Arginine Deprivation Inhibits the Warburg Effect and Upregulates Glutamine Anaplerosis and Serine Biosynthesis in ASS1-Deficient Cancers. *Cell Rep*. 2017;18(4):991-1004. doi:10.1016/j.celrep.2016.12.077